國立交通大學

電機與控制工程學系

碩士論文

以時域和頻域的方法來探討禪坐心電圖的特性

Meditation ECG Characterization by Time- and Frequency-Domain Methods

研 究 生：李啟弘

指導教授：羅佩禎　教授

中 華 民 國 九 十 四 年 一 月

以時域和頻域的方法來探討禪坐心電圖的特性

Meditation ECG Characterization by Time- and Frequency-Domain Methods

研 究 生: 李啟弘　　Student : Chi-hung Lee

指導教授: 羅佩禎　博士　　Advisor : Dr. Pei-Chen Lo

國 立 交 通 大 學 電 機 與 控 制 工 程 學 系

碩 士 論 文

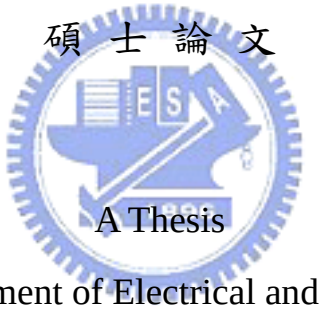

A Thesis

Submitted to Department of Electrical and Control Engineering

College of Electrical Engineering and Computer Science

National Chiao Tung University

In Partial Fulfillment of the Requirements

For the Degree of Master

In

Electrical and Control Engineering

January 2005

Hsinchu, Taiwan, Republic of China

中華民國九十四年一月

以時域和頻域的方法來探討禪坐心電圖的特性

研究生：李啟弘　　指導教授：羅佩禎

國立交通大學電機與控制工程學系碩士班

摘　　要

本研究的目的在於探討禪坐時心電圖的變化，結果將與靜坐休息下的控制組作比較。心率變異特性分析對評估心臟自主神經的調節功能已被證實是有效且是非侵入式的分析工具，所以我們可以藉由心率變異特性來評估禪定對心臟自主神經調節功能的影響。本研究總共收集了43位受測者的實驗資料(實驗組：25人；控制組：18人)，我們的目的是要分析兩組間統計上的差異。分析方法為時域分析和頻域分析，而其結果是根據一些要素如受測者的性別和坐姿來加以分析，最後量化的特徵將依時域和頻域分析中的各個參數以FCM(Fuzzy *C*-means)來作分類。

由實驗結果得到兩個結論：(1) 在時域分析方面，實驗組中採雙盤坐姿的受測者平均來說，在禪定過程當中所有的參數值(MRR, SDRR, RMSSD)都是減少的，而控制組平均而言，參數SDRR和RMSSD在休息過程中是呈現增加的趨勢；(2) 在頻域分析方面，代表交感神經活性的參數nLF和代表自律神經系統平衡的參數Ratio of LF/HF，實驗組中採單盤坐姿的受測者平均來說，是低於控制組的；相反的，代表副交感神經活性的參數nHF、HF，實驗組中採單盤坐姿的受測者平均來說，則是高於控制組的。

因此可以推測禪定與放鬆休息對心率變異和自主神經系統的調節有不同的效果.而不同的禪定姿勢所造成的效果亦不相同。

Meditation ECG Characterization by Time- and Frequency-Domain Methods

Student: Chi-hung Lee **Advisor: Pei-chen Lo**

Institute of Electrical and Control Engineering

National Chiao Tung University

Abstract

The purpose of this research is to discuss the variation of ECG during meditation, and the result will be compared with that of the control group under resting. The analysis of heart rate variability is verified to be effective for estimating the modulation of heart autonomic nerves, and it is also a non-invasive analyzing tool. So we may make use of HRV (heart rate variability) to evaluate the effect of meditation on the modulation of heart autonomic nerves. There are 43 subjects (experimental subjects: 25; control subjects: 18) in this research totally. We aim to analyze the statistical difference between two groups. The analyzing methods include time domain analysis and frequency domain analysis. The results are analyzed according to such factors as gender and meditation posture of the subjects. Finally quantitative features are classified by FCM (Fuzzy *C*-means) depending on each parameter in time and frequency domain analysis.

Two conclusions are drawn from the results：(1) In the time-domain analysis, all the parameters (MRR, SDRR, and RMSSD) tend to decrease when the experimental subjects adopting full-lotus posture enter the meditation session. In the control group, SDRR and RMSSD increase during the resting process. (2) In the frequency-domain analysis, the parameter reflecting the activation of sympathetic system, nLF, and the parameter indicating the balance of autonomic nervous system(ANS), ratio of LF/HF, are both higher for the control subjects in comparison with those of the experimental subjects who adopt half-lotus posture. On the contrary, the parameters reflecting the activation of parasympathetic system, nHF, and HF of the control subjects are lower than those of the experimental subjects who adopt half-lotus posture.

Therefore we may infer that the effects of meditation on the HRV and on the modulation of ANS are different from those of resting. In addition, the results obtained from meditators using various meditation postures are also distinct.

誌 謝

本篇論文的完成，首先要感謝我的指導教授羅佩禎老師，因為她適時的指導讓我在專業知識的獲取和研究學問的方法上都獲益良多。同時，也要感謝邱俊誠教授和楊谷洋教授對本論文提出許多建設性的指導與建議。

在碩士班兩年多的學習過程中，我要感謝剛鳴、瑄詠、憲政、權毅、適達以及清泉幾位博士班學長姐經常給我指導、建議與鼓勵。特別是剛鳴學長一年多來，對本論文的不吝賜教，使得本論文得以更加完整。而實驗室的同學岳昌和清文，也感謝你們和我一起努力。另外要感謝學弟偉源、富滄、進忠和偉凱，在我研究之餘陪我一起度過。

最後，我要感謝我的 師父與我的父母，謝謝你們對我的指引與支持，還有許多同修和家人對我的關心和照顧，讓我在完成學業的過程中，收穫滿行囊。

Contents

List of Tables

List of Figures

Chapter 1

Introduction

1.1 Background and Motivation

There are now considerable clinical evidences and a number of theories describing meditation's impact on psychological and physiological symptoms. Ramita Bonadonna mentioned that meditation practice could positively influence the experience of chronic illness and could serve as a primary, secondary and tertiary prevention strategy [33]. Vernon A. Barnes discovered that Transcendental Meditation program appeared to have a beneficial impact on cardiovascular functioning at rest and during acute laboratory stress in adolescents at-risk for hypertension [38]. Linda E. Carlson proved that Mindfulness-Based Stress Reduction meditation program enrollment was associated with enhanced quality of life and decreased stress symptoms in breast and prostate cancer patients [16]. Elizabeth Monk-Turner found that the subjects practicing meditation benefited most in the aspect of experiencing fewer symptoms of aching muscles or joints that resulted in less use of drugs and tranquilizers [7]. Laurie Keefer demonstrated that constant practice meditation was particularly effective in reducing the symptoms of abdominal pain and flatulence ; Relaxation response meditation is a beneficial treatment for irritable bowel syndrome in both the short-term and the long-term cases [17,18]. John Ding-E Young and Eugene Taylor denoted that there were many physiological analogies between the long-term meditators and hibernators on the phylogenetic scale [13]. Gregory A. Tooley revealed that meditation could affect plasma melatonin levels either by decreasing hepatic metabolism of the hormone or

via a direct effect on pineal physiology. Facilitation of higher physiological melatonin levels at proper times of day might be one way of health promoting effects of meditation [8]. John J. Miller showed that an intensive but time-limited group stress reduction intervention based on mindfulness meditation could have long term beneficial effects in the treatment of people diagnosed with anxiety disorders [14].

The advantage of meditation has drawn our attention. Our research group has been focusing on meditation EEG analysis for several years. We have a great achievement in the development of EEG analysis and interpretation algorithms. And the methods and technologies supporting our research work are getting matured. In recent years, we began extending our research field to other physical signals such as ECG (electrocardiograph), GSR (galvanic skin response), etc. In ECG study, Renlong Tsai used several methods including time domain analysis, frequency domain analysis, time-frequency domain analysis and poincare plot to examine the characteristics of HRV (heart rate variability) of the experimental and control groups. Furthermore, he discussed the correlation between the HRV parameters and ANS (autonomic nervous system). Since he only analyzed few subjects, we need to get a statistically meaningful conclusion by analyzing a larger amount of samples. Thus, in this research we sample more subjects from each group in order to identify the difference of the HRV characteristics between two groups.

1.2 Domestic and International Research Overview

In 1981 Akselrod [34] found that the HRV spectrum was able to tell the difference from the sympathetic effect to the parasympathetic one. Numerous signal-processing methods were adopted to analyze the correlation between HRV

and ANS. And ANS was evaluated for quantifying the variation of heart rate modulation under different kinds of diseases. In other words, results of the spectrum analysis of HRV might provide a tool to explore the ANS without invasion. Therefore HRV has become the dominant agent in the research of autonomic nervous system function. Several kinds of clinical applications of HRV are described separately**:**

I. Cardiovascular disease

HRV is a powerful index of prognosis for the patient of acute myocardial infarction. SDRR (standard deviation of RR intervals), LF (low frequency power) may be the prognosis index of mortality for the patient with heart exhaustion. When one's SDRR falls down, his mortality rises up [27]. The clinical reason is that the sympathetic dominates and the modulation effect of sinoatrial node vagi is getting weaker. The decreasing degree of time domain index of HRV is related to how serious the disease is. The correlation between the frequency index of HRV and the disease is more complicated. When one has minor heart failure, his LF increases obviously and HF (high frequency power) decreases. When one has serious heart exhaustion, both his LF and HF power reduce gradually and the rest power distributes in VLF (very low frequency power) band [28,19].

II. Hypertension

In the heart research project, Framingham found that LF corresponded obviously to the hypertension in all of the indexes such as SDRR, LF, HF, LF/HF ratio, and so forth for the HRV estimation of the hypertensive. It is more likely for the one with low LF to become a hypertensive patient [35].

III. Cerebral blood vessel disease

The patient of Parkinson's disease has lower values of SDRR, LF and HF than the healthy subjects of control group at night [23]. In the research of acute head injury in children, when the cerebral perfusion pressure is smaller than 40 mmHg, LF/HF ratio may decrease rapidly [1].

IV. Brain death

For the patient with brain death, the spectrum of LF is becoming zero; otherwise, the spectrum of HF is still quite weak, and LF/HF ratio may drop down [2].

V. Diabetes mellitus

In the experiment, Ewing confirmed that LF and HF were apparently less for the patient with pathological changes of autonomic nervous system. Thus HRV can be a tool of evaluating pathological changes of ANS for diabetics [42]. Pathological changes of ANS for diabetics usually exhibit some conditions: (1) mostly, all power spectrums reduce; (2) when one stands without raising his LF, it indicates the abnormality of the sympathetic reflection; (3) total power reduces exceptionally and LF/HF ratio keeps constant; and (4) when LF tends towards left, its physiological meaning needs to be evaluated further [28].

VI. Gynecologic disease

LF is higher and HF is lower in corpus luteum period than those in follicle period. The activation of sympathetic is higher in corpus luteum period than that in follicle period [36].

Some independent variables affecting HRV are described as follows **:**

I. Gender

The LF of female is lower than that of male, and HF/LF ratio is higher for women [20]. There are no significant differences between men and women for older people. For younger people, men have lower heart rates than women. And all 24-hour time domain indexes of HRV, except those that reflect vagal modulation of heart rate, are significantly higher than those in women [37].

II. Age

With aging, power spectrum relating to the phenomena of sympathetic and parasympathetic diminishes [20,37]. HF/LF ratio is similar between aged people and the young [20].

III. Sport

Experienced athletes exhibit higher modulation effect of parasympathetic and they have better ANS function than the control group. SDRR, LF, HF, and total power are higher in veteran sportsmen, while LF/HF ratio is lower in this group [43].

IV. Alternating between Day and Night

For children, LF/HF ratio is higher during the day than at night. Other HRV indexes such as SDRR, VLF, LF, RMSSD, and HF increase by night and decrease by day [24]. For adult, heart rate, LF/HF ratio, and LF increase during the day; and HF and RR interval increase at night [26].

V. Sleep

For young men, sleeping from awake state to non-REM (rapid eye movement) state, their R-R intervals increase and HF power rises [6]. For the normal, LF/HF ratio reduces obviously from awake state to non-REM state, whereas it rises in REM state. However, there exists a reverse trend for the myocardial infarction patients.

LF/HF ratio increases obviously from awake state to non-REM state, and it rises further in REM state. Myocardial infarction causes the disability of the vagal activity. It explains why sudden death attacks myocardial infarction patients at night [39].

VI. Occupation

HF is lower for the high consumption of physical strength and the difference of LF/HF ratio is unclear. The function of ANS may decay gradually in the laborers who burn the candle at both ends [40].

VII. Pregnancy and Menopause

LF is lower in a mother-to-be than in a normal woman. HF is lower and LF/HF ratio rises up for the women during menopause. It indicates that the control function of ANS is disordered. Hormone substitute therapy may improve excessive sympathetic activation [29].

1.3 Scope of This Research Study

This thesis is composed of five parts. Chapter 1 is to describe the research background and motivation, introduce domestic and international researches, and illustrate the organization of this thesis. In Chapter 2, the basic principles of ECG and the relationship between autonomic nervous system and cardiovascular system will be presented. The QRS detection algorithm, the methods for analyzing HRV in time and frequency domain, and the clustering method are illustrated in Chapter 3. Chapter 4 discusses the statistical meaning and clustering results of the ECG features between the experimental and control groups. Chapter 5 summaries this research work and brings forth further research topics to be conducted in the future.

Chapter 2

Background of Physiological Signal Systems

Many physiological signals of human being can be detected and transformed to electric signals. Then we can do some works such as recording, displaying, and analyzing with the help of clinical electronic meter. These signals can aid to the diagnosis of the cause of disease by proper interpretation. Therefore, physiological signals are very valuable in clinical reference. Among all the physiological signals, noninvasive measurements are carried out most often in hospitals, which include ECG, EMG(electromyograph), EEG(electroencephalograph), blood pressure, temperature, etc. Because this research is to analyze the characteristics of HRV (heart rate variability), we put emphasis on the process and analysis of cardiac-electric signals. We thus will go a step further to discuss the features and mechanism of cardiac-electric signals. Biological and physiological background will be illustrated in this chapter. First, principles of ECG, and definitions of ECG profile are introduced. Next, the relation between ANS (autonomic nervous system) and cardiovascular system and their mutual interaction are explained. Then the physiological indexes affecting cardiac output (CO) are listed. Finally, the correlation between HRV and ANS will be depicted.

2.1 Introduction to Electrocardiogram

In the early embryo period, a heart can throb although it just formed and it cannot stop pulsing at any moment until a person die. Heart itself owns the feature of pulsating automatically and rhythmically. The reason is that heart has a kind of

specialized conducting system inclusive of four parts, that is, SA node (sino-atrial node), AV node (atrio-ventricular node), Bundle of His, and Purkinje fibers. Figure 2.1 shows the anatomic description.

SA node is the pacemaker of heart. It controls the regular pulse of heart entirely. Depolarization waves originate in it, like pebbles falling into a pool. They spread around tier by tier. Depolarization waves propagate to atria (right first and left last), causing atria systole, and "P" wave appears in ECG. Besides, they also spread to AV node. AV node connects with Bundle of His, and Purkinje fibers are the extended part of the fibers of Bundle of His. Purkinje fibers are distributed such as a threadlike net on subenocardial surface. Thus the depolarization waves caused by the pacemaker propagate to atria all around and induce the two atria to draw back. Then they pass to AV node, spread to ventricles widely, and make two ventricles contract simultaneously. Therefore, the order of heart excitation is: SA node → myocardium (atria) → AV node → Bundle of His → Purkinje fibers → myocardium (ventricle) [44].

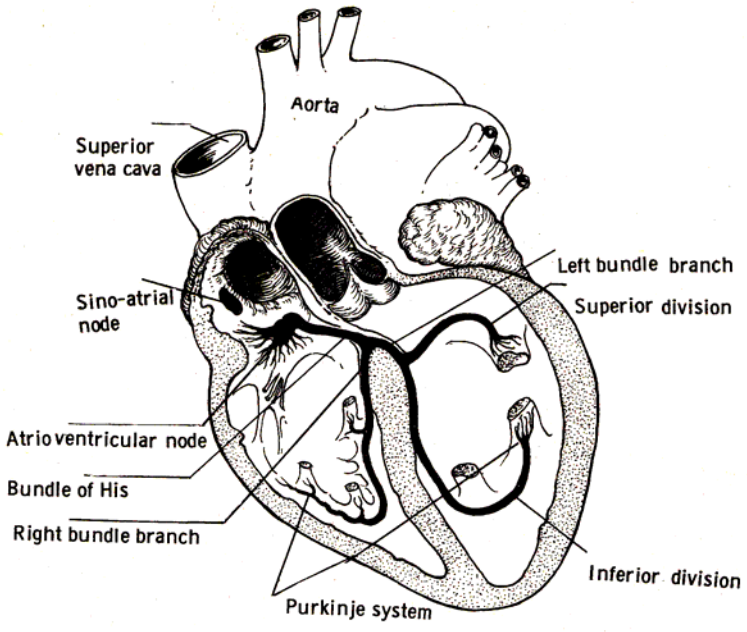

Fig. 2.1 The conduction system of Heart [44]

When heart beats, the depolarization waves resulting from myocardium not only extend to the whole heart, but also make electrical current change. This current will spread to the surface of body so that we may record it with electrocardiograph. The graph we get is called the ECG (electrocardiogram). In general, there are two ways to record ECG; one is bipolar lead and the other is unipolar lead.The method of bipolar recording is to attach the recording electrodes to two hands and two legs, and select right-leg electrode as a reference. Lead I is the voltage difference between left hand and right hand. Lead II is the voltage difference between right hand and left leg. Lead III is the voltage difference between left leg and left hand. (Figure 2.2A) The method of unipolar recording is to connect left hand with left leg to a joint. The voltage between the joint and the right hand is measured. The other way is to connect right hand and left leg to a joint. The voltage between the joint and the left hand is compared. This way is usually called augmented unipolar limb lead, and right leg is still the reference. (Figure 2.2B) Another method of unipolar is to attach six electrodes to the special locations on chest. The voltages measured by the six electrodes at adjoining locations are V_1, V_2, V_3, V_4, V_5, and V_6. (Figure 2.2C)

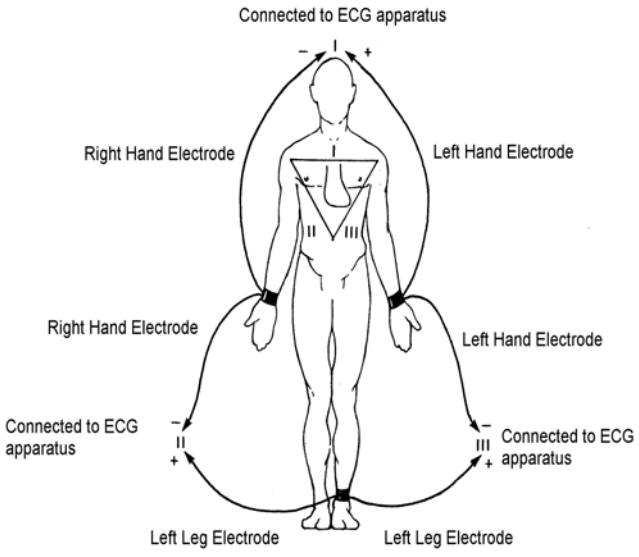

Fig 2.2 (A) Bipolar Standard leads [45]

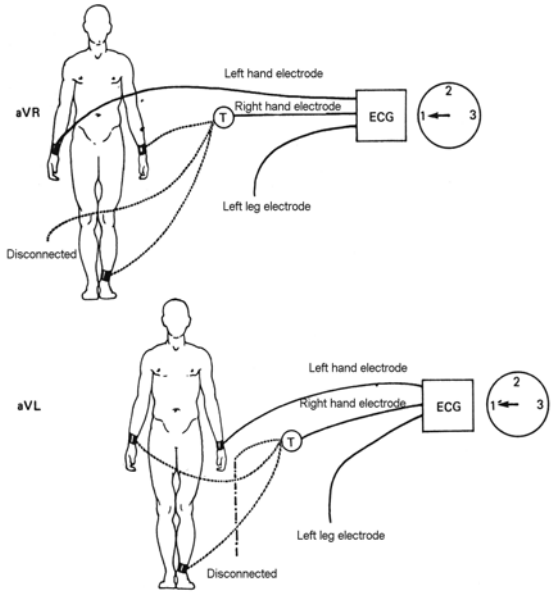

Fig 2.2 (B) Augmented Unipolar leads [45]

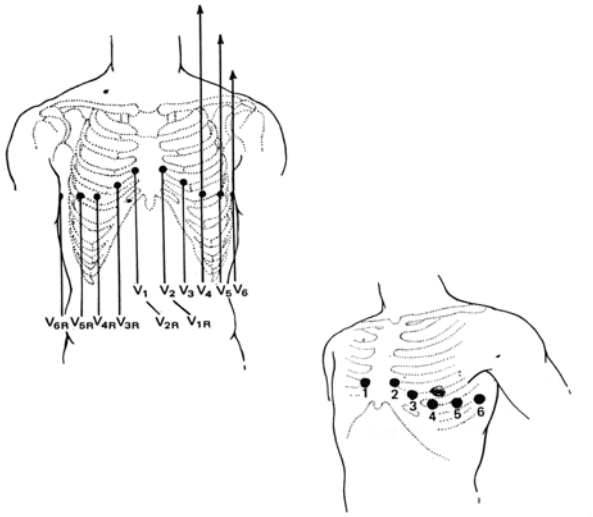

Fig 2.2 (C) Unipolar Chest leads [45]

Due to the negative potential in the quiescent state (-80mv or so), or so-called polarization, once heart cells are stimulated electrically, and become depolarized, they bear positive potential that activation potential induces the systole reaction. At the same time, ECG traces the potential variation of periodic activity of the heart. The standard wave patterns of ECG are shown in Figure 2.3. The physiological meaning of each normal electrocardiographic complex is described below:

P wave: This deflection is due to the atria depolarization

Q wave: This first negative deflection is caused by the ventricle depolarization. The first positive deflection (R) follows.

R wave: This first positive deflection caused by the ventricle depolarization.

S wave: This first negative deflection follows the first positive deflection (R) during the period of ventricle depolarization.

T wave: This deflection is due to the ventricle repolarization.

U wave: The deflection succeeds the T wave and leads the next P wave. (A positive wave in usual) The mechanism generating this wave forms is unclear yet. One proposal referred this phenomenon to the slower repolarization of the conducting system among ventricles (Purkinje fibers).

The characteristic interval values are introduced briefly as follows:

RR interval: RR interval stands for the time interval between two successive R waves. The BPM (beat per minute) can be derived by 60/RR interval (60 divided by RR interval).

PR interval: This is the period of AV conduction mainly. The period consists of some processes as follows: (1) atria depolarization (2) normal conduction delay in AV node (about 0.07 sec) (3) the period of depolarization waves passing Bundle of His and its branches until the beginning of ventricle depolarization. The normal value of PR interval is usually from 0.12sec to 0.2sec.

QRS interval: This period represents the whole time that ventricle depolarization takes. The normal value of QRS interval is usually from 0.04sec to 0.11sec.

QT interval: The period is from the starting point of Q wave to the ending of T wave. It stands for the period of electric power contracting of heart.

ST interval: The period is from the ending of QRS complexes to the starting point of T wave. The point connecting the QRS complexes and ST interval is called junction J.

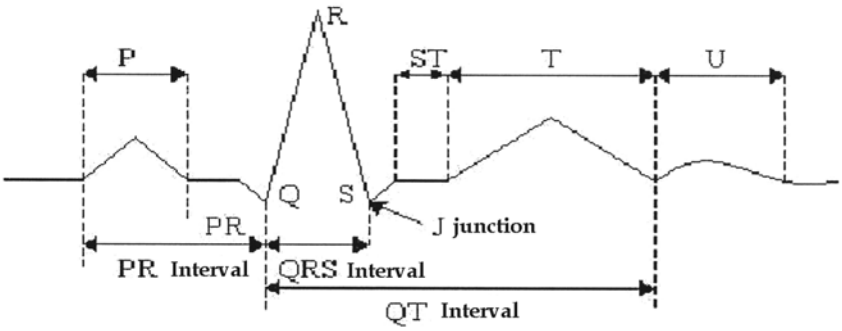

Fig. 2.3 The standard wave patterns of ECG

2.2 Autonomic Nervous System and Cardiovascular System Modulation

Autonomic nervous system controls the motor nerves of internal organs of human bodies. It is also called visceral nervous system. It is distributed in smooth muscles, cardiac muscles, and all kinds of glands. The major function of ANS is in the regulation of homeostasis. In the regulative process, sensory nerves may convey transient variations to central nervous system any time, and then it may affect viscera by autonomic nerves. Autonomic nervous system is composed of sympathetic nervous system and parasympathetic nervous system. Almost all the internal organs are dominated by both of sympathetic and parasympathetic nerves. In general, the functions of these two nervous systems are contending, but also coordinating to each other harmonically.

About the nerves control of heart, SA node, a pacemaker of heart, dominates heart rate, which is also affected by autonomic nerves. For example, when one takes exercise, the metabolic function of the whole body cells rise up. Heart rate needs to speed up so that blood may convey enough oxygen and nutrients to the tissues and cells of the whole body. At this time, the sympathetic nerves dominating heart will become excited. Then heart rate speeds up, and the systole strength of myocardium increases. The reason is that the neurotransmitter (norepinephrine) secreted by sympathetic nerve ends acts on the receiver of the surface of myocardium cells.

The parasympathetic nerves dominating heart are the vagus. When a person rests his body after the exercise, vagus becomes excited. The activation of pacemaker (SA node) is restrained so that heart rate lowers down. The conducting effect of the conducting system of heart is blocked, and the systole strength of myocardium is reduced. The reason is that the neurotransmitter (acetylcholine) secreted by parasympathetic nerve ends acts on the receiver of the surface of myocardium cells.

From the above, the functions of sympathetic nervous system and parasympathetic nervous system are contending.

About vasomotor center and the modulation of circulatory system, to maintain the normal blood pressure of human body is very important. It is involved in the complex neural control and endocrine effect. First, we need to know that our blood pressure changes all the time. Thus, our inner body needs a set of receivers, which can detect the variation of blood pressure at any moment, then transform it into a nervous impulse, and pass it to central nervous system. After central nervous system deals with the signal of blood pressure, cardiovascular system will be modulated by the action of autonomic nerves.

When blood pressure rises up, baroreceptors stimulated by the blood pressure induce nervous impulses to pass to the vasomotor center of medulla oblongata along the sinus nerves and vagus. After these nervous impulses are analyzed and processed, they will restrain the action of sympathetic nerves and promote the activation of parasympathetic nerves. The result is that heart rate slows down, blood vessels become diastolic, and then blood pressure decreases. On the contrary, if blood pressure falls, the processing result of the vasomotor center is to enhance the activation of sympathetic nerves, and restrain that of parasympathetic nerves. Therefore, heart rate speeds up, arteriole becomes systolic to increase resistance, and then blood pressure rises again. From the above, the functions of sympathetic nervous system and parasympathetic nervous system are coordinating to each other harmonically.

2.3 Physiological Indexes Affecting Cardiac Output

The major function of the heart is to pump blood into blood vessels and make blood flow throughout the whole body. This function can be estimated by cardiac output (CO), that is, the blood volume pumped out by the heart in per minute. This should be the product of heart rate (HR), and stroke volume (SV). It may be expressed as below: $CO(ml/min)=HR(min^{-1})\times SV(ml)$. Therefore heart rate and stroke volume determine the magnitude of cardiac output. The normal heart rate of adults at rest is 70 beats/min, and stroke volume is 70 ml/beat. That means cardiac output is 4,900 ml/min. Heart rate is affected most by autonomic nervous system. The excitation of sympathetic nerves not only increases action potential frequency of SA node, but strengthens myocardium systole. Both of them increase cardiac output. The excitation of parasympathetic nerves can decrease heart rate effectively. Although it influences systole little, it causes the cardiac output to reduce. In endocrine glands, epinephrine and thyroxine can stimulate heart rate as well. Besides, body temperature and ionic concentration in blood can also change heart rate. Stroke volume is the difference between the maximum volume of ventricle (during the diastolic period) and the minimum volume of ventricle (during the systole period). Stroke volume is affected both by the myocardium itself and some external factors such as the sympathetic activation. Frank-Starling's law of the heart states that the more ventricle congests, the stronger ventricle systole is, and more blood can be pumped out. Under the constant volume of ventricle, the activation of sympathetic can stimulate myocardium to enhance the systole power, and then produces larger stroke volume than under the original volume. Similarly, epinephrine may increase stroke volume as well. The modulated conditions of heart rate and stroke volume can be explained by the Fig. 2.4

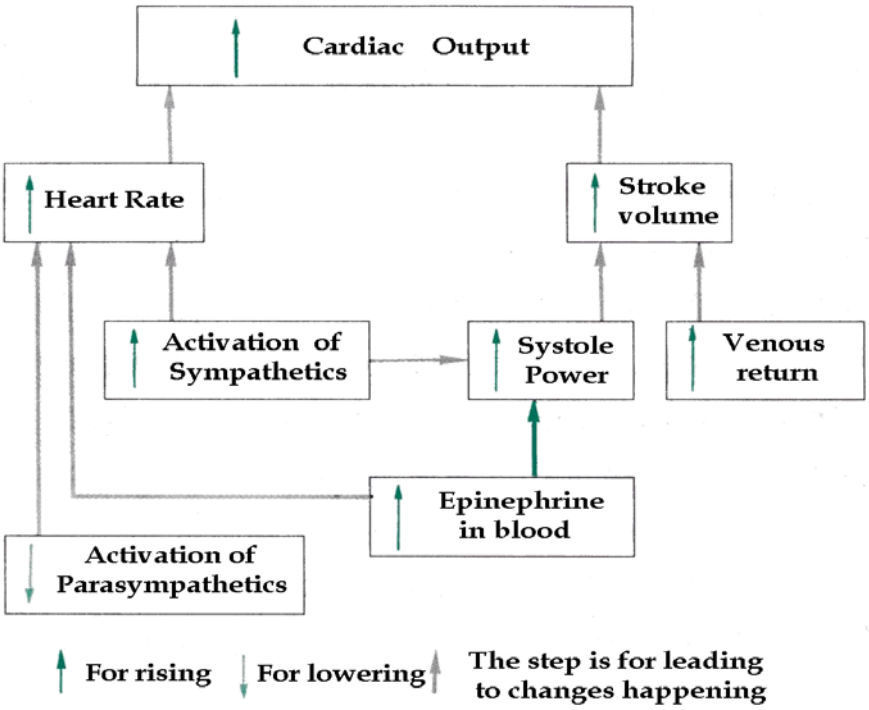

Fig. 2.4 Physiological modulating factors of cardiac output [21]

2.4 Analysis of Heart Rate Variability

2.4.1 History of heart rate variability

Heart rate and other hemodynamic indexes (such as the blood pressure, and the cardiac output) may vary periodically. This phenomenon was investigated systematically since 18th century. In 1733, Hales [46] first reported that there existed variance in blood pressure and heart rate between each heartbeat, and respiratory cycle, blood pressure, and intertbeat interval were mutually correlated. In 1846, Ludwig [46] utilized 24-hour electrocardiograph recording to analyze the heart rate, and found heart rate variability in synchronization with respiratory variation. Currently, the phenomenon of respiratory signal embedded in the signal of heart rate variability is accepted widely by medical science scope. In the 24-hour record of continuous electrocardiogram and blood pressure, it appears that some unknown

variations exist besides the respiratory variation. In 1965, Cooley and Turkey [46] developed the Fast Fourier Transform algorithm to estimate the frequency of signals with great improvement in computational efficiency. In 1975, Hyndman [46] first applied the power spectral analysis to the heart rate variability. They discovered that there were three spectral peaks on the power spectrum of the heart rate sequences. The low-frequency peak (0.04Hz) is related to cyclic fluctuations in peripheral vasomotor tone associated with thermoregulation. The mid-frequency peak (0.12Hz) is related to the frequency response of the baroreceptor reflex associated with homeostasis. High-frequency peak (0.3Hz) is related to respiratory cycle. Next, in 1981, Akselrod [10] and others found that low frequency part was related to mediation of sympathetic and parasympathetic, fluctuations in peripheral vasomotor tone, and the activation of rennin-angiotensin system. Middle frequency part was associated with baroreceptor reflex, and modulation of blood pressure. High frequency part was related to respiratory cycle. In recent years, analyzing the power spectrum of heart rate variability has been the most common method for studying the function of autonomic nervous system. Other related researches that selected the function of parasympathetic as an index showed that when the function of cardiovascular system was abnormal (such as coronary artery diseases, myocardial infarction, diabetes, hypertension, heart failure and aging, etc.), the activation of parasympathetic would decrease obviously. As a consequence, the analysis of heart rate variability (HRV) provides a potential tool to diagnose the heart diseases.

2.4.2 Methods of analyzing heart rate variability

HRV analysis has become an important tool in cardiology. The reason is that ECG recording can be noninvasive and easy to perform. In addition, it provides reliable prognostic information on patients with heart disease. HRV is mainly

influenced by two factors**:** one is the discharging rate of SA-node cells, and the other one is the mediation of autonomic nervous system. The natural discharging rate of SA-node is fixed, and it won't change with the variance of environment. Autonomic nervous system may increase or decrease the discharging rate of SA-node to maintain homeostasis so that heart rate rises up or lowers down to meet the physiological need. One way to classify the methods of analyzing HRV is to group them into 2 categories: linear and nonlinear. The linear methods involve time domain analysis and frequency domain analysis. The representative methods in time domain are: the standard deviation of normal-to-normal R-R interval (SDRR), the standard deviation of the average value of normal-to-normal R-R intervals in 5 minutes over a 24 h period (SDANN), the root-mean-square value of difference of successive R-R intervals (RMSSD), the proportion of instantaneous difference over 50 ms between 2 consecutive normal-to-normal R-R intervals (pNN50), and etc [11]. Frequency domain methods are generally based on Fast Fourier transform that converts signals into spectral features. The boundaries of the most commonly used frequency bands are as follows: ultra low frequency ($f < 0.0033$ Hz), very low frequency ($0.0033 \text{ Hz} \leqq f < 0.04$ Hz), low frequency ($0.04 \text{ Hz} \leqq f < 0.15$ Hz), and high frequency ($0.15 \text{ Hz} \leqq f < 0.4$ Hz). The frequency domain methods are more often used in clinic or in engineering. And it is easier to be realized for the real-time and on-line analysis. Among the nonlinear analyzing methods, the most typical ones are Lyapounov exponents measurement[30], 1/f behavior[22], Approximate Entropy measurement[9], Geometrical methods[41], etc.

2.4.3 Characteristics of power spectrum of HRV

In 1981, Akselrod [10] and others found that power spectrum of HRV could reflect the mediation phenomenon of sympathetic and parasympathetic for physical mechanism. Therefore the research prologue of the relationship of HRV and ANS was opened. In the power spectrum of HRV, we usually observe three distinct spectral peaks. They are low-frequency, mid-frequency, and high-frequency components respectively. As Fig. 2.5 shows, different definitions of low-frequency, mid-frequency, and high-frequency components have been proposed in the former research literatures. Among them, the definitions adopted most often are low-frequency band (0.02~0.08 Hz), mid-frequency band (0.08~0.15 Hz), and high-frequency band (0.15~0.4 Hz) respectively. Former researches have reported two major findings: (1) when parasympathetic was inhibited by medicine, the mid- and high-frequency peaks lowered by a large scale, while the low-frequency peak reduces a little; (2) If both sympathetic and parasympathetic were inhibited together, then all peaks disappeared. Thus, researchers speculate that mid- and high-frequency components might stand for the effect of parasympathetic, while the low- and mid-frequency components might represent the function of sympathetic. Hence, the power spectrum analysis of HRV can be developed to form a new physiological index for analyzing the mediation condition of ANS. Recently, [31] the characteristics of the power spectrum of HRV mentioned above are classified into high-frequency band (0.15~0.4 Hz) and low-frequency band (0.04~0.15 Hz). High-frequency band of the spectrum was the index of activation of the parasympathetic system, low-frequency band of the spectrum was the index of co-mediation of both sympathetic and parasympathetic. The ratio of low-frequency power to high-frequency power was the index of activation balance of parasympathetic to sympathetic. By making use of these three

indexes, the modulating conditions of sympathetic and parasympathetic with physical variances can be monitored. This research adopts this spectrum range as well.

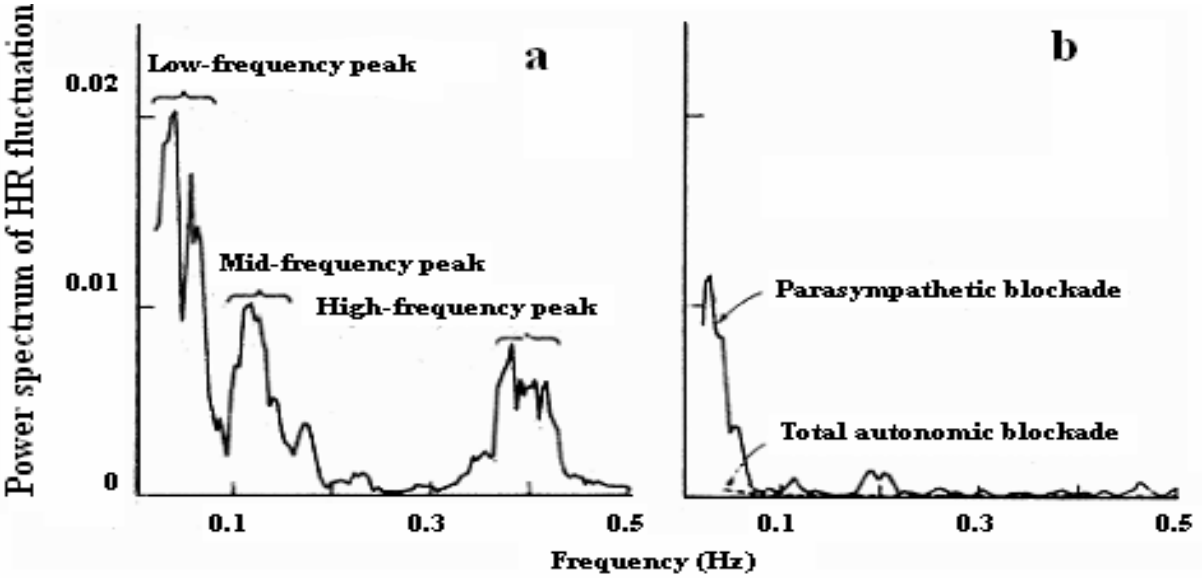

Fig. 2.5(a) Power spectrum of HRV with 3 major peaks [34]

Fig. 2.5(b) Power spectrum of HRV under parasympathetic blockade and combined parasympathetic and sympathetic blockade[34]

Chapter 3

Theoretical Model and Methods

The methods adopted in this research are mainly to analyze electrocardiographic signals collected by noninvasive methods. The whole process of signal analysis is illustrated in Fig 3.1. The meaning of each block will be discussed in the following sections. The features of HRV will be analyzed after collecting ECG signals. Therefore the positions of R wave in ECG signals need to be detected first, and then some linear methods are utilized to analyze the features of HRV in time and frequency domain. Finally, in order to see the difference of the HRV features between experimental group and control group, we use *t*-test to do statistical analysis, and Fuzzy *C*-means algorithm to do classification.

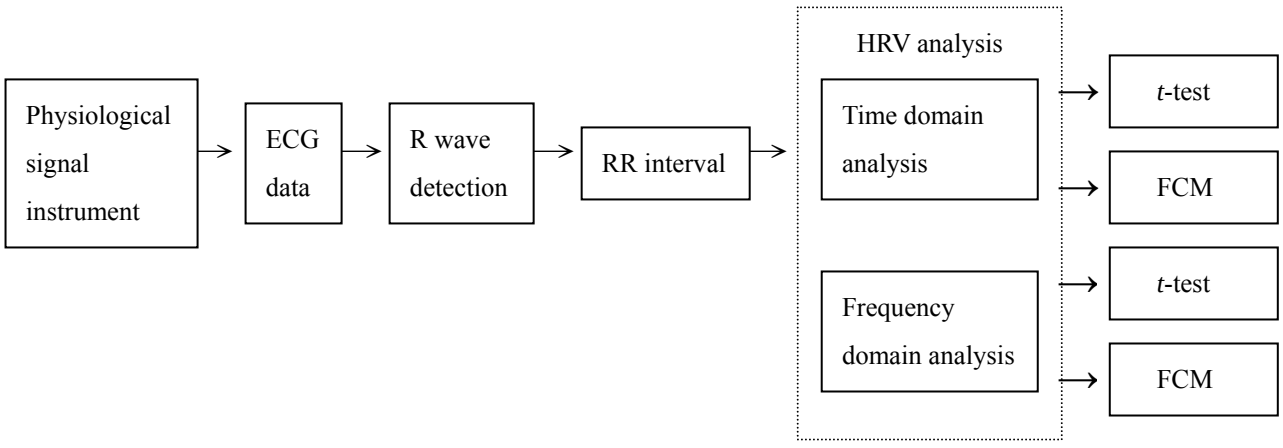

Fig 3.1 The processing procedure for ECG signal

3.1 Physiological signal collecting system

The physiological signal collecting system in this research is shown as Fig 3.2. The physiological signals passing through adhesive electrodes attached to the body surface of a subject are amplified by BioAmp (PowerLab ML136, biological signal amplifier) made by ADInstruments. Next, signals are delivered to pc through USB interface, and built-in collecting software, chart4, takes record. The physiological signals which are measured synchronously include ECG, EMG, and GSR.

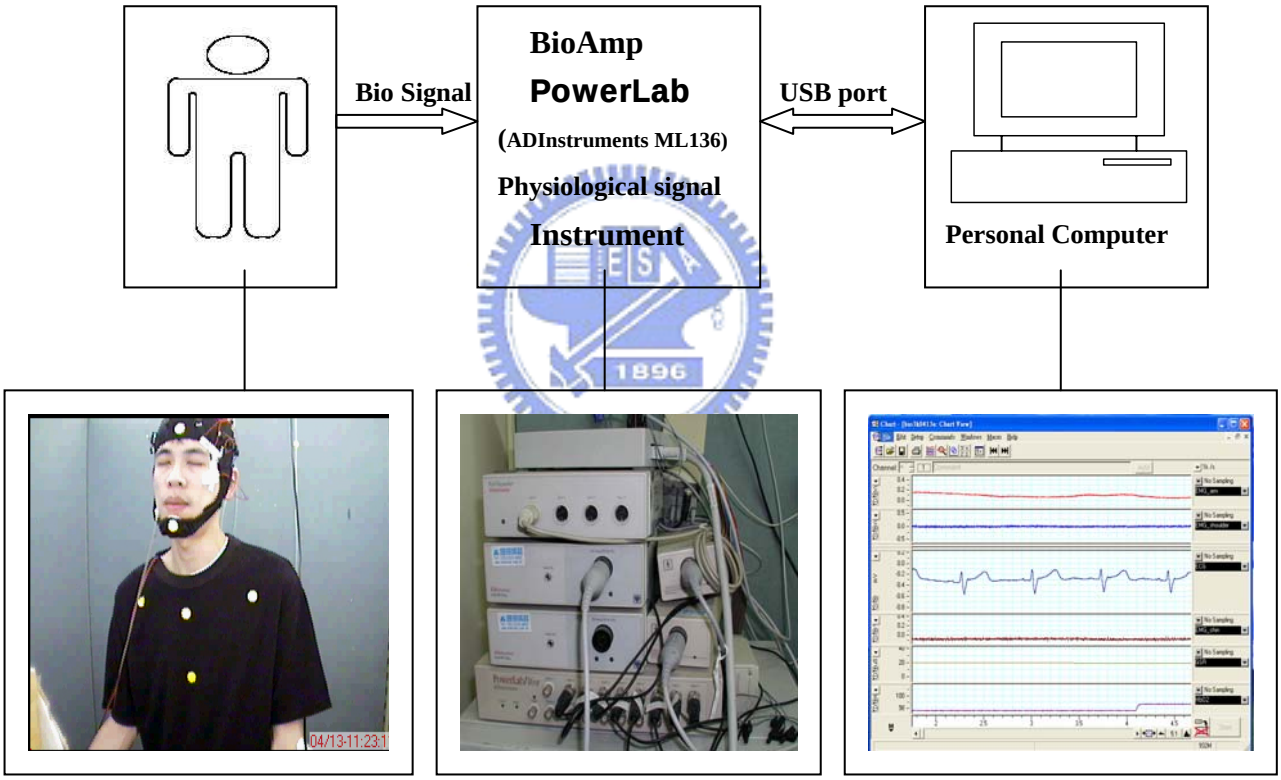

Fig.3.2 The physiological signal collecting system

ECG signals measurement

In this research, we make use of bipolar limb lead I to do the work, collecting and processing of ECG signals. Then we connect lines to BioAmp made by ADInstruments to amplify ECG signals as shown in Fig.3.3. BioAmp has 3 different input ends; they are 2 differential input ends and 1 reference potential end respectively. In general, we put the reference on inner side of the right ankle, and positive and negative electrodes of two differential input ends on inner sides of left and right wrists respectively.

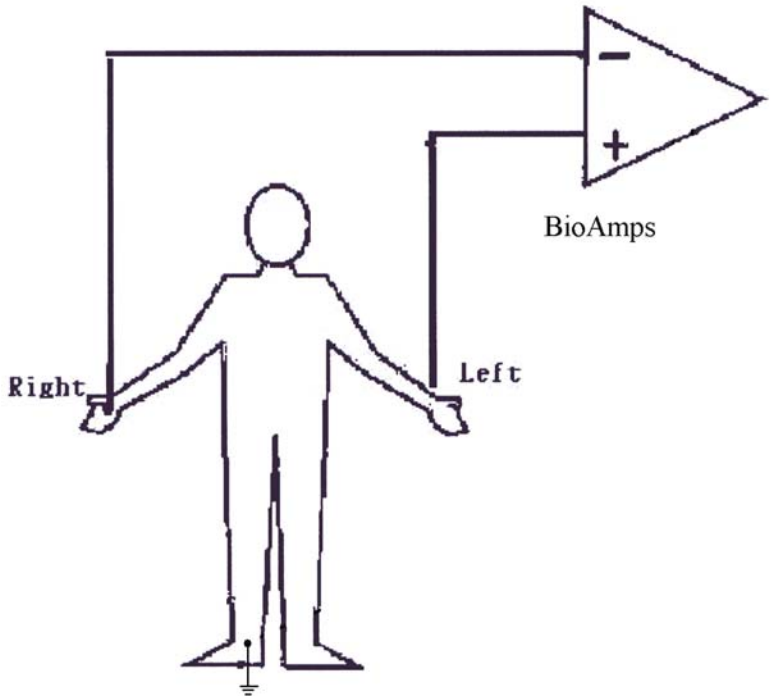

Fig. 3.3 Bipolar limb lead I

3.2 QRS detection and heart rate calculating

The magnitude of R wave is the biggest and the characteristic of R wave is the most obvious in ECG. (as shown in Fig 3.4) Generally speaking, in the analysis of heart rate, the position of QRS complex is needed to be detected at first, and then the position of the peak of R wave is found out by the setting of threshold. Next, the heart rate is calculated from R-R intervals, and the unreasonable heart rate signals must be rejected. (atria premature contractions and ventricular premature contractions) Thus, the heart rate variability can be obtained and the characteristics of HRV in time domain and frequency domain can be analyzed. The whole processing program is shown in Fig 3.5.

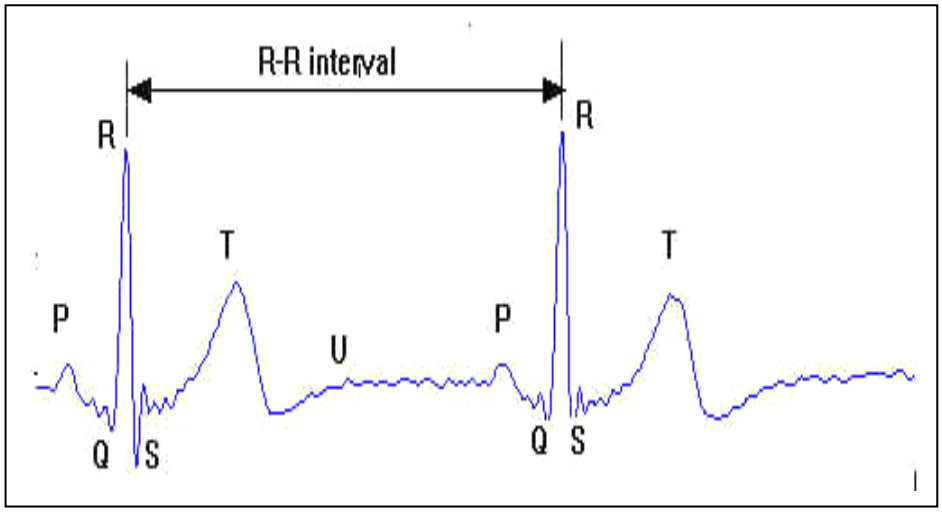

Fig 3.4 Standard Electrocardiograph

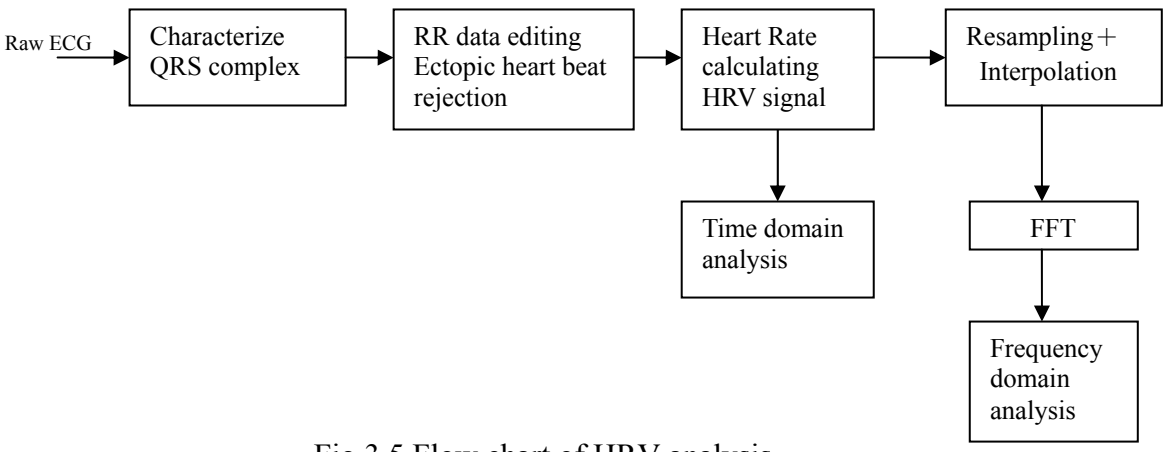

Fig 3.5 Flow chart of HRV analysis

3.2.1 Tompkins QRS detection algorithm

In this research, the QRS detection algorithm mainly bases on Tompkins QRS detection algorithm [32]. The algorithm includes 5 processes: band-pass filter, derivative, squaring, moving window integration, and adaptive thresholds (as shown in Fig 3.6). The signals after processing are shown in Fig. 3.7. After band-pass filtering, the amplitudes of P wave and T wave are suppressed due to their lower-frequency characteristics. The influences of baseline wander and high frequency noise are reduced. The main parts of the frequency response of QRS complexes are located in the main frequency band of the band pass filter; thus the QRS complexes are specially highlighted. In order to elevate the relative intensity of QRS complexes further, electrocardiographic signals are processed with differentiating and squaring to eliminate the influences of P wave and T wave on R wave. Then the signals dealt with the programs mentioned above are calculated with moving window integration so that each QRS complex corresponds to a signal peak. After using proper threshold detection, the correct position of the peak of R wave can be found. The detail explanations will be described as following.

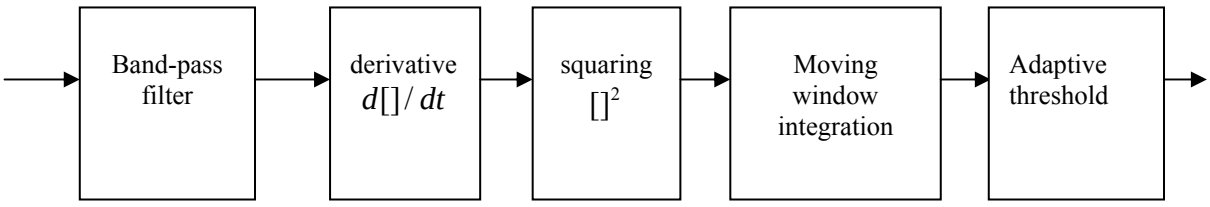

Fig. 3.6 Tompkins QRS detection algorithm

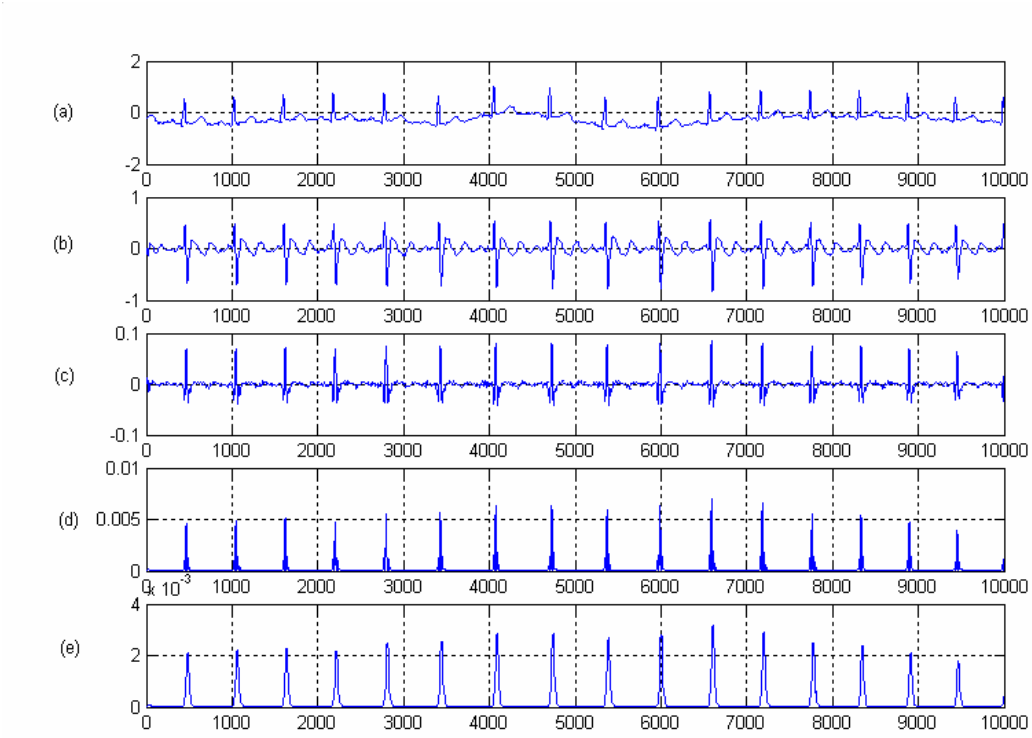

Fig 3.7 Flow chart of R wave detection algorithm (a) Original signal (b) Output of band-pass filter (c) Output of differentiator (d) Output after squaring (e) Result after moving window-integration

(1) Bandpass Filter

The bandpass filter reduces the influence of muscle noise, 60 Hz interference, baseline wander, and T-wave interference. The desirable passband which maximizes the QRS energy is approximately 5-15 Hz. This class of filters having poles and zeros only on the unit circle permits limited passband design flexibility. Due to the sampling rate, we could not design a bandpass filter directly for the desired passband of 5-15 Hz using this specialized design technique. Therefore, we cascaded the low-pass and high-pass filters described below to achieve a 3 dB passband about 5-12 Hz, which reasonably close to the design goal. Fig 3.8 shows the result of the ECG signal with high frequency noise and baseline wander after passing through the bandpass filter.

Low-Pass Filter

The transfer function of the second-order low-pass filter is:

$$H(z) = \frac{(1 - z^{-6})^2}{(1 - z^{-1})^2} \tag{3.1}$$

High-Pass Filter

The design of the high-pass filter is based on subtracting the output of a first-order low-pass filter from an all-pass filter. The transfer function for such a high-pass filter is:

$$H(z) = \frac{(1 + 32z^{-16} + z^{-32})}{(1 + z^{-1})} \tag{3.2}$$

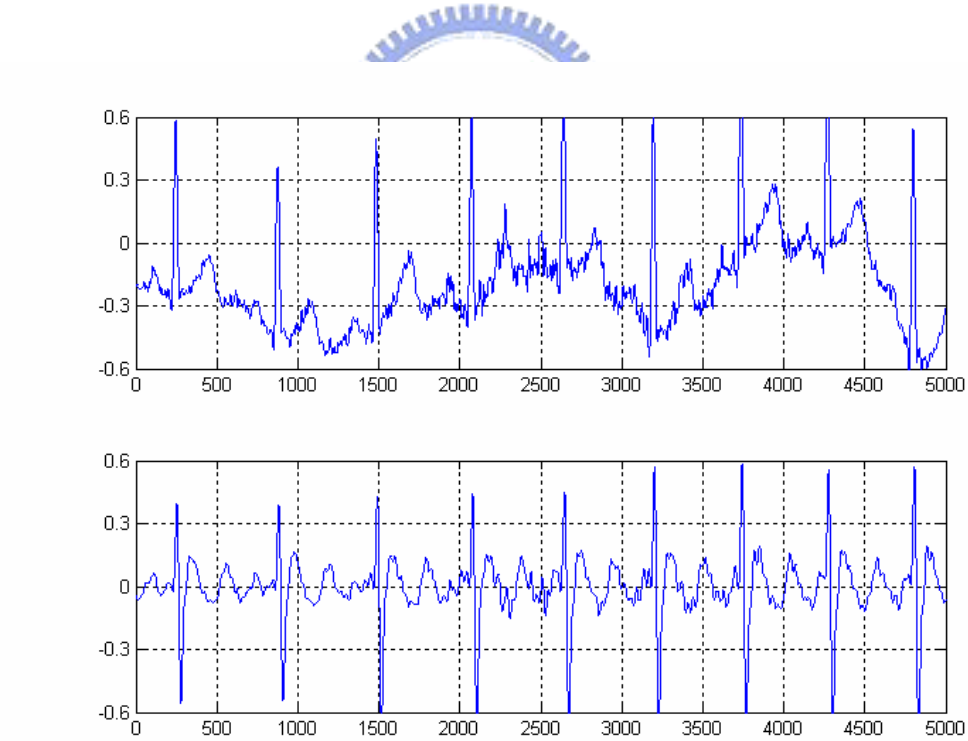

Fig 3.8(a) ECG signal with baseline wandering and high frequency noise interference (b) The same ECG signal after bandpass filter

(2) Derivative

After filtering, the signal is differentiated to provide the QRS-complex slope information. We use a five-point derivative with the transfer function:

$$H(z) = (1/8)(-1 - 2z^{-1} + 2z^{-3} + z^{-4}) \tag{3.3}$$

(3) Squaring Function

After differentiation, the signal is squared point by point. The equation of this operation is:

$$y(n) = [x(n)]^2 \tag{3.4}$$

This makes all data points positive and does nonlinear amplification of the output of the derivative emphasizing the higher frequencies.

(4) Moving-Window Integration

The purpose of moving-window integration is to obtain waveform feature information about both the slope and the width of the QRS complex. In this research, the window is 24 samples wide. It is calculated from:

$$y(n) = (1/24)[x(n) + x(n-1) + \ldots + x(n-23)] \tag{3.5}$$

(5) Adjusting the Thresholds

The signal after moving window integration, its positions of R waves can be detected out by setting a proper threshold. Because the amplitude of electro-cardiographic signals is different from one to another, and there even exists difference in amplitude for the same subject, thus the setting of a threshold must be adaptive so that signal won't be missed or judged incorrectly. Therefore we adopt

the adaptive threshold method for R-wave detection. The half mean value of first 3 QRS peaks is taken as the initial value,

$$\text{threshold} = (1/2)(1/3)(\text{peak1} + \text{peak2} + \text{peak3}) \tag{3.6}$$

Then the new threshold is adjusted according to the new QRS peak. Its revising criterion is by equation (3.7)

$$\text{new\_threshold} = \text{new\_value} \quad 0.5 \times 0.1 + \text{old\_threshold} \times 0.9 \tag{3.7}$$

The revising basis of new_threshold is made up of half 10% of the QRS peak detected latest, and the 90% of prior threshold so that thresholds can be compared, adjusted, and revised with the signal coming in continuously.

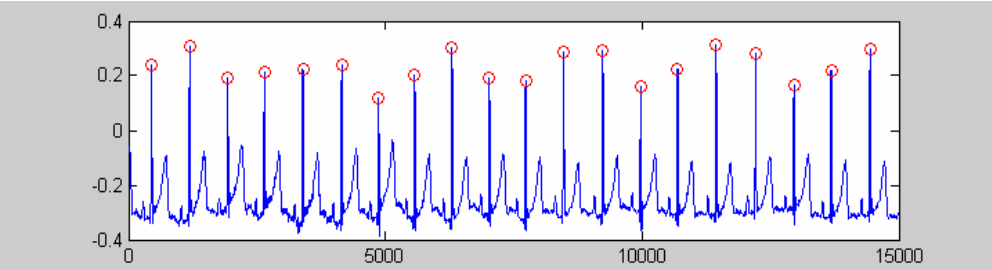

Fig. 3.9 Result of R wave Detection

3.2.2 Eliminating ectopic beats

To avoid ectopic beat such as PAC (premature atria contractions as shown in Fig 3-10(a)) and PVC (premature ventricular contractions as shown in Fig 3-10(b)),which will affect the normal heart rate spectrum analysis, we need to eliminate unreasonable ECG signals before calculating heart rate. Generally, ectopic heartbeat means that premature contraction of heart causes shorter heartbeat duration. Due to the compensatory effect, next heartbeat duration will be longer than normal interval. As shown in Fig 3-11(a), the sum of the successive RR intervals is smaller than two times of the normal RR interval (RR1+RR4>RR2+RR3). It is very important to deal with ectopic heartbeat during the period from recognizing R wave

position to calculating RR interval because even small amounts of ectopic heartbeat will have a negative influence on heart rate variability indexes of short term or long term recordings.

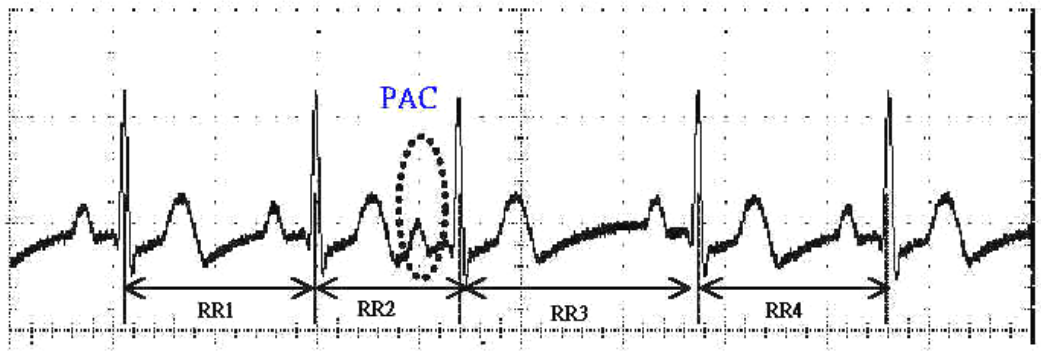

(a)

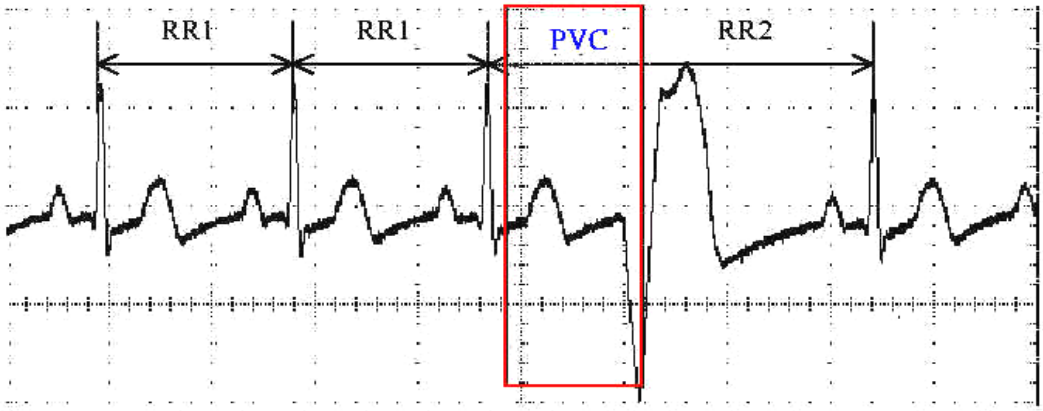

(b)

Fig.3.10 (a) premature atria contraction (PAC)
(b) premature ventricular contraction (PVC)

The revising way of ectopic beat is to exclude the point where ectopic heartbeat happened. Then the duration is picked up from the last R wave peak to the next one, and choose the middle point of this duration as the new position of R wave peak shown in Fig 3-11(b). In the figure, R2 is ectopic beat (RR1 is much smaller than the average, and RR2 is opposite). According to the way mentioned above, R2 is excluded, and a new point Rn is inserted in the middle between R1 and R3. Then the interval between R1 and Rn becomes (1/2)(RR1+RR2).

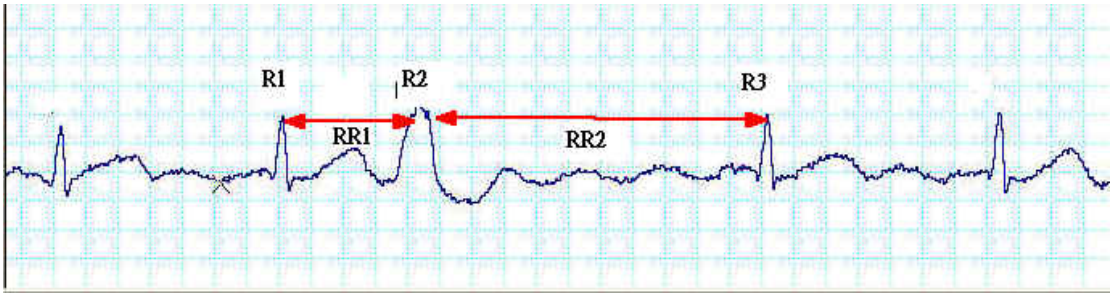

(a)

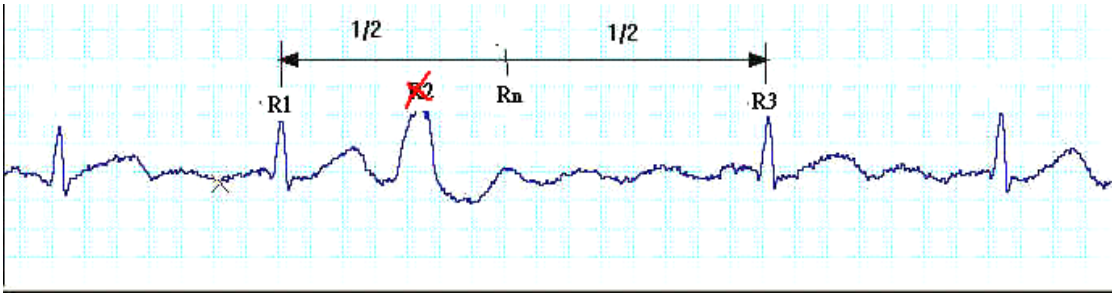

(b)

Fig.3-11(a) Abnormal ECG signal (b) Modification of ectopic heartbeat

3.2.3 Heart rate calculating

When the position of the R wave peak is detected precisely, the time interval of successive R waves represents heartbeat period. The time series made up of every RR interval is called HRV signal shown in Fig 3.12. Because RR interval is different from one to another, thus, this signal is unequal sampled. However, the objects analyzed by digital signal processing are generally equal-sampled signals. Therefore this signal must be transformed to equal-sampled signal before using general digital signal processing methods.

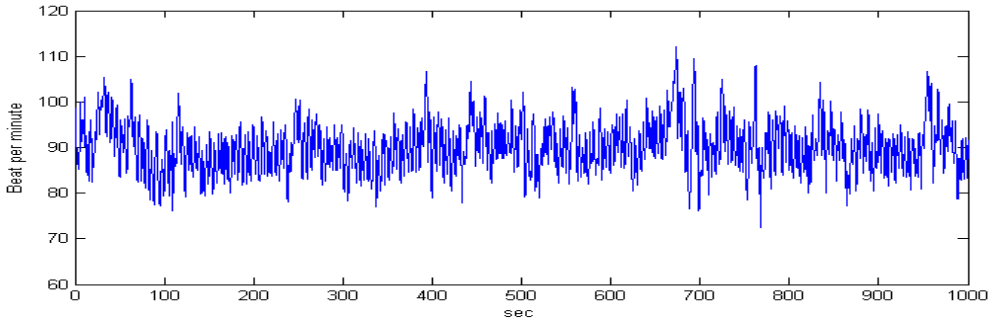

Fig.3.12 HRV signal

In this research, we adopt window interpolations, which Berger used in 1986 to calculate HRV by equal sampling [3]. We first found out all RR intervals, and then decided the re-sampling frequency. The equation (3.8) represents the heart rate after re-sampling.

$$r_i = f_r \times \frac{n_i}{2} \tag{3.8}$$

r_i is the heart rate at the *i*th resample point, f_r is re-sampling frequency, and n_i is the number of RR intervals that fell in the local window centered at the *i*th resample point. If re-sampling frequency is 5Hz, and original sampling frequency is 1000 Hz, there exists a new signal point separated by 200 sample points. Next we must get n_i, the number of RR intervals that fell in the local window centered at every resample point. There are 2 conditions to decide n_i. As shown in Fig 3.13(a), if the sampling interval before the sample point and the one after the sample point are distributed in the same RR interval (I_2), then n_i is a/ I_2. a is 2 sampling intervals ,that is, local window, and I_2 is the second RR interval in Fig3.13(b). If the sampling interval before the sample point and the one after the sample point are distributed in different RR intervals, then n_i should be decided by both of the RR intervals. Thus n_i is b/I_3+c/I_4. b and c are the time of sampling intervals distributed in 2 different RR intervals respectively. We make use of the methods mentioned above to calculate all the values of n_i, and bring them into equation 3.8 so that the equal-sampled HRV can be obtained.

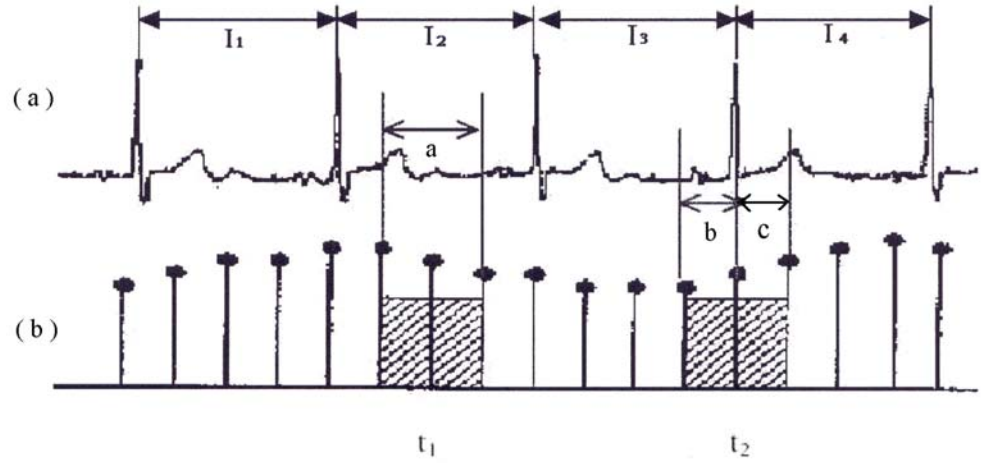

Fig. 3.13 Heart rate signal after equal sampling (a) a section of RR intervals (b) heart rate signal after equal sampling, when the center point of the local window falling at t1, $n_i = a/I_2$, at t2 $n_i = b/I_3 + c/I_4$.

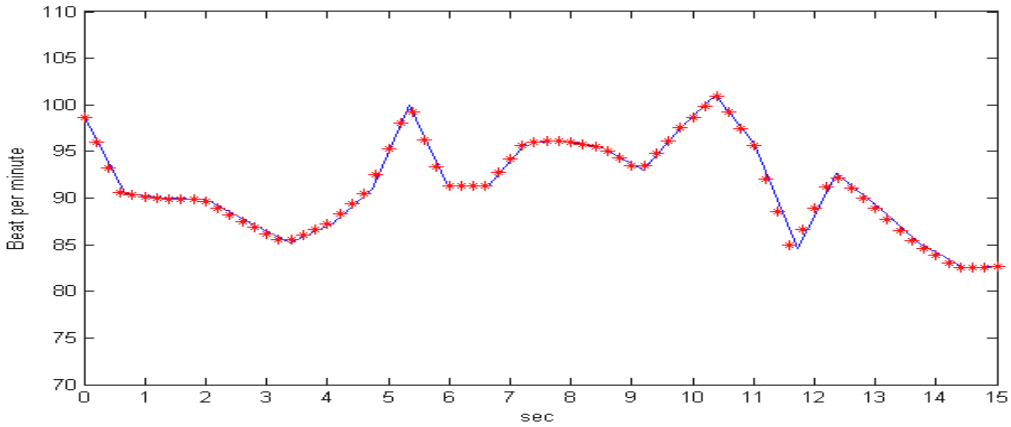

Fig. 3.14 Result after equal sampling (★ is the point after re-sampling)

3.2.4 Heart rate variability analysis methods

The heart rate variability will be analyzed in time and frequency domain. The spectrum of HRV needs to be analyzed to distinguish the action of sympathetic from that of parasympathetic. Then the correlation between the characteristics of HRV and the action of autonomic nervous system also needs to be examined. Therefore, we transform the HRV signal from time domain to frequency domain by Fast Fourier Transform and find out the power spectrum so that we can observe the modulation of sympathetic and parasympathetic from the power spectrum of HRV.

According to the meaning of HRV and many kinds of measurement standardized proposed by the European Society of Cardiology and the North American Society of Pacing and Electrophysiology in 1996, some common analytic parameters in time and frequency domain will be introduced [11]. In these methods, the ECG signal records are classified into 2 kinds: short-term 5 minutes record and long-term 24 hours record.

1. Time domain analysis

For HRV in time domain analysis, the major analytic parameter is the mean and standard deviation of HRV for 5 minutes. They can be calculated by statistical methods. Time domain analysis is to detect each QRS complex interval in continuous ECG, and define it as RR interval (RRI). Table 3.1 lists the variables and measurement of the statistical methods in time domain. In the list, SDANN is proposed to do long-term 24 hours analysis. However, the methods of short-term analysis and those of long-term analysis can't substitute each other, and they are adopted depending on the need of research. For HRV of short time 5 minutes, SDRR and RMSSD have better statistical meaning than pNN50 and NN50 do. Because this research is not a 24-hour record, SDRR and RMSSD are taken as reference indexes.

Table 3.1 Time domain parameters of HRV (*variables are the parameters adopted in this research)

Variable	Unit	Description
MRR*	s	Mean of RR intervals
SDRR*	ms	Standard deviation of all the RR intervals
SDANN	ms	Standard deviation of the mean values of all 5 minutes RR intervals in the whole record
RMSSD*	ms	Root-Mean-Square values of the differences of all the successive RR intervals
NN50 count	ms	Counts of the differences which are larger than 50 ms in all the RR intervals
PNN50	%	Percentages of NN 50 count in all RR intervals

2. Frequency domain analysis

Frequency analysis of HRV is to do FFT on the RR intervals after equal sampling. As shown in Fig 3.15, the area under the power spectrum curve can express the power of frequency response. The total areas under the curve are total power. The area under each frequency band can express the power of that frequency band, so the response power in the very low frequency band is called very low frequency power (VLF); the response power in the low frequency band is called low frequency power (LFP); the response power in the high frequency band is called high frequency power (HFP). The magnitude of high frequency power can be seen as the index of parasympathetic activation. The magnitude of low frequency power can be seen as the index of co-mediation of both sympathetic and parasympathetic, and the ratio of high frequency power to low frequency one can be regarded as the index of activation balance of parasympathetic to sympathetic.

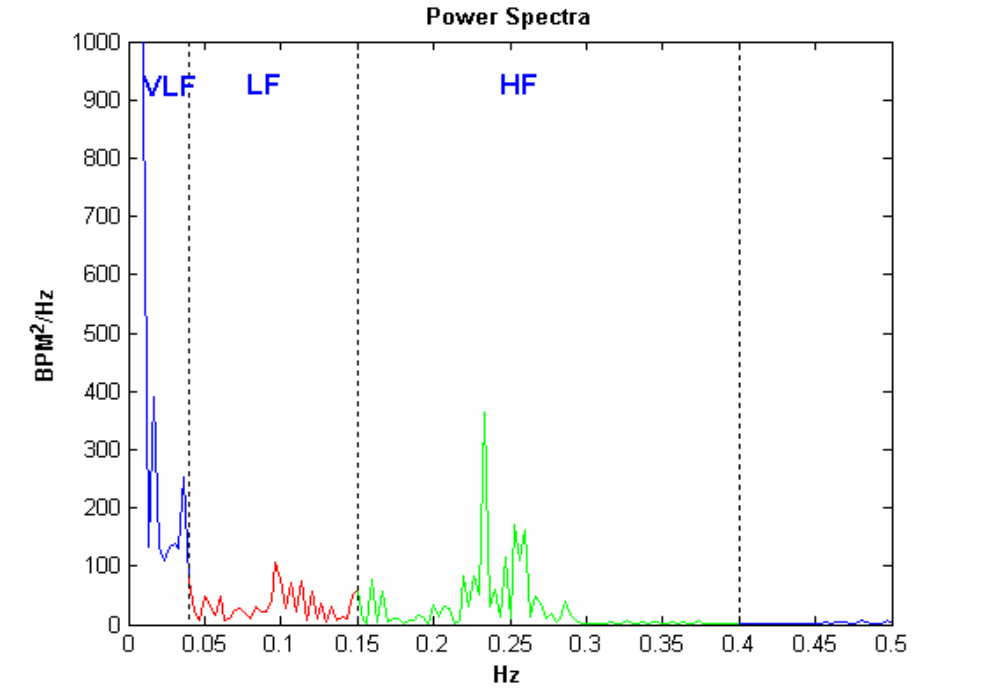

Fig. 3.15 Power spectrum of HRV

The spectrum components for short-term recording can be separated into 3 parts: VLF, LF, and HF. The power distribution and the center frequency of LF and HF are not fixed, but they may be affected by the modulation of autonomic nerves. The physiological meaning of VLF is seldom defined. The power of VLF, LF, and HF are usually calculated by absolute value (BPM^2/Hz). LFP and HFP can be also expressed as normalized unit as shown in equation (3.9).

$$LF(orHF)n.u = \frac{LF(HF)power}{Totalpower - VLFpower} \times 100\% \quad (3.9)$$

The normalized power of LF and HF expresses the mechanism behavior of control and balance of sympathetic and parasympathetic, and it may be seen as the relative value of evaluating LF(HF) power to total power. To describe the distribution of power spectrum completely, both absolute value and normalized value need to be calculated for comparing as shown in table 3.2. The magnitude of the power spectrum of VLF, LF, and HF bands, and the percentage occupied by them can show the mutual action of sympathetic and parasympathetic.

Table 3.2 Frequency domain parameters of HRV

Variable	Unit	Description
VLF	Bpm^2	Power in VLF range
LF	Bpm^2	Power in LF range
LF norm	Nu	LF power in normalized units LF/(total power - VLF)×100
HF	Bpm^2	Power in HF range
HF norm	Nu	HF power in normalized units HF/(total power - VLF)×100
LF/HF		Ratio of LF/HF

3.3 Analysis of Poincare scattering plot

In this section, we will discuss how to make use of geometrical methods to observe heart rate variability. The method adopted is Poincare plot, which originally is a noun applied in astronomy, and it is a 2 dimensional scattering plot composed of current cardiac cycle length (the RR interval on the ECG) against the preceding RR interval. It reflects the variation of successive RR intervals, and it is a scattering plot marking the data positions of all the successive RR intervals in rectangular coordinate system. Poincare plot may not only show the whole features of HRV, but also visually display the instant variations of interbeat. Thus Poincare plot reveals the nonlinear characteristics of HRV [4,10].

◆Methods for constructing and analyzing the Poincare scattering plot

1. The drawing principle of Poincare scattering plot

By utilizing the suitable quantity of the RR intervals of the successive heartbeats, we set the first RRI as the abscissa value and the second RRI as the ordinate value of the first heart beat point. Then the second RRI is set as the abscissa value and the third RRI is set as the ordinate value of the second heart beat point. Then following in this order, abscissa is the collection of RR[n], and ordinate is the collection of RR[n+1]. Then after all heart beat points in some period are determined, Poincare scattering plot can be composed.

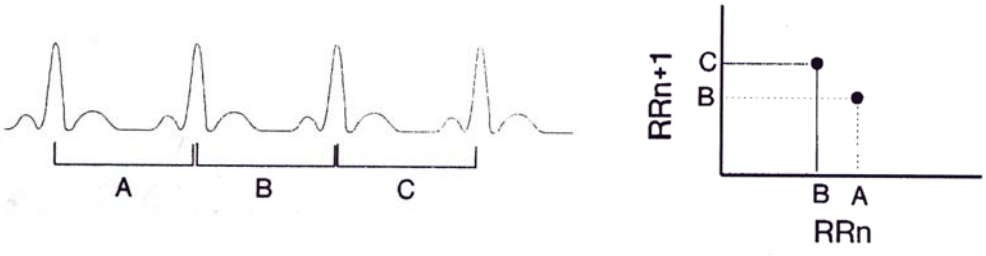

Fig. 3.16 Construction of the Poincare scattering plot

2. The analysis of typical patterns of Poincare scatter plot

The magnitude and regularity of HRV can be estimated from the area and shape of Poincare scatter plot. Generally speaking, according to the differences of the length distribution of RR intervals, Poincare plot can be classified by visual assessment into 4 typical patterns.

1) Comet shape

Figure 3.17 shows that RR intervals are located in the area of 500~1000 ms of 2 axes. Near the origin of the rectangular coordinate, the tail end is expanded symmetrically along the line of identity (slope=1) from the narrow bottom. The head end gets wider gradually, and the plot forms a unique comet pattern with big head and small tail. The scattering points most gather around the line of unitary slope passing through the origin. It expresses that the successive RR intervals are probably equal for normal people. The markings spreading around the angle of 45^{o} presents the phenomenon of sinus arrhythmia. In figure 3.17, on the upper part of scattering plot, due to the slow heart rate, RR intervals are getting longer. It presents the serious extent of sinus arrhythmia. However, on the lower part of scattering plot, scattering plot is getting narrow gradually. It explains that when heart beats are increasing, sinus arrhythmia is going to a small extent. The length of the scatter plot along the direction of the angle of 45^{o} represents the variation of the average heart rate. If the length is shorter, it represents that the variation of the average heart rate is small during the analysis period. The length of the line, along which scattering points spread, perpendicular to the line of identity represents the magnitude of the sharp variance of RR intervals. Generally speaking, the heavy density core of the scattering plot explains that successive RR intervals are nearly identical. It reflects the activation of sympathetic. The thin density part of the scattering plot represents that the differences of successive RR intervals are large. It reflects the activation of

parasympathetic [4].

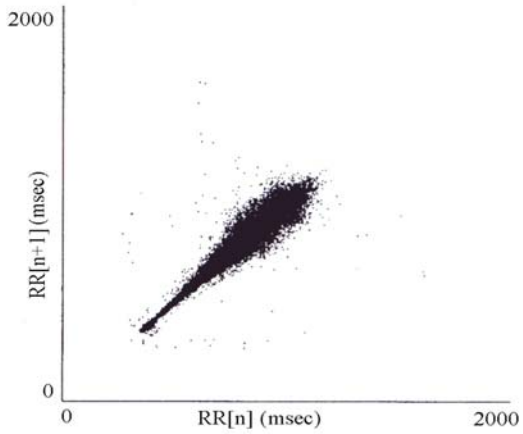

Fig. 3.17 Comet shape

2) Torpedo shape

Figure 3.18 expresses a short torpedo-shaped scattering plot. For any R-R interval, the next R-R interval is likely to deviate only minimally. However, this minimal deviation does not indicate a fixed heart rate but is suggestive of a heart rate pattern that changes gradually, yet maintained small beat-to-beat R-R variability. This figure explains that the sympathetic action is stronger, and the proportion of the parasympathetic action is less.

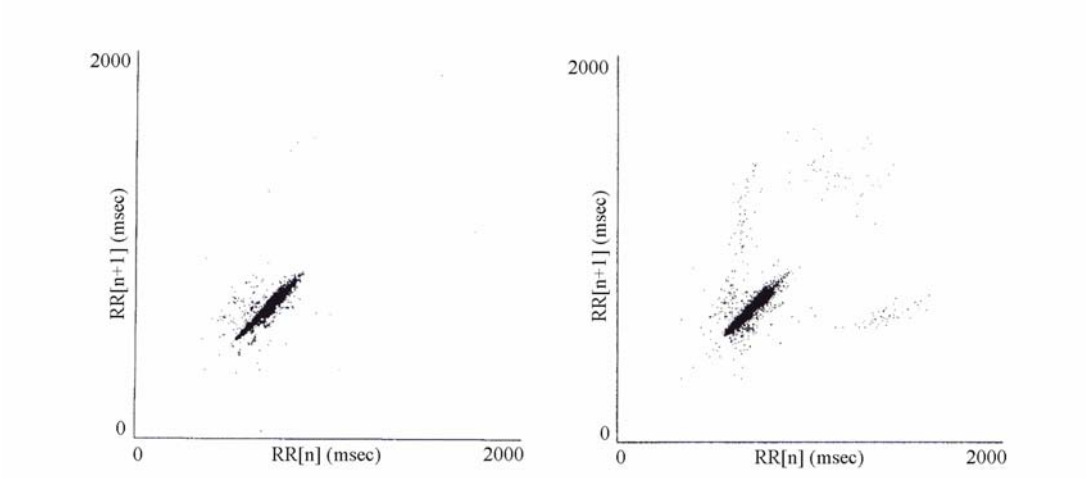

Figure 3.18 Torpedo shape

3) Fan shape

Figure 3.19 shows that points radiate in a relatively symmetric manner from a narrow base at the lower RR intervals. In the fan-shaped patterns, the overall range

of RR intervals is diminished, but the beat-to-beat RR interval dispersion is greater than that in comet-shaped patterns. The fan-shaped patterns have small increases in RR interval length that are associated with greater subsequent RR interval dispersion over a much shorter overall range.

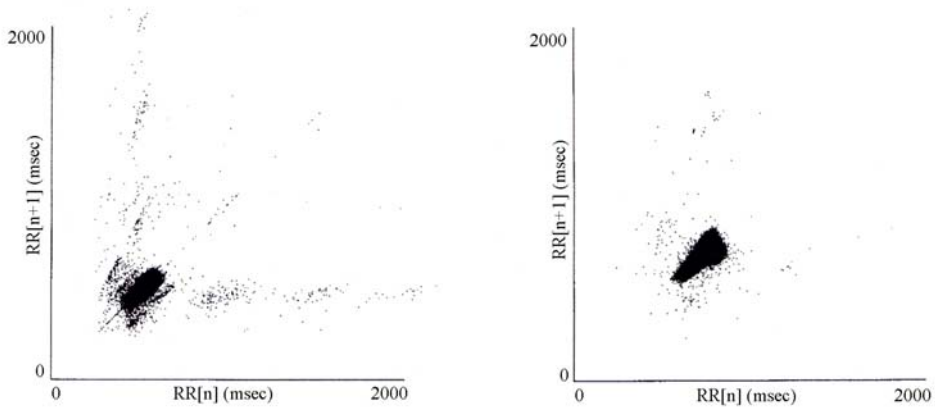

Figure 3.19 Fan shape

4) Complex shape

Figure 3.20 shows that the complex-shaped patterns are composed of several clusters of RR intervals. The complex patterns lacked the graded relationship between successive RR intervals found in the comet-shaped formation. Instead, the complex configurations exhibited discrete stepwise clusters of points with distinct gaps between the clusters. The complex patterns may result from stepwise changes in RR intervals.

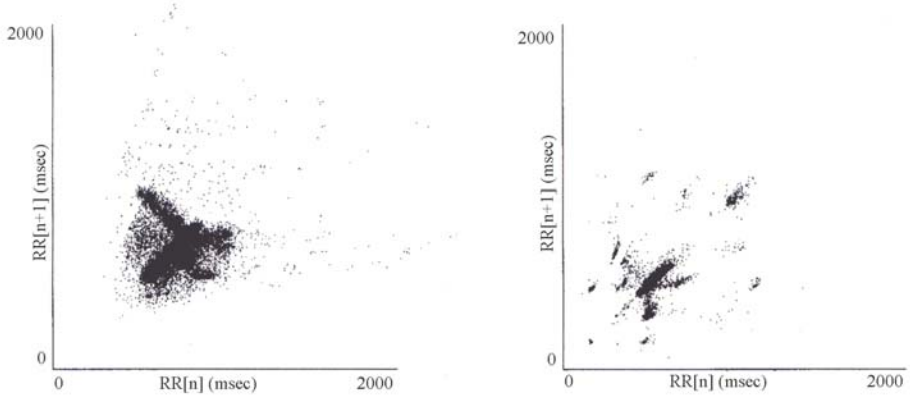

Figure 3.20 Complex shape

3. The quantitative analysis of Poincare scatter plot

Quantitative analysis entails fitting an ellipse to the scatter plot, with its center coinciding with the center point of the markings. The center point of the markings is at (RR_{aver},RR_{aver}),where RR_{aver} is the average RR-interval length for the tachogram. The longest length of the line which passes through the center point along the line of identity is defined as the length of the Poincare cloud, that is SD1. It stands for the level of long-term HRV. The longest length of the line which passes through the center point perpendicular to the line of identity is defined as the width of the Poincare cloud, that is SD2. It indicates the level of short-term HRV [15].

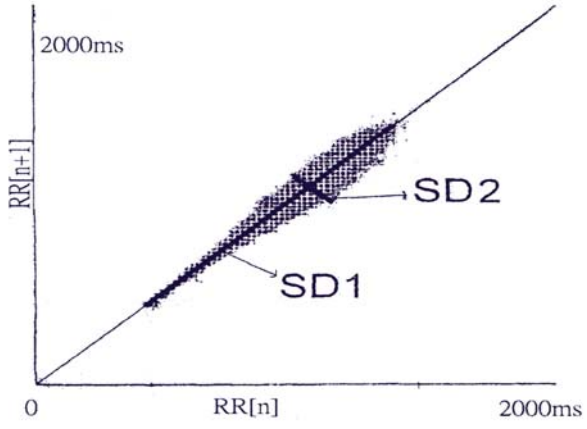

Fig. 3.21 On the poincare plot, long-axis length is SD1 short-axis length is SD2

4. Mathematical relation of HRV indexes between Poincare plot and time domain [5]

I. Time domain indices

The standard time domain measures of HRV are mentioned here again. Here the time-course of the RR intervals is denoted by RR_n. The standard deviation of the RR intervals, denoted by SDRR, is often employed as a measure of overall HRV. It is defined as the square root of the variance of the RR intervals

$$SDRR = \sqrt{E[RR_n^2] - \overline{RR}^2} \tag{3.10}$$

where the mean RR interval is denoted by $\overline{RR} = E[RR_n]$.

The standard deviation of the successive differences of the RR intervals, denoted by SDSD, is an important measure of short-term HRV. It is defined as the square root of the variance of the sequence $\triangle RR_n = RR_n - RR_{n+1}$(the delta-RR intervals).

$$SDSD = \sqrt{E[\Delta RR_n^2] - \overline{\Delta RR}_n^2} \tag{3.11}$$

Note that $\overline{\Delta RR_n} = E[RR_n] - E[RR_{n+1}] = 0$ for wide-sense stationary intervals. This means RMSSD is statistically equivalent to SDSD.

$$SDSD = RMSSD = \sqrt{E[(RR_n - RR_{n+1})^2]} \tag{3.12}$$

The Fourier transform of the autocorrelation function is the power spectrum of RR intervals. The autocorrelation function of the RR intervals is defined as

$$\gamma_{RR}(m) = E[RR_n RR_{n+m}] \tag{3.13}$$

Spectral analysis is normally performed on the mean-removed RR intervals and, therefore, the mean-removed autocorrelation function, called the auto-covariance function is often preferred

$$\phi_{RR}(m) = E[(RR_n - \overline{RR})(RR_{n+m} - \overline{RR})] \tag{3.14}$$

For stationary RR intervals, the auto-covariance function is related to the autocorrelation function, as right $\phi_{RR}(m) = \gamma(m) - \overline{RR}^2$.

The auto-covariance function is related to the variance of the RR intervals as $SDRR^2 = \phi_{RR}(0)$, and the mean square of the successive differences, $RMSSD^2 = 2(\gamma_{RR}(0) - \gamma_{RR}(1)) = 2(\phi_{RR}(0) - \phi_{RR}(1))$.

II. Poincare plot descriptors

To characterize the shape of the plot mathematically, most researchers have used the technique of fitting an ellipse to the plot, as Fig 3.22 shows. A set of axis is oriented with the line-of-identity. The axis of the Poincare plot are related to the new set of axis by a rotation of $\theta = \pi/4$ radian.

$$\begin{bmatrix} x_2 \\ x_1 \end{bmatrix} = \begin{bmatrix} \cos\theta & -\sin\theta \\ \sin\theta & \cos\theta \end{bmatrix} \begin{bmatrix} RR_n \\ RR_{n+1} \end{bmatrix} \tag{3.15}$$

In the reference system of the new axis, the dispersion of the points around the x_1 axis is measured by the standard deviation denoted by SD1. SD2 is the standard deviation around the x_2 axis. They are related to the time domain indices in the following manner:

$$SD2^2 = Var(x_2) = Var(\frac{1}{\sqrt{2}} RR_n - \frac{1}{\sqrt{2}} RR_{n+1})$$

$$= \frac{1}{2} Var(RR_n - RR_{n+1}) = \frac{1}{2} SDSD^2 = \frac{1}{2} RMSSD^2 \tag{3.16}$$

Thus, the SD2 measure of Poincare width is equivalent to the root-mean square of successive differences of RR intervals, except that it is scaled by $1/\sqrt{2}$. This means that we can relate SD2 to the auto-covariance function

$$SD2^2 = \phi_{\mathrm{RR}}(0) - \phi_{\mathrm{RR}}(1) \tag{3.17}$$

With a similar argument, it may be shown that the length of the Poincare cloud is related to the auto-covariance function

$$SD1^2 = \phi_{\mathrm{RR}}(0) + \phi_{\mathrm{RR}}(1) \tag{3.18}$$

By adding (3.17) and (3.18) together, we obtain the result

$$SD1^2 + SD2^2 = 2\phi_{RR}(0) = 2SDRR^2 \tag{3.19}$$

Finally

$$SD1^2 = 2SDRR^2 - 1/2\, RMSSD^2 \tag{3.20}$$

Equation (3.20) allows us to interpret SD1 in terms of existing time domain indexes of HRV. Fitting an ellipse to the Poincare plot does not generate indexes that are independent of the standard time domain |HRV indexes. Actually, the width of the Poincare plot is a linear scaling of the most common statistic used to measure short-term HRV, the RMSSD index. Therefore we won't discuss the analysis result of Poincare plot in chapter 4.

3.4 Pattern Recognition based on Fuzzy *c*-Means Algorithm

Consider a finite set of elements $X=\{x_1, x_2,\ldots, x_m\}$ as being elements of the n-dimensional Euclidean space $\mathbf{R}^n$, that is, $x_j \in \mathbf{R}^n$, j=1,2,…,m. The problem is to perform a partition of this collection of elements into *c* fuzzy sets with respect to a given criterion, where c is a given number of clusters. The criterion is usually to optimize an objective function that acts as a performance index of clustering. The end result of fuzzy clustering can be expressed by a membership matrix U such that

$$U=[u_{ij}]_{i=1\ldots c,\ j=1\ldots m} \tag{3.21}$$

where u_{ij} is a numerical value in [0,1] and expresses the degree to which the element x_j belongs to the *i*th cluster. However, there are two additional constraints on the value of u_{ij}. First, a total membership of the element $x_j X$ in all classes is equal to 1; that is,

$$\sum_{i=1}^{c} u_{ij} = 1 \qquad \text{for all } j=1,2,\ldots,m. \tag{3.22}$$

Second, every constructed cluster is nonempty and different from the entire set; that is

$$0 < \sum_{j=1}^{m} u_{ij} < m \qquad \text{for all } i=1,2,\ldots,c. \tag{3.23}$$

One of the widely used clustering methods is the fuzzy c-means(FCM) algorithm developed by Bezdek[1981]. This objective function of the FCM algorithm takes the form of

$$J(u_{ij}, v_i) = \sum_{i=1}^{c}\sum_{j=1}^{m} (u_{ij})^p \left\| x_j - v_i \right\|^2, \qquad p>1, \tag{3.24}$$

where *p* is called the exponential weight which influences the degree of fuzziness of the membership matrix.

With the above background, fuzzy clustering can be precisely formulated as an optimization problem:

Minimize $J(u_{ij}, v_i)$, $i=1,2,\ldots,c;\ j=1,2,\ldots,m$

subject to Eqs. (3.22) and (3.23).

To solve this minimization problem, we first differentiate the objective function in Eq. (3.24) with respect to v_i (for fixed u_{ij}, i=1,2,…,c, j=1,2,…,m) and to u_{ij} (for fixed v_i, i=1,2,…,c) and apply the conditions of Eq. (3.22), obtaining

$$v_i = \frac{1}{\sum_{j=1}^{m}(u_{ij})^p} \sum_{j=1}^{m}(u_{ij})^p x_j, \qquad i=1,2,\ldots,c \tag{3.25}$$

$$u_{ij} = \frac{(1/\|x_j - v_i\|^2)^{1/(p-1)}}{\sum_{k=1}^{c}(1/\|x_j - v_k\|^2)^{1/(p-1)}}, \qquad i=1,2,\ldots,c; \quad j=1,2,\ldots,m. \tag{3.26}$$

The system described by Eqs. (3.25) and (3.26) cannot be solved analytically. However, the FCM algorithm provides an iterative approach to approximating the minimum of the objective function starting from a given position. This algorithm is summarized in the following block diagram.

Algorithm FCM: Fuzzy *c*-Means Algorithm

Step1:

Select a number of clusters c(1<c<m) and exponential weight p (1<p<∞). Choose an initial partition matrix $U^{(0)}$ and a termination criterion ε. Set the iteration index l to 0.

Step2:

Calculate the fuzzy cluster centers $\{v_i^{(l)} \mid i=1,2,...,c\}$ by using $U^{(l)}$ and Eq.(3.25).

Step3:

Calculate the new membership matrix $U^{(l+1)}$ by using $\{v_i^{(l)} \mid i=1,2,...,c\}$ and Eq.(3.26).

Step4:

Calculate $\Delta=\|U^{(l+1)}-U^{(l)}\| = \max_{i,j} |u_{ij}^{(l+1)} - u_{ij}^{(l)}|$. If $\Delta>\varepsilon$, then set $l=l+1$ and goto step 2. If $\Delta \leqq \varepsilon$, then stop.

End FCM

Chapter 4

Statistical meaning and Clustering of ECG

The aim of this research is to observe the regulation of heart rate behavior and the corresponding influence of the autonomic nervous system of meditators. This goal is achieved by analyzing heart rate variability. In order to investigate the effect on the circulatory system under meditation and normal rest, we recruited some subjects who had meditation experience (the experimental group), and some healthy subjects without any meditation experience (the control group).

There involved 43 subjects in this study (Exp:25 ; Ctrl:18). We are to study if there exist statistical differences between these two groups. The parameters in time and frequency domain discussed in the previous chapter will be applied as the indexes in the statistical analysis.

However, in statistics, we can only see the vague differences between two groups. To explore the subtle variations between the experimental and control group, we will apply the Fuzzy *C*-means algorithm in this part of study.

4.1 The analysis of ECG in time domain

The analysis of experimental results in time domain is divided into two parts. The first part is the statistical analysis. The second part is the FCM analysis. The following subsections illustrate the details.

4.1.1 Statistical analysis

There involve 25 subjects (male: 17 female: 8) in the experimental group. Their meditation experiences are from one year to thirteen years. (mean: 6.9 years ; std: 3.3 years) The average age is 30±4 years. Everyone is free to take either full-lotus posture or half-lotus posture that they are used to. They sit on the chair designed for meditation. On the other hand, the 18 subjects (male:9 female:9) in the control group don't have any meditation experience. Their average age is 23±2 years. The experiment is held under the same environment, except that they sit on an armed chair.

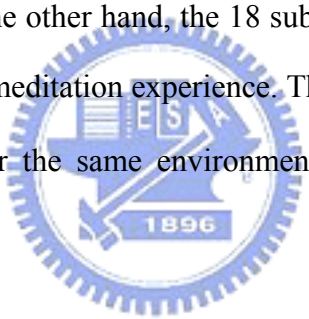

The whole experimental procedure is scheduled as Fig. 4.1. We collected five distinct sections of signal so as to interpret the effect of practicing meditation on human bodies. The first section is the five minutes before the beginning of meditation (rest). In this section, the subject needs to quiet down on the seat and takes some pre-tests such as eye open, and eye close that are instructed by the operator. Then the subjects in the experimental group will practice meditation for forty minutes continuously, while the subjects in the control group will rest for thirty minutes. The second section is the five minutes after the beginning of meditation (rest). The third one is the five minutes after the experimental subject meditates for seventeen minutes, and the five minutes after the control subject rests for twelve

minutes. The fourth one is the five minutes before the ending of meditation (rest). Finally the last one is the five minutes after the ending of meditation (rest). In this section, subjects keep the original position and take some post-tests such as mental calculation.

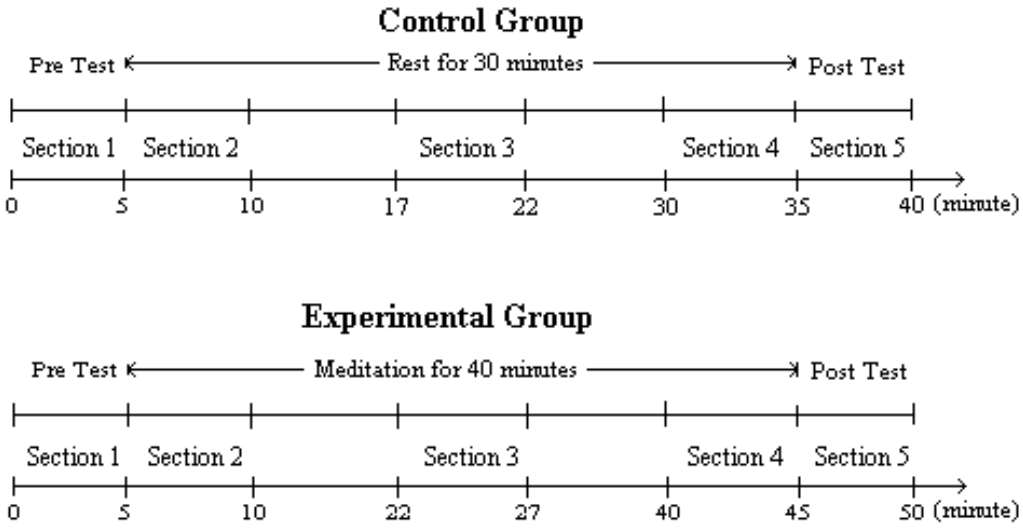

Fig. 4.1 Experimental procedure

First we discuss the mean value of heart rate (MRR). Fig. 4.2.1 shows the mean value of MRR of each group in 5 distinct sections. The MRR value of control group is larger than that of experimental group in every section. The MRR value of control group doesn't change much during the resting course, and it presents somewhat descending trend from Section4 to Section5. The MRR value of experimental group shows a falling tendency through the meditating process; yet, it rises a little from Section4 to Section5. Moreover, in Section3 and Section4, the distribution of MRR value can be distinguished statistically between 2 groups ($p<0.05$). These phenomena may indicate that meditation posture can probably speed up the heart rate, and practicing meditation for a while can make heart rate rise more. That is, meditation has the similar effect of taking slight exercise. On the other hand, resting doesn't influence heart rate.

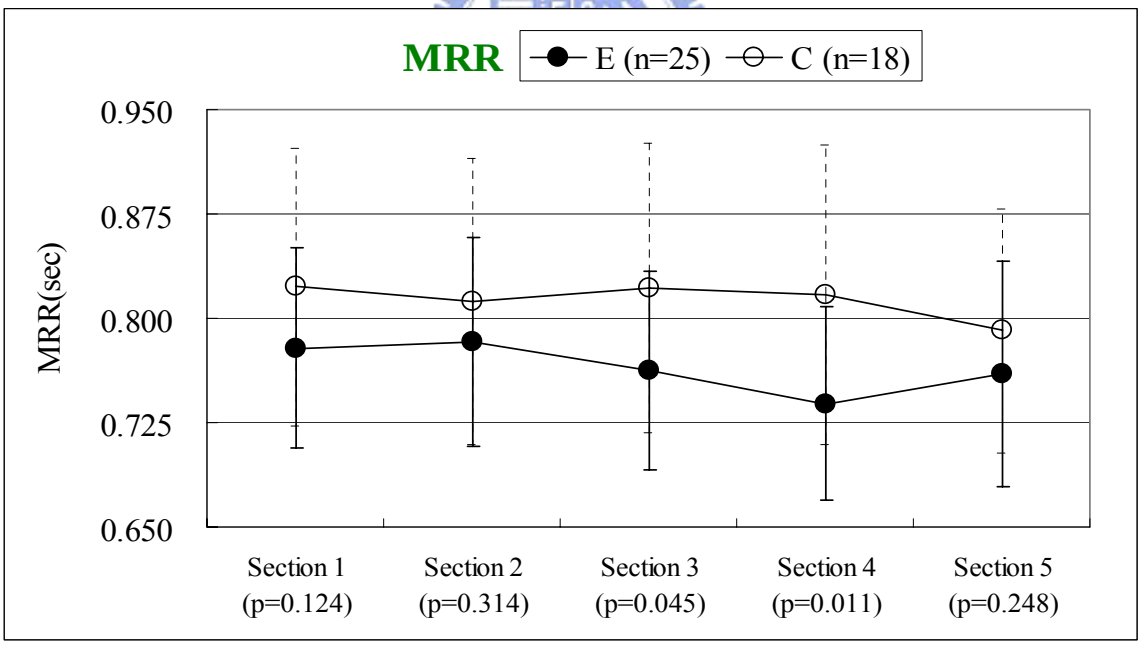

$\overline{MRR}(E)$	0.779±0.072	0.783±0.075	0.762±0.071	0.739±0.07	0.760±0.081
$\overline{MRR}(C)$	0.823±0.1	0.812±0.103	0.822±0.104	0.817±0.108	0.791±0.088

Fig. 4.2.1 Mean value of MRR (mean value of RR intervals for 5 minutes) of each group in five distinct sections (solid circle E: Experimental group; open circle C: Control group)

It is of great interest to analyze various factors like the gender and the meditation postures. The label of identification and number of subjects in each group are listed in Table 4.1

Table 4.1 Label of identification and number of subjects in each group

Group	Posture	Gender	New Group label	Number
Experiment	Full-lotus	male	E_full_male	11
Experiment	Half-lotus	male	E_half_male	6
Experiment	Full-lotus	female	E_full_female	6
Experiment	Half-lotus	female	E_half_female	2
Control		male	C_male	9
Control		female	C_female	9

Fig. 4.2.2 shows the mean value of MRR of each group in 5 distinct sections. A clear distinction between experimental and control group is that the MRR values of control group present descending tendency from Section4 to Section5, and those of experimental group show the opposite trend.

Based on the same position, heart rate of the male is faster than that of the female in experimental group, and it shows the opposite in control group. In the experimental group, we may easily find that the heart rates of the subjects who adopt full-lotus posture present increasing trend during the meditation procedure. However, little variation of the heart rates is observed in the subjects who adopt half-lotus posture. That is, better effect of exercise is expected for the subjects who take the full lotus position.

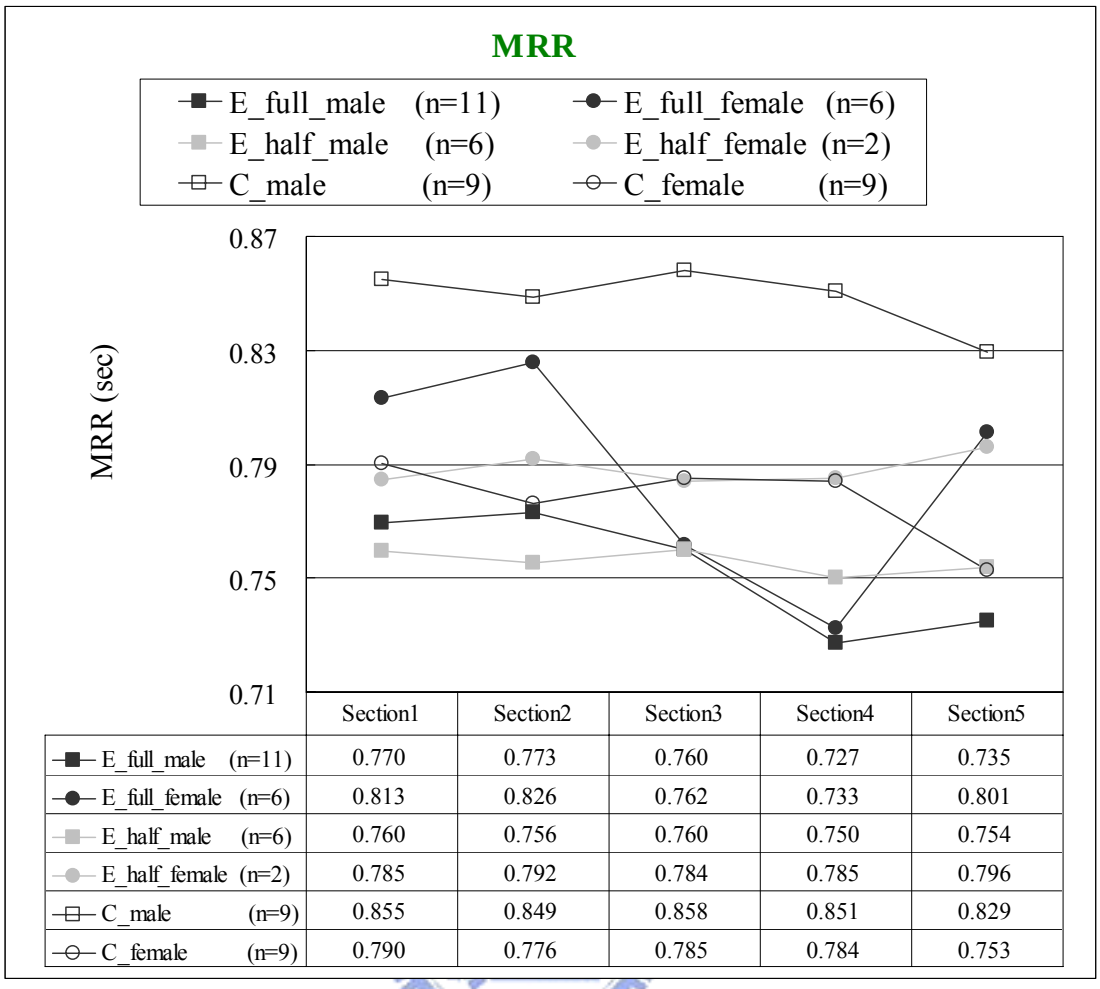

	Section1	Section2	Section3	Section4	Section5
E_full_male (n=11)	0.770	0.773	0.760	0.727	0.735
E_full_female (n=6)	0.813	0.826	0.762	0.733	0.801
E_half_male (n=6)	0.760	0.756	0.760	0.750	0.754
E_half_female (n=2)	0.785	0.792	0.784	0.785	0.796
C_male (n=9)	0.855	0.849	0.858	0.851	0.829
C_female (n=9)	0.790	0.776	0.785	0.784	0.753

Fig. 4.2.2 Mean value of MRR (mean value of RR intervals) of each group in five distinct sections

We further analyze the standard deviation of the heart rate (SDRR). Fig. 4.3.1 shows the mean value of SDRR of both the experimental and control group in 5 distinct sections. The SDRR value of control group is larger than that of experimental group in most sections. The SDRR value of experimental group doesn't change much during the meditating course. The SDRR value of control group shows a rising tendency through the resting process, and it presents somewhat descending trend from Section4 to Section5. Moreover, like the parameter, MRR, in Section3 and Section4, the distribution of SDRR value can be distinguished statistically between 2 groups ($p<0.05$). These phenomena may probably indicate

that practicing meditation can make heart rate variability lower and more stable. On the other hand, resting makes heart rate variability among subjects increase with the resting time getting longer.

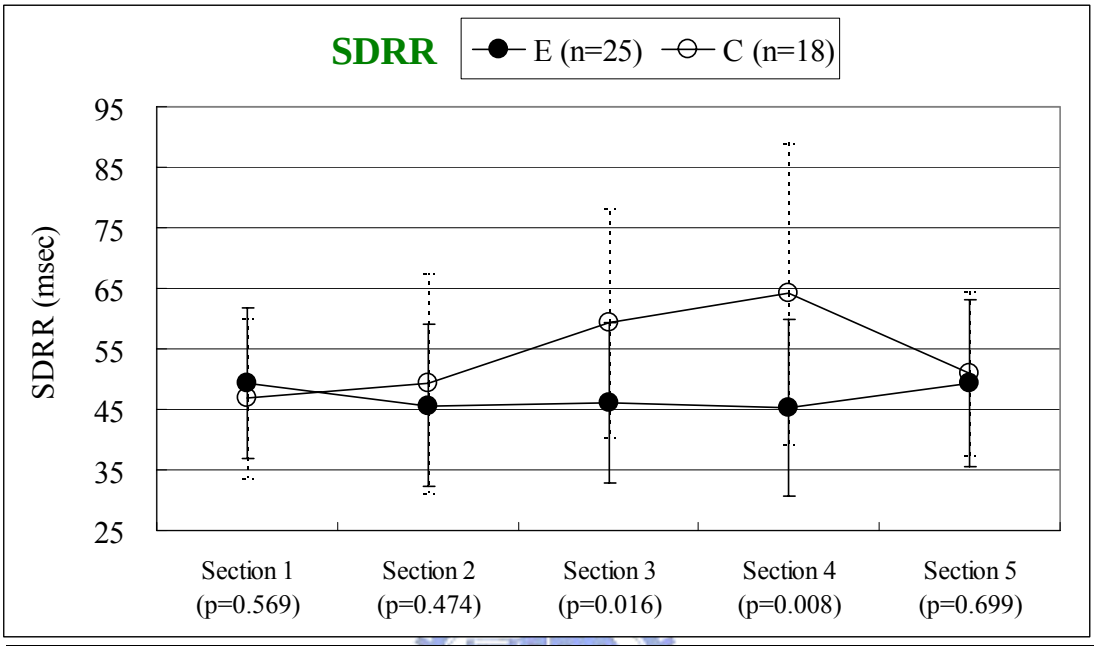

$\overline{SDRR}(E)$	49.2±12.5	45.7±13.4	46.1±13.4	45.2±14.5	49.2±13.8
$\overline{SDRR}(C)$	46.9±13.2	49.3±18.2	59.4±18.9	64.2±24.9	50.9±13.6

Fig. 4.3.1 Mean value of SDRR (standard deviation of RR intervals) of each group in five distinct sections (solid circle E: Experimental group; open circle C: Control group)

Fig. 4.3.2 shows the mean value of SDRR of the six groups defined in Table 4.1 in 5 distinct sections. A clear distinction between experimental and control group is that the SDRR values of control group present descending tendency from Section4 to Section5. Heart rate variability of the male is larger than that of the female in control group. Similarly, this phenomenon is observed in the experimental subjects adopting half-lotus posture. However, experimental subjects adopting full-lotus posture exhibit no such trend between male and female. Considering the experimental group, we may easily find that the SDRR values of the subjects who adopt full-lotus posture present decreasing trends during the meditation procedure.

However, there exist rising tendencies in the SDRR values of the subjects who adopt half-lotus posture.

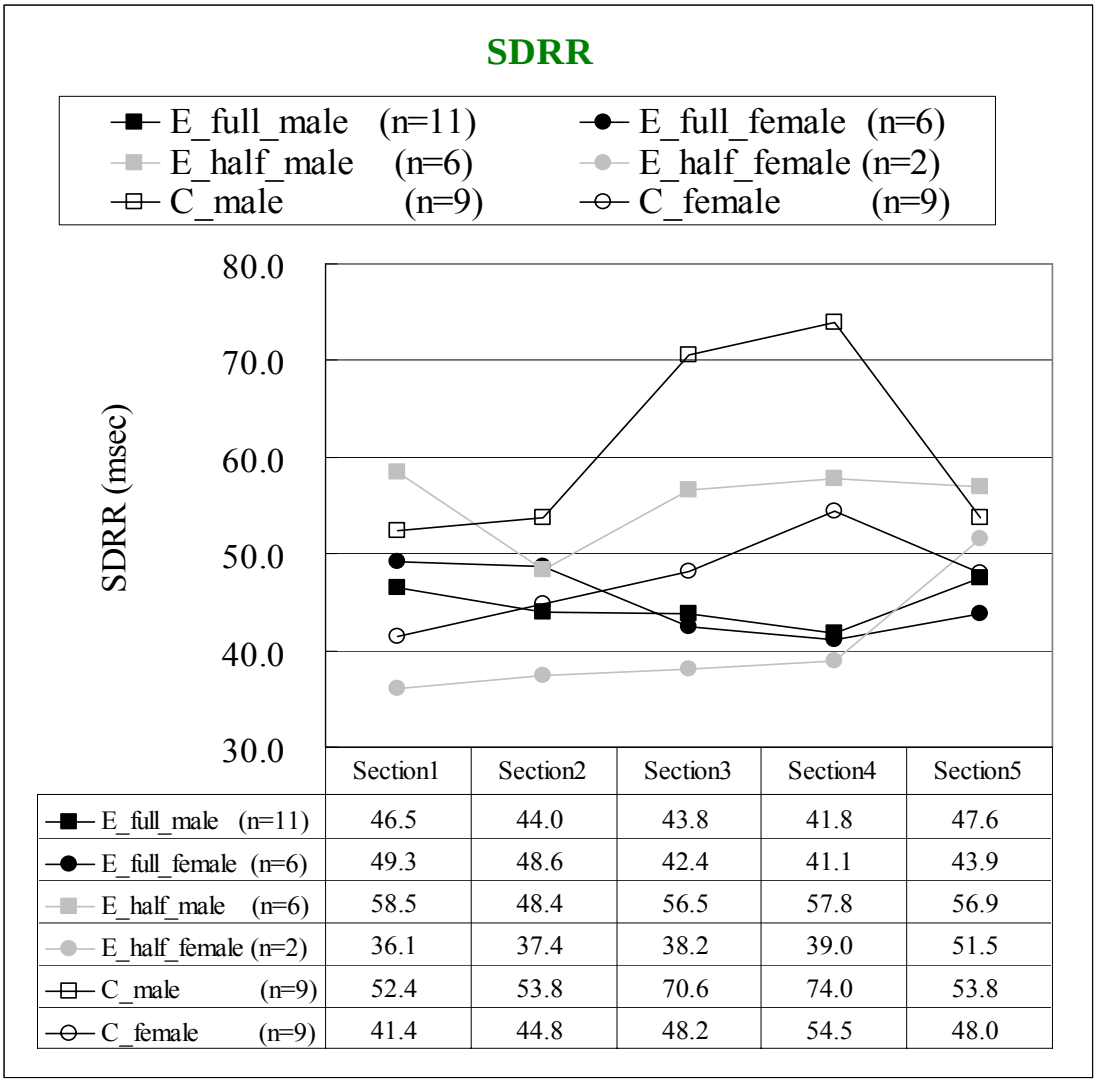

	Section1	Section2	Section3	Section4	Section5
E_full_male (n=11)	46.5	44.0	43.8	41.8	47.6
E_full_female (n=6)	49.3	48.6	42.4	41.1	43.9
E_half_male (n=6)	58.5	48.4	56.5	57.8	56.9
E_half_female (n=2)	36.1	37.4	38.2	39.0	51.5
C_male (n=9)	52.4	53.8	70.6	74.0	53.8
C_female (n=9)	41.4	44.8	48.2	54.5	48.0

Fig. 4.3.2 Mean value of SDRR (standard deviation of RR intervals) of each group in five distinct sections

The third RR parameter to be analyzed is the root mean square (rms) value of the differences of all the successive RR intervals (RMSSD). Fig. 4.4.1 shows the mean value of RMSSD of both the experimental and control group in 5 distinct sections. The RMSSD value of the experimental group is crisscrossed with that of the control group in 5 sections. The RMSSD value of the experimental group presents a falling trend during the meditating course and it shows somewhat rising trend from Section4

to Section5. The RMSSD value of control group shows ascending tendency through the resting process, and it presents somewhat descending tendency from Section4 to Section5. However, the distribution of RMSSD value can not be distinguished statistically between 2 groups ($p<0.05$) in all the sections. These phenomena may probably indicate that practicing meditation can make instantaneous heart rate variability decrease a little. On the other hand, relaxing can make instantaneous heart rate variability increase a bit.

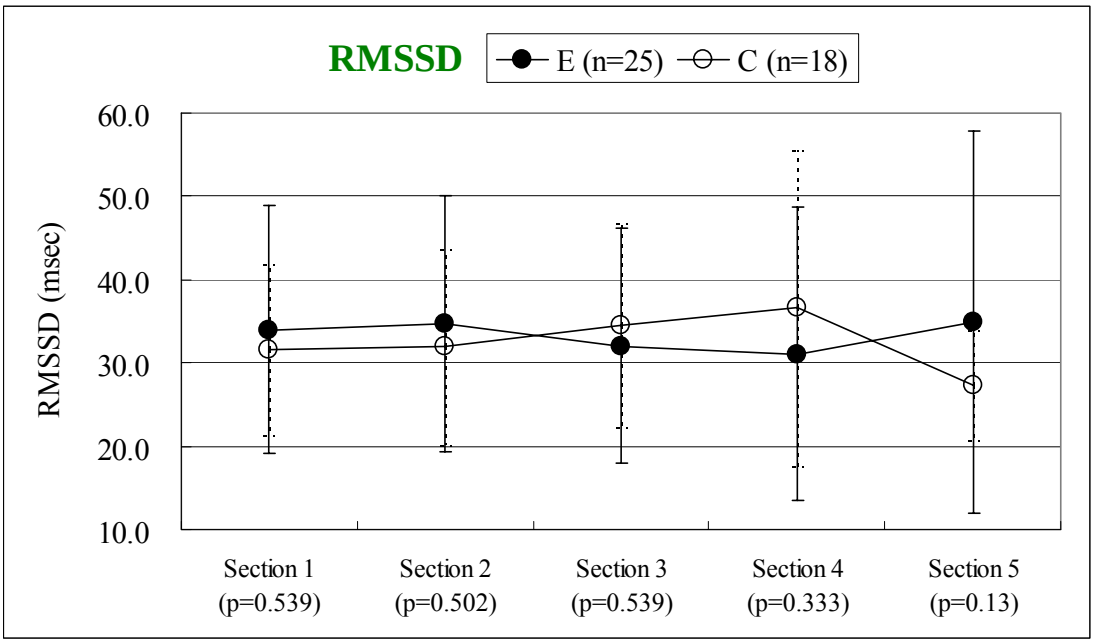

$\overline{RMSSD}(E)$	34.0±14.9	34.7±15.4	32.1±14.2	31.0±17.6	34.9±23.0
$\overline{RMSSD}(C)$	31.6±10.3	31.9±11.7	34.6±12.3	36.6±18.9	27.3±6.6

Fig. 4.4.1 Mean value of RMSSD (root mean square value of the difference of all the successive RR intervals) of each group in five distinct sections (solid circle E: Experimental group; open circle C: Control group)

Fig. 4.4.2 shows the mean value of RMSSD of the six groups defined in Table 4.1 in 5 distinct sections. A clear distinction between the experimental and the control group is that RMSSD values of the control group present descending tendency from Section4 to Section5, and those of experimental group probably show ascending trend. Based on the same position, instantaneous heart rate variability of

the male is larger than that of the female in the control group. It shows the same phenomena for the experimental subjects adopting half-lotus posture. However, the male have smaller RMSSD values than the female for the experimental subjects adopting full-lotus posture. The male subjects adopting half-lotus posture in the experimental group have the largest RMSSD value in all the sections.

In the experimental group, we may easily find that the RMSSD values of the subjects who adopt full-lotus posture present decreasing trend during the meditation procedure. However, it presents increasing trend for the male subjects who adopt half-lotus posture during the meditation course. There is little variation in RMSSD for the female subjects who adopt half-lotus posture during the meditation course.

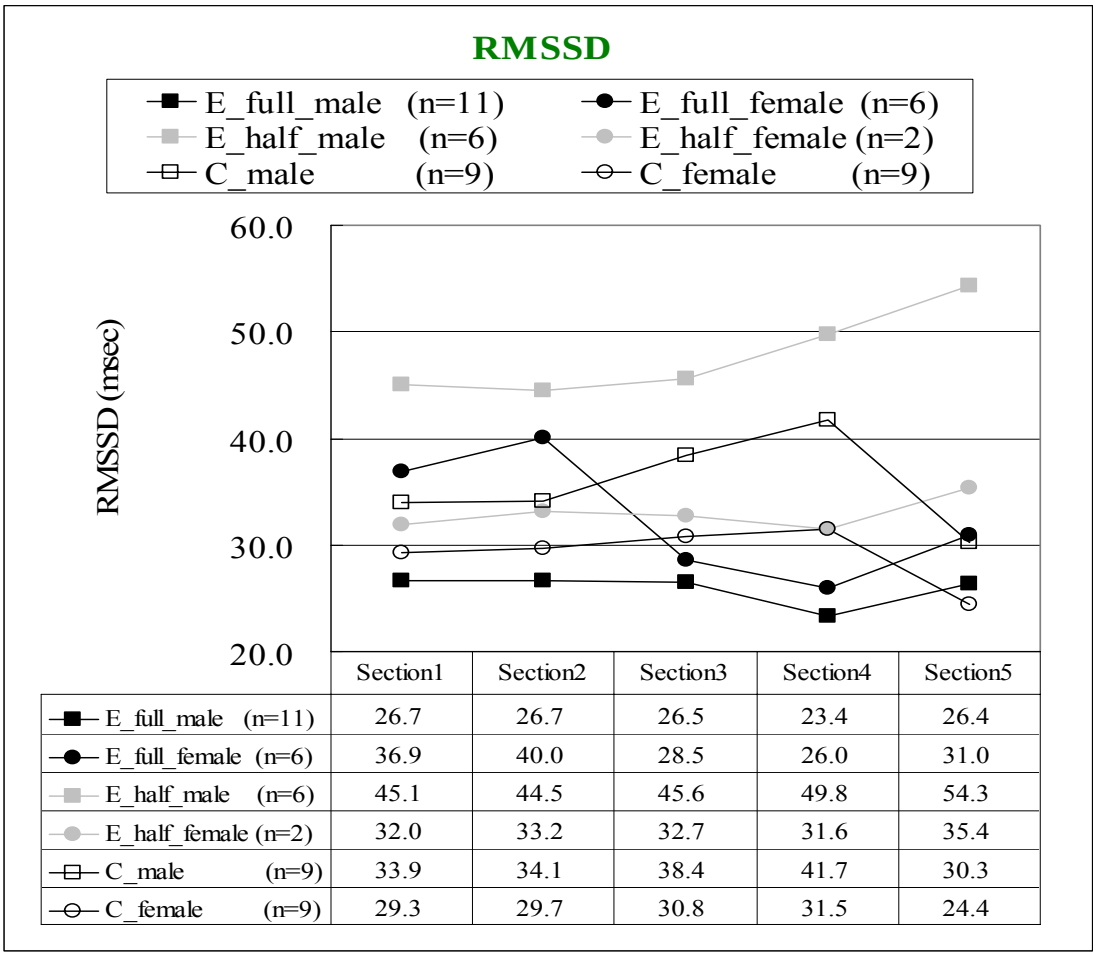

	Section1	Section2	Section3	Section4	Section5
E_full_male (n=11)	26.7	26.7	26.5	23.4	26.4
E_full_female (n=6)	36.9	40.0	28.5	26.0	31.0
E_half_male (n=6)	45.1	44.5	45.6	49.8	54.3
E_half_female (n=2)	32.0	33.2	32.7	31.6	35.4
C_male (n=9)	33.9	34.1	38.4	41.7	30.3
C_female (n=9)	29.3	29.7	30.8	31.5	24.4

Fig. 4.4.2 Mean value of RMSSD (root mean square value of the difference of all the successive RR intervals) of each group in five distinct sections

The analysis above focused on the diversity among different groups for each individual parameter. Next, we are to investigate if there exist relations among different parameters evaluated in time domain. Therefore we summarize the results discussed previously in Tables 4.2-4.5.

Table 4.2 (Value in the parentheses) means the subtraction of the parameter in Section4 from that in Section5

Parameter / Comparative Item	Group Label	MRR	SDRR	RMSSD
Tendency from Section4 to Section5	E	Rise(0.022sec)	Rise(4.0msec)	Rise(3.9msec)
	C	Fall(-0.026sec)	Fall(-13.4msec)	Fall(-9.3msec)
	E_full_male	Rise(0.008sec)	Rise(5.8msec)	Rise(3.0msec)
	E_full_female	Rise(0.069sec)	Rise(2.8msec)	Rise(5.0msec)
	E_half_male	Rise(0.003sec)	Fall(-0.9msec)	Rise(4.5msec)
	E_half_female	Rise(0.011sec)	Rise(12.5msec)	Rise(3.9msec)
	C_male	Fall(-0.022sec)	Fall(-20.2msec)	Fall(-11.4msec)
	C_female	Fall(-0.031sec)	Fall(-6.5msec)	Fall(-7.1msec)

As shown in Table 4.2, from Section 4 to Section 5, MRR and RMSSD tend to rise in all the experimental groups, and SDRR also tends to rise in the experimental groups except the male subjects in half-lotus posture. However, MRR, SDRR and RMSSD all present falling tendency for both the male and female in the control groups from Section 4 to Section 5. It probably exhibits that the heart rate slows down and HRV increases for the subjects in the experimental group from the end of meditation to the post-test section. The condition is just opposite for control group during the same period.

Table 4.3 P-value

Comparative Item \ Parameter		MRR	SDRR	RMSSD
P-value between Experimental and Control group during Section3 and Section4	Section 3	0.045	0.016	0.539
	Section 4	0.011	0.008	0.333

The items listed in Table 4.3 are the P-values (in double tailed t-test) used to compare the dissimilar degree between the experimental and control group in Section 3 and Section 4 respectively. For MRR and SDRR, the difference between two groups is obvious in Section 3 and more apparent in Section 4. For RMSSD, the difference is vague in both of the Section3 and Section4. This means there exist different states of heart rate and HRV between the experimental subjects after meditation and the control ones after resting for a period of time. Moreover, the difference increases with the time getting longer. It infers that the effect of meditation on cardiovascular system is different from that of resting.

Table 4.4 Parameter (male) $_{\text{Section I}}$ – parameter (female) $_{\text{Section I}}$ based on the same posture in 5 sections (M: male; F: female)

Group Label \ Parameter	MRR(sec)	SDRR(msec)	RMSSD(msec)
C	M＞F(0.064, 0.072, 0.073, 0.067, 0.077)	M＞F (11.0, 8.9, 22.4, 19.5, 5.8)	M＞F (4.6, 4.5, 7.6, 10.3, 5.9)
E_full_lotus	M＜F(-0.043, -0.053, -0.002, -0.006, -0.067)	M≈F (-2.7, -4.6, 1.4, 0.6, 3.7)	M＜F (-10.2, -13.3, -2.0, -2.6, -4.6)
E_half_lotus	M＜F(-0.025, -0.036, -0.024, -0.035, -0.042)	M＞F (22.4, 11.0, 18.4, 18.8, 5.4)	M＞F (13.1, 11.3, 12.9, 18.3, 18.9)

The items listed in Table 4.4 are the results of comparing the magnitude of each parameter between male and female in the same position during the five sections. In the control group, all the parameters of the male are larger than those of the female. For the experimental subjects in half lotus posture, MRR of the male is smaller than that of the female, SDRR and RMSSD of the male are larger than those of the female. However, for the experimental subjects in full lotus posture, MRR and RMSSD of the male are smaller than those of the female, and the male have similar SDRR as the female. From the above, it therefore infers that meditation in full lotus posture causes the comparative result of the magnitude of the time domain parameters between the male and the female to be opposite to the resting.

Table 4.5 Tendency from Section 2 to Section 4 (during meditation course or resting course)

Parameter / Group Label	MRR		SDRR		RMSSD	
	Tendency	Sect3- Sect2	Tendency	Sect3- Sect2	Tendency	Sect3- Sect2
		Sect4- Sect3		Sect4- Sect3		Sect4- Sect3
E	falling	-0.021 sec	vague	0.4 msec	Falling	-2.6 msec
		-0.024 sec		-0.8 msec		-1.1 msec
C	vague	0.009 sec	rising	10.1 msec	Rising	2.7 msec
		-0.004 sec		4.8 msec		2.0 msec
E_full_male	falling	-0.013 sec	falling	-0.2 msec	Falling	-0.2 msec
		-0.033 sec		-2.0 msec		-3.1 msec
E_full_female	falling	-0.064 sec	falling	-6.2 msec	Falling	-11.5 msec
		-0.029 sec		-1.3 msec		-2.5 msec
E_half_male	vague	0.004 sec	rising	8.1 msec	Rising	1.1 msec
		-0.010 sec		1.3 msec		4.2 msec
E_half_female	vague	-0.008 sec	rising	0.8 msec	Falling	-0.5 msec
		0.001 sec		0.8 msec		-1.2 msec
C_male	vague	0.010 sec	rising	16.8 msec	Rising	4.2 msec
		-0.007 sec		3.4 msec		3.4 msec
C_female	vague	0.009 sec	rising	3.4 msec	Rising	1.1 msec
		-0.001 sec		6.2 msec		0.7 msec

It is discovered that (Table 4.5), from Section 2 to Section 4, all the time domain parameters (MRR, SDRR, and RMSSD) of the experimental subjects in full lotus posture present falling trend. However, SDRR and RMSSD of the control subjects and the experimental subjects in half lotus posture (except the female subjects in half lotus position) tend to rise, and their trends of MRR are indistinct from Section 2 to Section 4. Accordingly, it infers that meditation in full lotus position can make heart rate speed up and HRV lower down, that causes different effects on the heart rate and HRV analyzed on the subjects meditating in half lotus position and on the control subjects.

4.1.2 Analysis with Fuzzy *C*-Means Clustering

Feature clustering helps establishing a systematic data structure for medical research and clinical application. We thus apply the Fuzzy *C*-means algorithm to the quantitative features to study their clustering behaviors. There are totally 43 subjects in the experimental and the control groups; that is, there are 43 patterns entirely. According to the Table 4.2 and 4.5, the tendency of the three parameters, MRR, SDRR, RMSSD, from Section 2 to Section 4 and from Section 4 to Section 5 can be distinguished between the experimental and control group. Therefore the differences of these 3 parameters between Section 2 and Section 4 and those between Section 4 and Section 5 are chosen as feature vectors respectively. In order to make each dimension of the feature vectors work well, the values of each feature vector is normalized into the range between 0 and 1. Firstly, we discuss the classified results about the differences of the 3 parameters from Section 2 to Section 4. As shown in Fig. 4.5, the patterns are divided into 4 clusters based on the 3-dimensional feature vectors reconstructed by subtraction of MRR (Section4-Section2), subtraction of SDRR (Section4-Section2), and subtraction of RMSSD (Section4-Section2). The classified condition of each group is tabulated in Table 4.6. From Table 4.6, we may see that Cluster 1 is mainly composed of the experimental subjects in full lotus position, and Cluster 2 consists of all groups. Cluster 3 is mostly occupied by the control subjects. Cluster 4 is made up of the control subjects and the male experimental subjects in half lotus position. From the Fig. 4.5(a)(c), the differences of MRR and RMSSD from Section 2 to Section 4 are negative for the subjects in Cluster 1. The differences of SDRR from Section 2 to Section 4 are positive for the subjects in Cluster 3. From the Fig. 4.5 (b)(d), the tendencies of MRR and RMSSD of the experimental subjects in full lotus posture are mostly descending from Section 2 to Section 4, and the tendencies of SDRR of the control subjects are mostly

ascending from Section 2 to Section 4. These results are in accordance with those in the statistical analysis.

Table 4.6 The classified results of the differences of the 3 parameters from Section 2 to Section 4; the number of subjects (of a group) being classified to a particular cluster.

Group \ Cluster	Cluster 1	Cluster 2	Cluster 3	Cluster 4	Unclassified
E_full_male	3	4	2	0	2
E_full_female	3	1	1	0	1
E_half_male	0	3	0	2	1
E_half_female	0	2	0	0	0
C_male	1	2	3	2	1
C_female	0	1	7	1	0

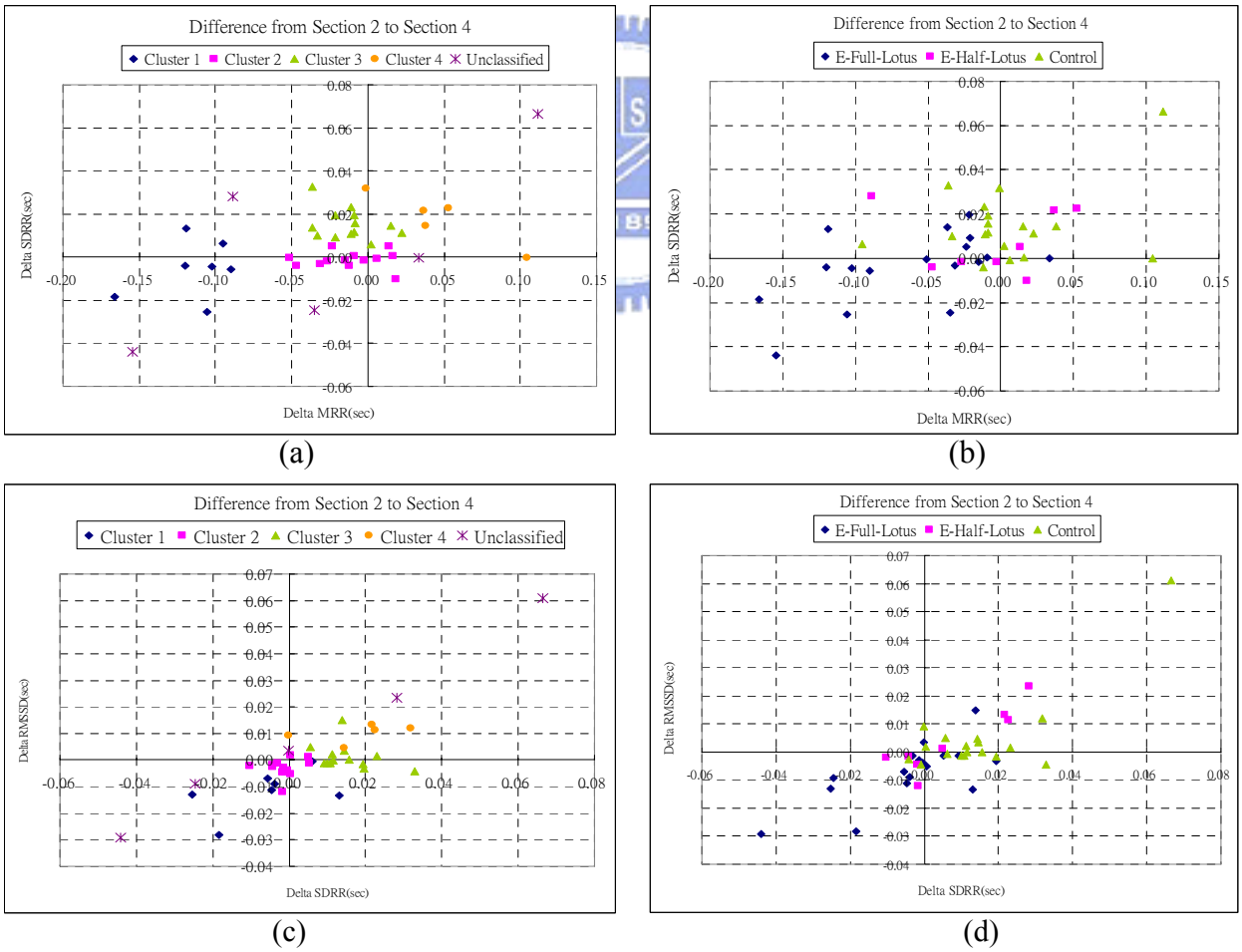

Fig. 4.5 The classified results of the differences of the 3 parameters from Section 2 to Section 4 using Fuzzy *C*-means algorithm

Then we discuss the classified results about the differences of the 3 parameters from Section 4 to Section 5. As shown in Fig. 4.6, the patterns are divided into 4 clusters based on the 3-dimensional feature vectors reconstructed by subtraction of MRR (Section4-Section2), subtraction of SDRR (Section4-Section2), and subtraction of RMSSD (Section4-Section2). The classified condition of each group is tabulated in Table 4.7. From Table 4.7, we may see that Cluster 1 is mainly composed of the experimental subjects in full lotus position and the female control subjects. Cluster 2 mainly consists of all the experimental groups. Cluster 3 is occupied by the control subjects wholly. Cluster 4 is made up of the control subjects and the male experimental subjects. From the Fig. 4.6(a),(c), the differences of MRR, SDRR, and RMSSD from Section 4 to Section 5 are almost positive for the subjects in Cluster 2. The differences of MRR, SDRR, and RMSSD from Section 4 to Section 5 are all negative for the subjects in Cluster 3. From the Fig. 4.6(b),(d), in the experimental group, the number of the subjects whose MRR ,SDRR, and RMSSD present ascending tendencies from Section 4 to Section 5 is more than that of the subjects whose MRR ,SDRR, and RMSSD present descending tendencies during the same period. On the contrary, in the control group, the number of the subjects whose MRR, SDRR, and RMSSD present descending tendencies from Section 4 to Section 5 is more than that of the subjects whose MRR, SDRR, and RMSSD present ascending tendencies during the same period. These results are also in accordance with those in the statistical analysis.

Table 4.7 The classified results of the differences of the 3 parameters from Section 4 to Section 5; the number of subjects (of a group) being classified to a particular cluster.

Cluster / Group	Cluster 1	Cluster 2	Cluster 3	Cluster 4	Unclassified
E_full_male	4	6	0	1	0
E_full_female	2	1	0	0	3
E_half_male	1	3	0	1	1
E_half_female	0	2	0	0	0
C_male	0	1	2	5	1
C_female	3	0	4	1	1

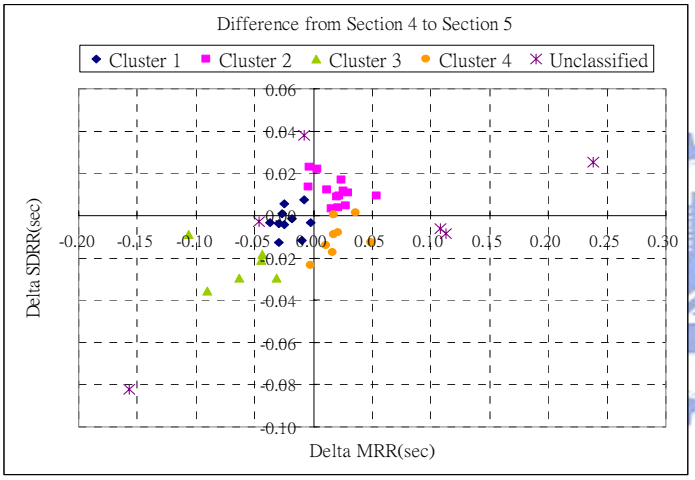

(a)

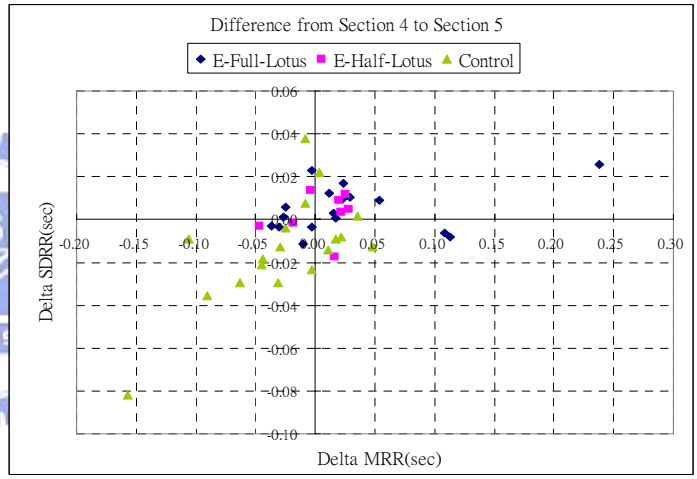

(b)

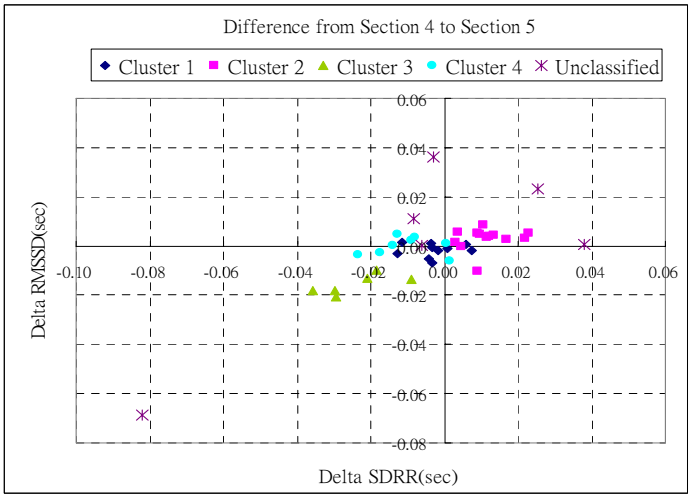

(c)

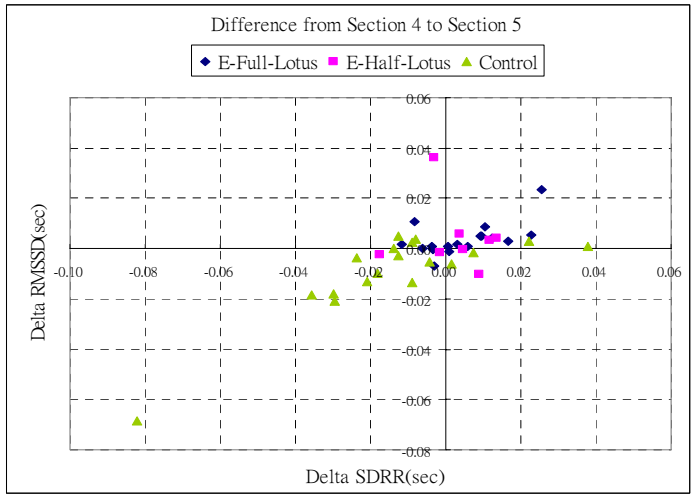

(d)

Fig. 4.6 The classified results of the differences of the 3 parameters from Section 4 to Section 5 using Fuzzy *C*-means algorithm

4.2 Analysis of RR Interval in frequency domain

Like the analysis in time domain, the frequency analysis will involve two parts. The first part is the statistical analysis. The second part is the FCM analysis. Details are illustrated below.

4.2.1 Statistical analysis

Similar to the strategy in the time-domain analysis, data of the RR intervals are segmented into 5 sections. The method of frequency domain analysis is based on FFT(Fast Fourier Transform) algorithm. From the Fourier Spectrum, we estimate some parameters like the pHF, pLF, nHF, nLF and the ratio of pLF/pHF.

We first discuss the low-frequency power (pLF). Fig. 4.8.1 shows the mean value of pLF in 5 distinct sections for both the experimental(E) and the control(C) group. The pLF value of control group shows a rising tendency from Section 1 to Section 4, and it presents apparently descending trend from Section 4 to Section 5. The pLF value of experimental group only changes slightly from the beginning to Section 4. The pLF value of the control group is larger than that of the experimental group from Section 2 to Section 4. However, the pLF value of control group is smaller than that of experimental group in Section 1 and Section 5. In Section1 and Section4, the distribution of pLF value can be distinguished statistically between 2 groups ($p<0.05$).

Because pLF is the index of the co-mediation of sympathetic and parasympathetic, thus we may probably indicate that practicing meditation can make autonomic nervous system more stable. On the other hand, resting makes the activation of autonomic nervous system increase with the increase of resting time.

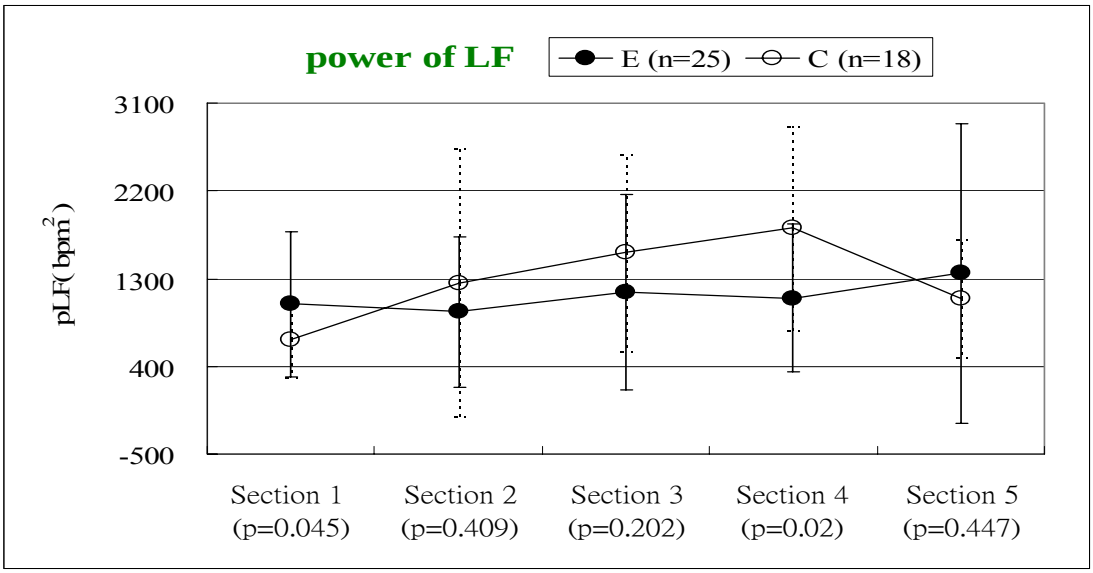

$\overline{pLF}(E)$	1038±749	958±776	1161±1002	1101±759	1355±1540
$\overline{pLF}(C)$	675±386	1260±1378	1566±1013	1815±1054	1093±610

Fig. 4.7.1 Mean value of pLF (low-frequency power) of each group in five sections (solid circle E: Experimental group; open circle C: Control group)

As the analysis in time domain, we will analyze the result by dividing the subjects into six groups. As shown in Fig. 4.7.2, the most significant difference between control group and experimental group is that the pLF value of control group indicates a sharply decreasing trend from Section 4 to Section 5. However, that of experimental group shows a lightly decreasing or sharply increasing tendency from Section 4 to Section 5. In the control group, male have the magnitude and trend of the pLF value similar to those of the female. Regardless of the positions, female apparently have smaller pLF value than male in the experimental group. In the sight of experimental group, the magnitude and trend of pLF value is similar from Section 1 to Section 4 for the male adopting both full-lotus and half-lotus posture. However, this trend reverses in the last section between these two groups. The pLF value only varies slightly from Section 1 to Section 5 for the female who adopt full-lotus posture. The pLF value tends to rise from the beginning to the end for the female who adopt half-lotus posture.

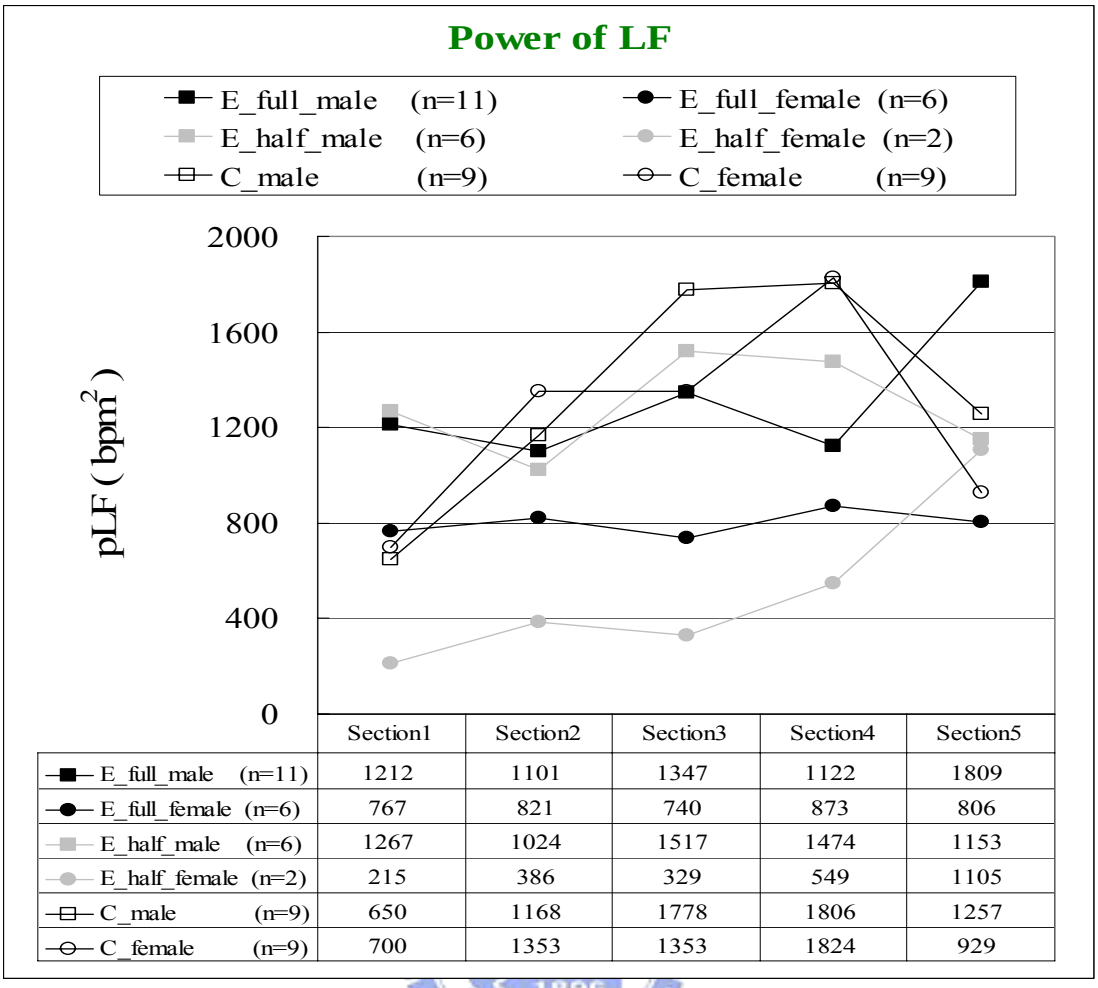

	Section1	Section2	Section3	Section4	Section5
E_full_male (n=11)	1212	1101	1347	1122	1809
E_full_female (n=6)	767	821	740	873	806
E_half_male (n=6)	1267	1024	1517	1474	1153
E_half_female (n=2)	215	386	329	549	1105
C_male (n=9)	650	1168	1778	1806	1257
C_female (n=9)	700	1353	1353	1824	929

Fig. 4.7.2 Mean value of pLF (low-frequency power) of each group in five distinct sections

Then we discuss the high-frequency power (pHF). Fig. 4.8.1 shows the mean value of pHF in 5 distinct sections for both the experimental(E) and the control(C) group. The pHF value shows a rising tendency from Section 1 to Section 3, and it presents somewhat descending trend from Section3 to Section5 for both of the control and experimental groups. Generally speaking, the pHF value of the experimental group is larger than that of the control group during all sections.

However, during all sections, the distribution of pHF value can not be distinguished statistically between 2 groups ($p<0.05$). As pHF is the index of the activation of parasympathetic, thus we may probably indicate that practicing meditation can make parasympathetic more active than normal resting.

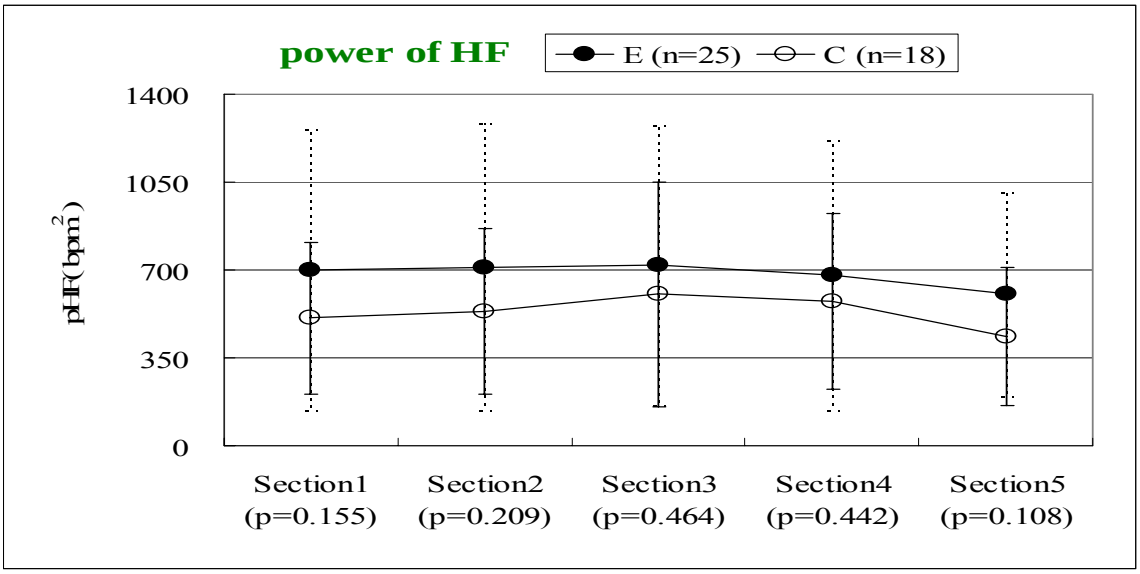

$\overline{pHF}(E)$	701±562	712±574	718±559	679±538	604±408
$\overline{pHF}(C)$	508±304	535±330	604±447	573±350	433±275

Fig. 4.8.1 Mean value of pHF (high-frequency power) of each group in five sections (solid circle E: Experimental group; open circle C: Control group)

As the analysis in pLF, we will analyze the result by dividing the subjects into six groups. As shown in Fig. 4.8.2, the pHF values of the subjects adopting half-lotus position in the experimental group are larger than those of the subjects in the control group. In the control group, male have the trend of the pHF value similar to that of female, and the magnitude of pHF of the male is smaller than that of the female. For the subjects who take full-lotus position in the experimental group, the pHF value of the female is higher than that of the male. However, the condition is just opposite for the subjects who take half-lotus position in the experimental group.

In the sight of experimental group, the pHF value of the male adopting full-lotus position is the smallest of all the groups. On the contrary, the pHF value of the male adopting half-lotus position is the largest of all the groups. The pHF value varies intermediately from Section 1 to Section 5 for the female who adopt half-lotus posture. The tendency of the pHF value is probably falling from the beginning to the end for the female who adopt full-lotus posture.

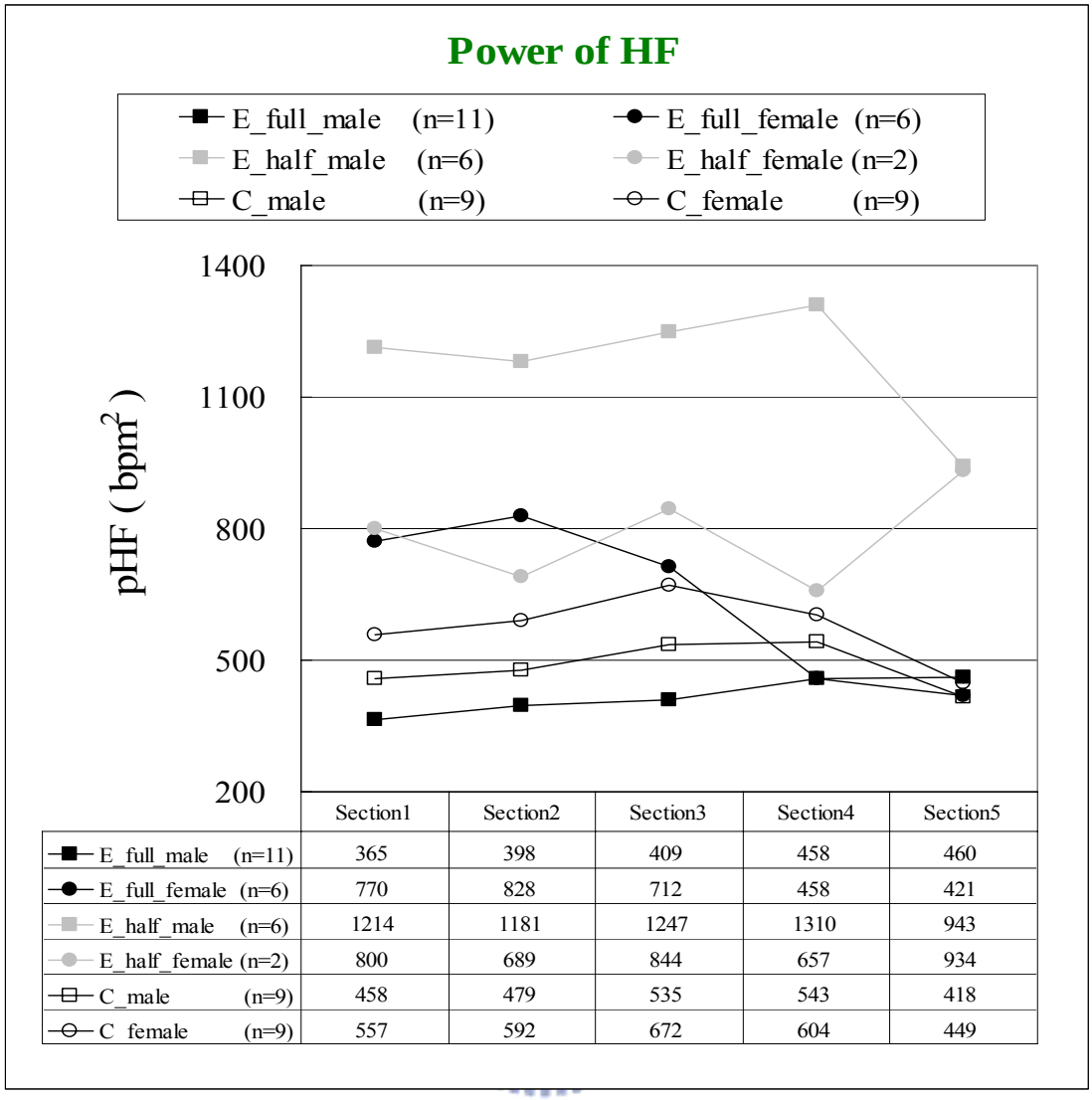

	Section1	Section2	Section3	Section4	Section5
E_full_male (n=11)	365	398	409	458	460
E_full_female (n=6)	770	828	712	458	421
E_half_male (n=6)	1214	1181	1247	1310	943
E_half_female (n=2)	800	689	844	657	934
C_male (n=9)	458	479	535	543	418
C_female (n=9)	557	592	672	604	449

Fig. 4.8.2 Mean value of pHF (high-frequency power) of each group in five distinct sections

Then we discuss the normalized low-frequency power (nLF). Fig. 4.9.1 shows the mean value of nLF in 5 distinct sections for both the experimental(E) and the control(C) group. The nLF value of the control group shows a rising tendency from Section 1 to Section 4, and it presents somewhat descending trend from Section 4 to Section 5 like the case of pLF. The nLF value of the experimental group presents a falling trend from Section 1 to Section 2, and it shows a slightly rising tendency from Section 2 to Section 5.

The nLF value of the control group is larger than that of the experimental group from the beginning to the end. During all the sections, except the Section 1, the

distribution of nLF value can be distinguished statistically between 2 groups ($p<0.05$). As nLF is also the index of the co-mediation of sympathetic and parasympathetic, thus we may probably indicate that practicing meditation can make autonomic nervous system more stable. On the other hand, resting makes the activation of autonomic nervous system increase with the increase of resting time.

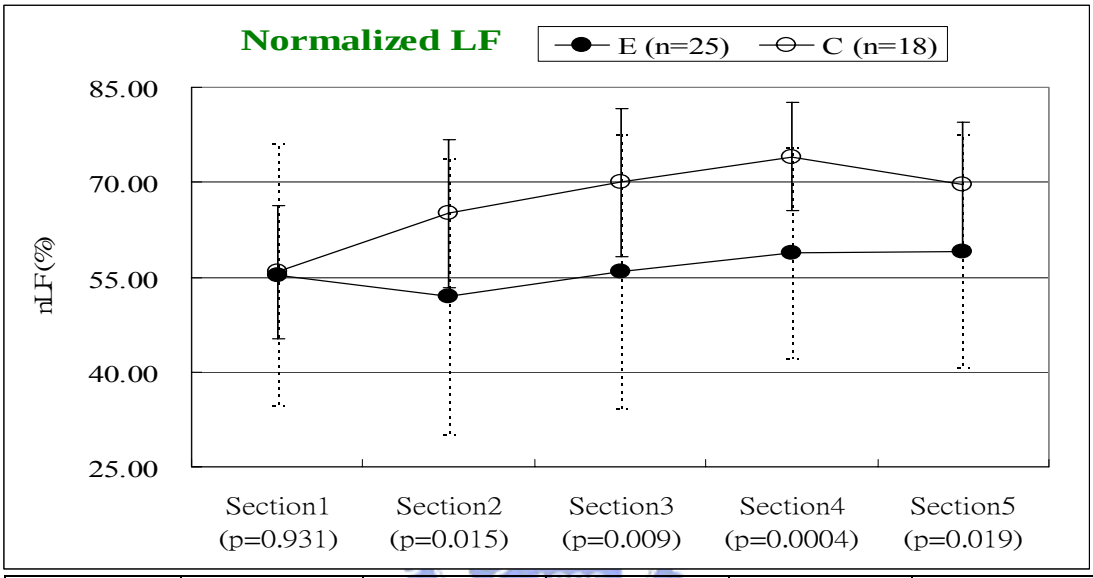

$\overline{nLF}(E)$	55.38±20.72	51.95±21.82	55.86±21.60	58.85±16.66	59.10±18.42
$\overline{nLF}(C)$	55.80±10.55	65.05±11.67	69.97±11.63	74.05±8.57	69.72±9.82

Fig. 4.9.1 Mean value of nLF (normalized low-frequency power) of each group in 5 sections (solid circle E: Experimental group; open circle C: Control group)

Then we will discuss the result by separating the subjects into six groups. As shown in Fig. 4.9.2, the nLF value of the members in the control group and the male subjects adopting full-lotus position in the experimental group is probably larger than sixty, and however, that of the rest members of the experimental group is smaller than sixty. Based on the same posture, like the pLF, the male have the magnitude and trend of the nLF value similar to that of female in the control group. For the subjects adopting full-lotus position, female have smaller nLF value than

male in the experimental group. There exists the same phenomenon for the subjects adopting half-lotus position.

In the sight of experimental group, the magnitude of nLF value is the highest for the male subjects adopting full-lotus position, and it varies a little during all the sections. For the male subjects adopting half-lotus position, the nLF value also somewhat varies during all the sections. The nLF value probably shows a increasing tendency for the female in the experimental group.

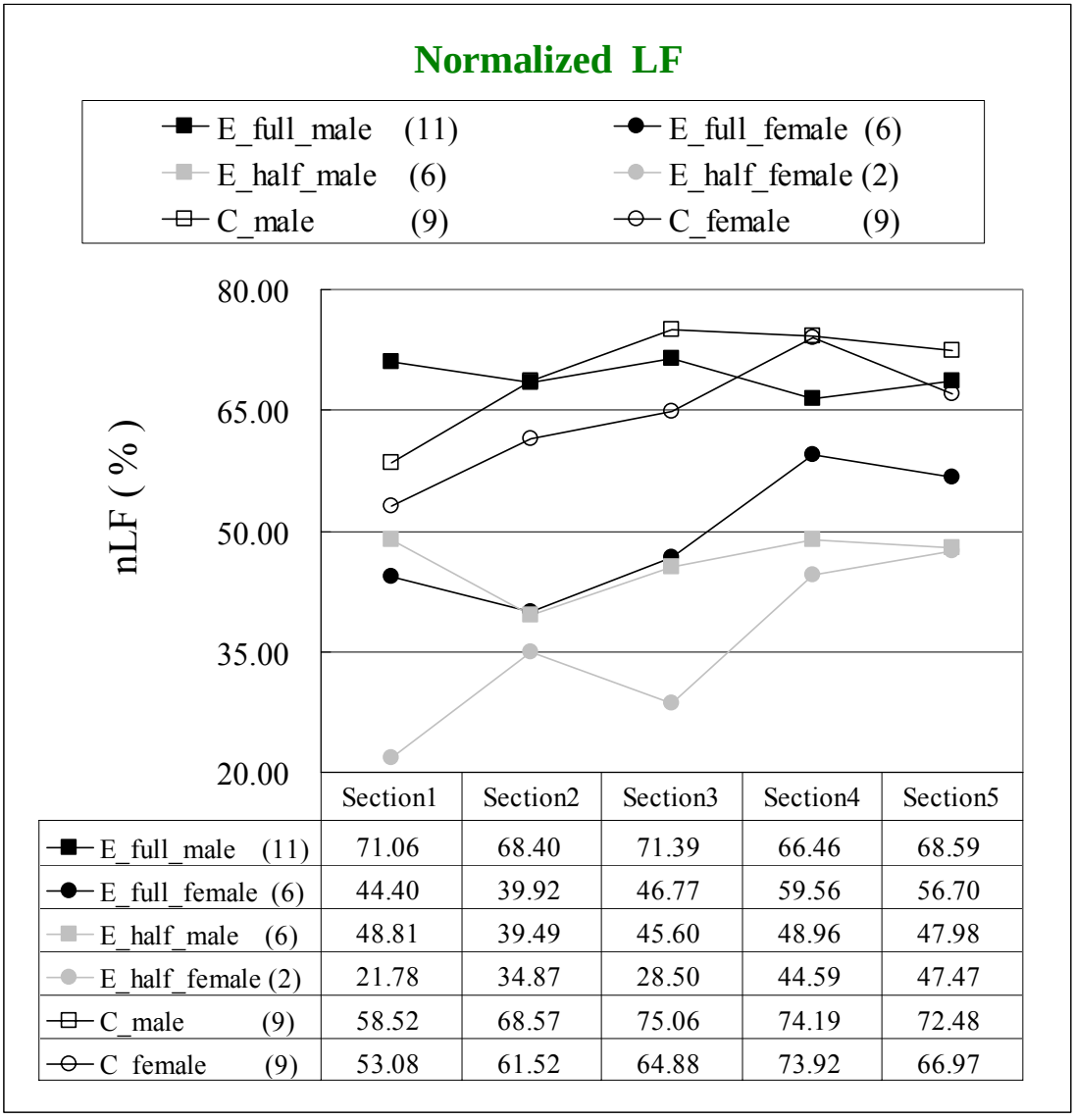

	Section1	Section2	Section3	Section4	Section5
E_full_male (11)	71.06	68.40	71.39	66.46	68.59
E_full_female (6)	44.40	39.92	46.77	59.56	56.70
E_half_male (6)	48.81	39.49	45.60	48.96	47.98
E_half_female (2)	21.78	34.87	28.50	44.59	47.47
C_male (9)	58.52	68.57	75.06	74.19	72.48
C_female (9)	53.08	61.52	64.88	73.92	66.97

Fig. 4.9.2 Mean value of nLF (normalized low-frequency power) of each group in five distinct sections

Then we discuss the normalized high-frequency power (nHF). Fig. 4.10.1 shows the mean value of nHF in 5 distinct sections for both the experimental(E) and the control(C) group. The nHF value of control group shows a falling tendency from Section 1 to Section 4, and it presents somewhat rising trend from Section 4 to Section 5. The nHF value of experimental group presents ascending trend from Section 1 to Section 2, and it shows a slightly descending tendency from Section 2 to Section 5. The trend of nHF is opposite to that of nLF.

The nHF value of control group is smaller than that of experimental group from Section 2 to Section 5. During all the sections, except the Section 1, the distribution of nHF value can be distinguished statistically between 2 groups ($p<0.05$). As nHF is also the index of the activation of parasympathetic, thus we may probably indicate that practicing meditation can make parasympathetic more active.

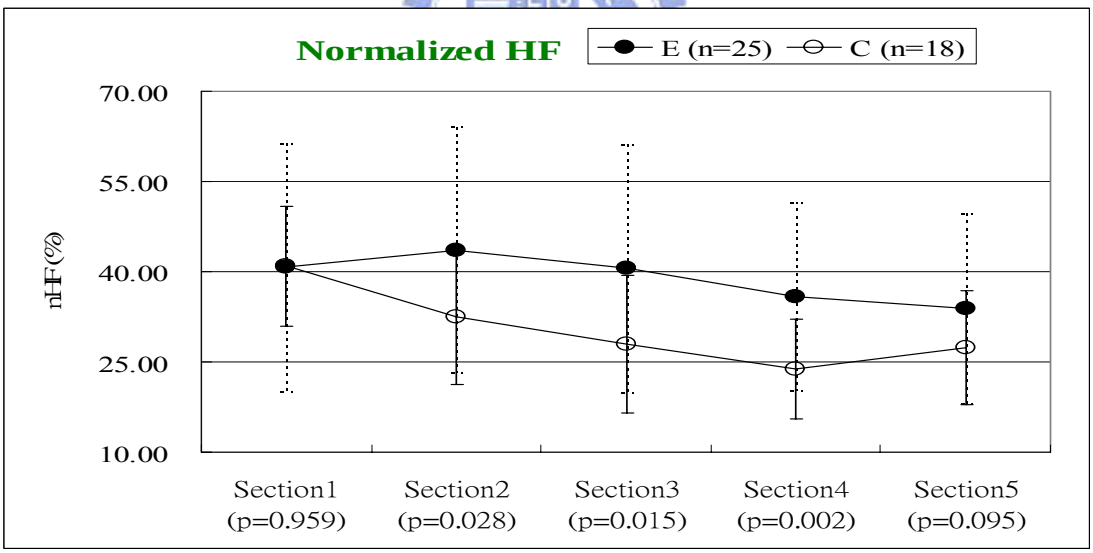

$\overline{nHF}(E)$	40.72±20.59	43.64±20.43	40.50±20.67	35.87±15.52	33.92±15.75
$\overline{nHF}(C)$	40.96±9.97	32.51±11.26	27.95±11.45	23.87±8.25	27.31±9.48

Fig. 4.10.1 Mean value of nHF (normalized high-frequency power) of each group in 5 sections (solid circle E: Experimental group; open circle C: Control group)

Then we will discuss the result by dividing the subjects into six groups. As shown in Fig. 4.10.2, the nHF value of the members in the control group and the

male subjects adopting full-lotus position in the experimental group are probably smaller than forty, and however, that of the rest members of experimental group are probably larger than forty. Based on the same posture, like the nLF, the male have the magnitude and trend of the nHF value similar to those of the female in control group. For the subjects adopting full-lotus position, the female have larger nHF value than the male in experimental group. There exists the same phenomenon for the subjects adopting half-lotus position. In the sight of experimental group, the magnitude of nHF value is the lowest for the male subjects adopting full-lotus position, and it varies a little during all the sections. For the male subjects adopting half-lotus position, and the female in experimental group, the nHF value probably shows a decreasing tendency though there exist some vibrations during the process of experiment.

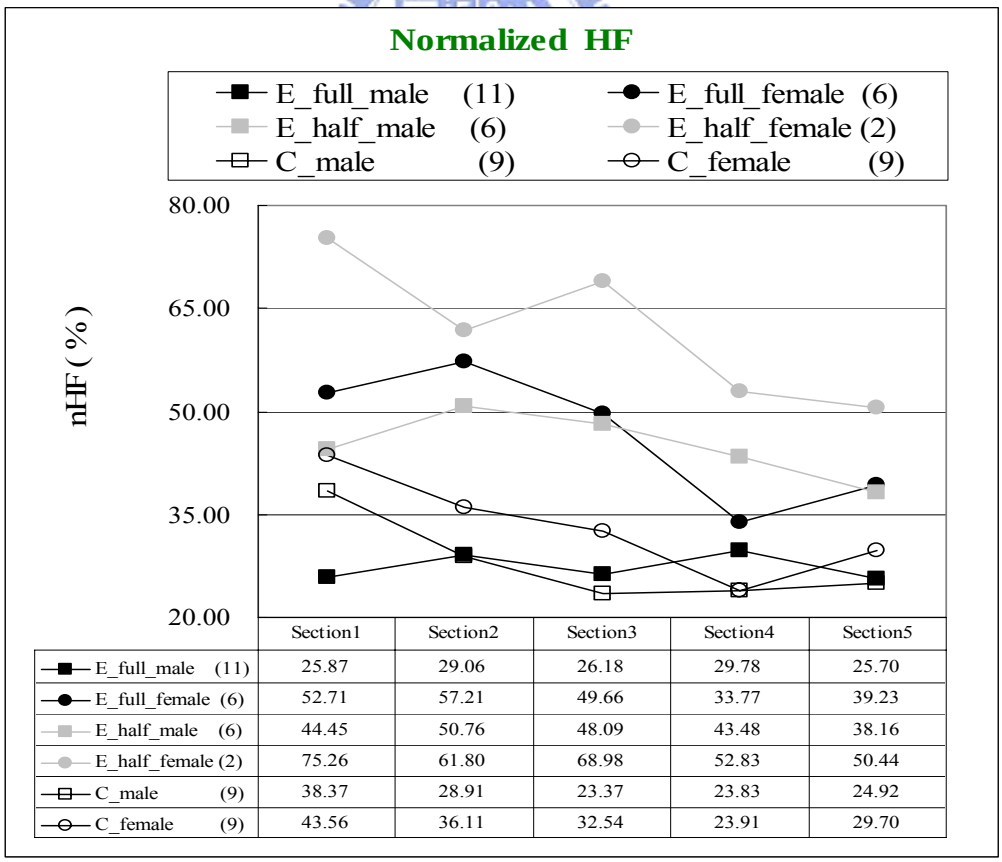

	Section1	Section2	Section3	Section4	Section5
E_full_male (11)	25.87	29.06	26.18	29.78	25.70
E_full_female (6)	52.71	57.21	49.66	33.77	39.23
E_half_male (6)	44.45	50.76	48.09	43.48	38.16
E_half_female (2)	75.26	61.80	68.98	52.83	50.44
C_male (9)	38.37	28.91	23.37	23.83	24.92
C_female (9)	43.56	36.11	32.54	23.91	29.70

Fig. 4.10.2 Mean value of nHF (normalized high-frequency power) of each group in five distinct sections

We now discuss the ratio of pLF/pHF. Fig. 4.11.1 shows the mean value of the ratio of pLF/pHF in 5 distinct sections for both the experimental(E) and the control(C) group. The ratio of pLF/pHF of control group shows a rising tendency from Section 1 to Section 4, and it presents somewhat descending trend from Section 4 to Section 5. The ratio of pLF/pHF of experimental group presents a falling trend from Section 1 to Section 2, and it shows a slightly rising tendency from Section 2 to Section 5. The ratio of pLF/pHF of control group is larger than that of experimental group from Section 2 to Section 5. The distribution of the ratio of pLF/pHF can be distinguished statistically between 2 groups ($p<0.05$) only in Section 4. As the ratio of pLF/pHF is the balancing index of the activation of sympathetic and parasympathetic, thus we may probably indicate that the balance of the activation of sympathetic and parasympathetic is better in the experimental group than that in the control group, because the ratio of pLF/pHF is closer to 1 for experimental group.

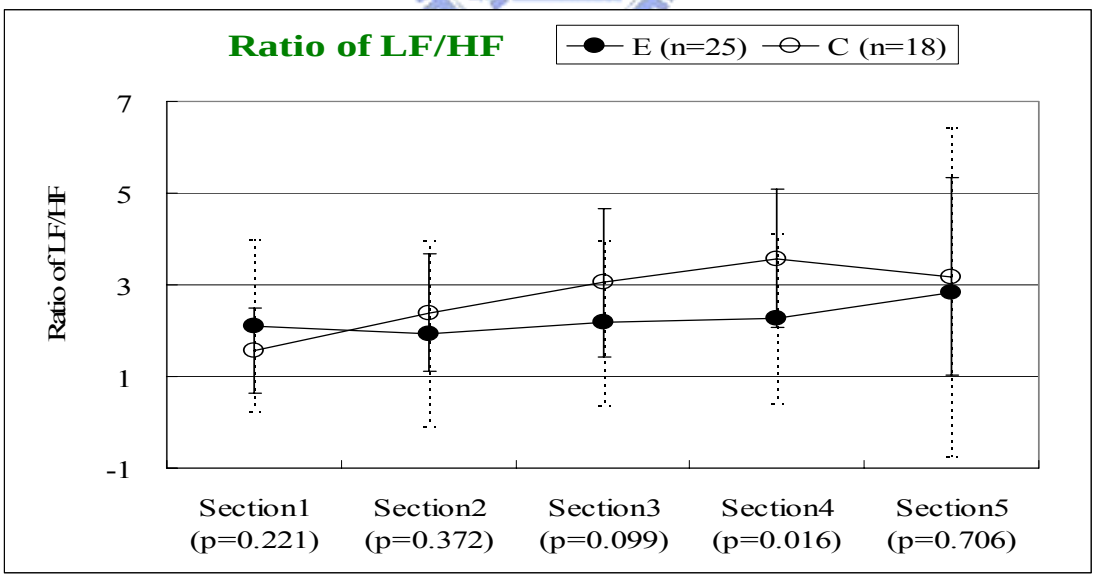

$\overline{LF/HF}(E)$	2.11±1.88	1.93±2.04	2.17±1.78	2.27±1.86	2.84±3.59
$\overline{LF/HF}(C)$	1.57±0.93	2.39±1.29	3.05±1.62	3.57±1.51	3.18±2.15

Fig. 4.11.1 Mean value of the ratio of LF/HF for each group in five sections (solid circle E: Experimental group; open circle C: Control group)

Then we will discuss the result by dividing the subjects into six groups. As shown in Fig. 4.11.2, the most difference between the control group and experimental group is that the ratio of LF/HF value of control group indicates a decreasing trend from Section 4 to Section 5, and however, that of the experimental group shows increasing tendency from Section 4 to Section 5. Based on the same posture, the male have the magnitude and trend of the ratio of LF/HF value similar to those of the female in the control group. For the subjects who take full-lotus position in the experimental group, the ratio of LF/HF value of the female is lower than that of the male. Then the condition is same for the subjects who take half-lotus position in the experimental group.

In the sight of the experimental group, the magnitude of the ratio of LF/HF value is the highest during all sections for the male adopting full-lotus position. That is, the sympathetic is activated most, and the parasympathetic is inhibited most for the male adopting full-lotus position. For the male adopting half-lotus posture, the ratio of LF/HF value keeps between 1 and 2. That is, the sympathetic is a little more activated than the parasympathetic for the male adopting half-lotus position. The ratio of LF/HF approaches 1 from Section 1 to Section 3 for the female who adopt full-lotus posture. That is, the activation of sympathetic and that of parasympathetic are almost balanced for the female adopting full-lotus position in the prior three sections. The ratio of LF/HF is probably less than 1 for the female who adopt half-lotus posture. That is, the parasympathetic is a little more activated than the sympathetic for the female adopting half-lotus position.

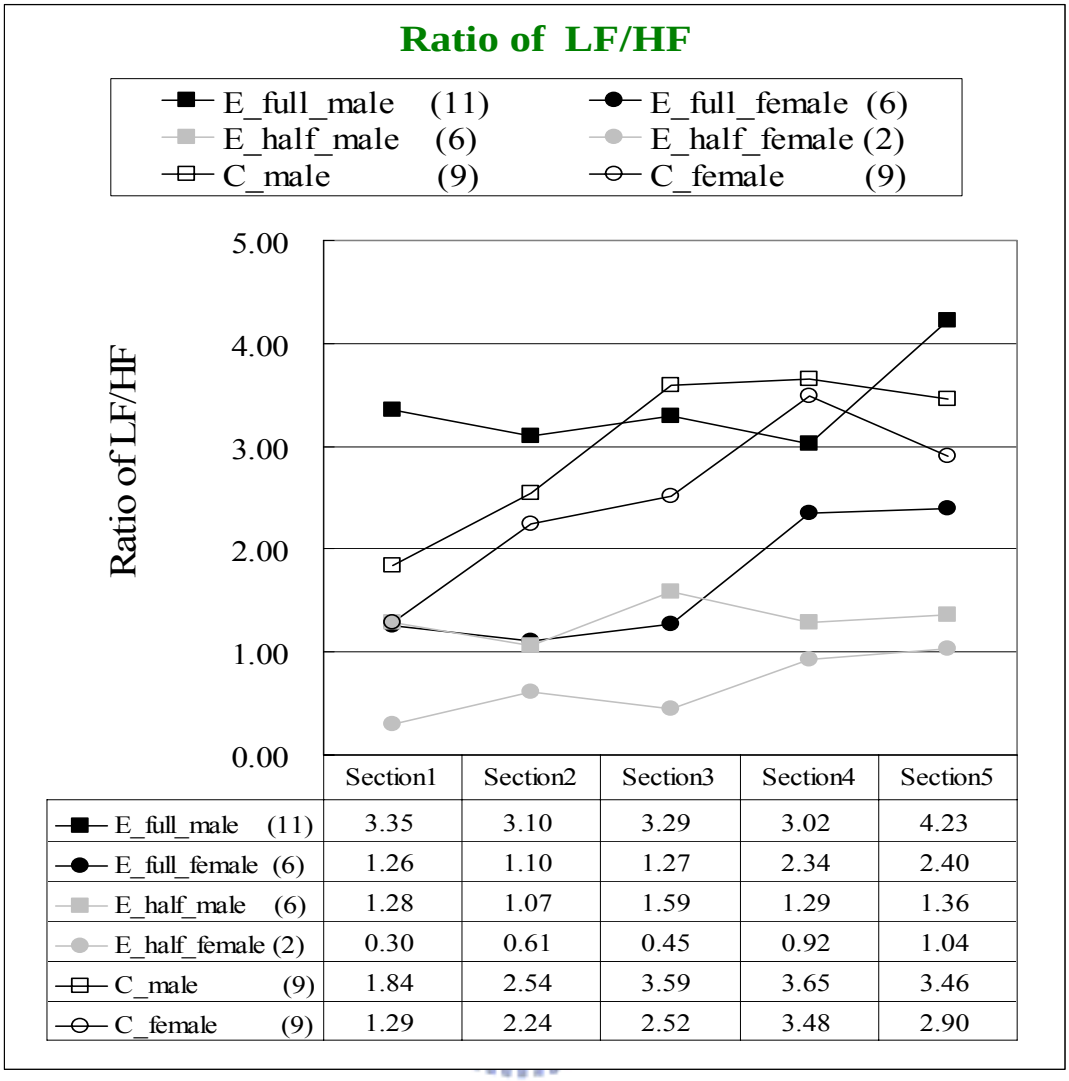

	Section1	Section2	Section3	Section4	Section5
E_full_male (11)	3.35	3.10	3.29	3.02	4.23
E_full_female (6)	1.26	1.10	1.27	2.34	2.40
E_half_male (6)	1.28	1.07	1.59	1.29	1.36
E_half_female (2)	0.30	0.61	0.45	0.92	1.04
C_male (9)	1.84	2.54	3.59	3.65	3.46
C_female (9)	1.29	2.24	2.52	3.48	2.90

Fig. 4.11.2 Mean value of the ratio of LF/HF for each group in five distinct sections

The analysis above focused on the diversity among different groups for each individual parameter. Next, we are to investigate if there exist relations among different parameters evaluated in frequency domain. Therefore we summarize the results discussed previously in Tables 4.8-4.15.

Table 4.8 P-value

Comparative Item \ Parameter		pLF	pHF	nLF	nHF	LF/HF Ratio
P-value between Experimental and Control group from Section 1 to Section 5	Section 1	0.045	0.155	0.931	0.959	0.221
	Section 2	0.409	0.209	0.015	0.028	0.372
	Section 3	0.202	0.464	0.009	0.015	0.099
	Section 4	0.020	0.442	0.0004	0.002	0.016
	Section 5	0.447	0.108	0.019	0.095	0.706

The items listed in Table 4.8 are the P-values (in double tailed t-test) used to compare the dissimilar degree between the experimental and control group from Section 1 to Section 5. For nLF and nHF, the difference between two groups is very obvious from Section 2 to Section 4, but for pLF and LF/HF Ratio, the difference is apparent only in Section4. nLF is the co-mediation parameter of the sympathetic and the parasympathetic and nHF is the parameter standing for the activation of the parasympathetic. From Table 4.8, the difference of these two parameters between the experimental and control group is getting more obvious with the increase of the meditation (resting) time. Therefore it infers that meditation has a different effect on the modulation of the autonomic nervous system from resting.

Table 4.9 Parameter (male) $_{\text{Section I}}$ – parameter (female) $_{\text{Section I}}$ based on the same posture in 5 sections (M: male; F: female)

Parameter / Group Label	E_Full_Lotus	E_Half_Lotus	Ctrl
pLF (bpm^2)	M＞F (445, 280, 608, 250, 1003)	M＞F (1052, 638, 1188, 925, 49)	M≈F (-50, -185, 424, -19, 328)
pHF (bpm^2)	M＜F (-404, -430, -304, 1, 40)	M＞F (414, 491, 403, 653, 9)	M＜F(-100, -113, -137, -62, -31)
nLF (%)	M＞F (26.66, 28.48, 24.62, 6.9, 11.89)	M＞F (27.03, 4.62, 17.1, 4.37, 0.51)	M＞F (5.44, 7.04, 10.18, 0.27, 5.5)
nHF (%)	M＜F(-26.84, -28.16, -23.48, -4, -13.52)	M＜F(-30.81, -11.04, -20.89, -9.35, -12.28)	M＜F(-5.19, -7.21, -9.17, -0.08, -4.79)
LF/HF Ratio	M＞F (2.09, 1.99, 2.02, 0.68, 1.83)	M＞F (0.98, 0.46, 1.14, 0.37, 0.32)	M＞F (0.54, 0.3, 1.07, 0.17, 0.56)

The items listed in Table 4.9 are the results of comparing the magnitude of each parameter between male and female in the same position during the five sections. The parameters, nLF and LF/HF Ratio, of the male are larger than those of the female in all groups. For the experimental subjects in full lotus posture and the control subjects, pHF and nHF of the male are smaller than those of the female. For the experimental subjects in half lotus posture, nHF of the male is also smaller than that of the female; nevertheless, pHF of the male is larger than that of the female. The parameter pLF of the male is larger than that of the female for the experimental subjects and in the control group, the magnitude of pLF is similar between the male and female. Therefore we may find that no matter which group the subjects belong to, the comparative results of the magnitude of the frequency domain parameters between the male and the female are almost in accordance among three groups except the pHF value in E_Half_Lotus group and pLF value in control group.

Table 4.10 Difference between the mean of each parameter of each group and that of all groups in Section 1

Parameter / Comparative Item	Group Label	PLF	pHF	nLF	nHF	LF/HF Ratio
Difference between the mean of each parameter of each group and that of all groups in Section 1	E_full_male	410	-329	21.45	-20.83	1.80
	E_full_female	-35	76	-5.21	6.01	-0.30
	E_half_male	465	520	-0.80	-2.25	-0.27
	E_half_female	-587	106	-27.83	28.56	-1.25
	C_male	-152	-236	8.91	-8.33	0.28
	C_female	-102	-137	3.47	-3.14	-0.26

Table 4.11 Difference between the mean of each parameter of each group and that of all groups in Section 2

Parameter / Comparative Item	Group Label	pLF	pHF	nLF	nHF	LF/HF Ratio
Difference between the mean of each parameter of each group and that of all groups in Section 2	E_full_male	125	-297	16.27	-14.92	1.32
	E_full_female	-154	134	-12.21	13.24	-0.67
	E_half_male	48	486	-12.64	6.78	-0.71
	E_half_female	-590	-5	-17.26	17.82	-1.16
	C_male	192	-216	16.44	-15.07	0.76
	C_female	378	-103	9.39	-7.86	0.46

Table 4.12 Difference between the mean of each parameter of each group and that of all groups in Section 3

Parameter / Comparative Item	Group Label	pLF	pHF	nLF	nHF	LF/HF Ratio
Difference between the mean of each parameter of each group and that of all groups in Section 3	E_full_male	170	-328	16.03	-15.29	1.18
	E_full_female	-438	-24	-8.60	8.19	-0.85
	E_half_male	340	511	-9.77	6.62	-0.53
	E_half_female	-849	107	-26.87	27.51	-1.67
	C_male	600	-201	19.69	-18.10	1.47
	C_female	176	-64	9.51	-8.93	0.40

Table 4.13 Difference between the mean of each parameter of each group and that of all groups in Section 4

Parameter / Comparative Item	Group Label	pLF	pHF	nLF	nHF	LF/HF Ratio
Difference between the mean of each parameter of each group and that of all groups in Section 4	E_full_male	-152	-213	5.18	-4.83	0.57
	E_full_female	-402	-214	-1.72	-0.83	-0.11
	E_half_male	199	639	-12.32	8.88	-1.16
	E_half_female	-726	-15	-16.69	18.23	-1.53
	C_male	531	-129	12.91	-10.77	1.20
	C_female	550	-68	12.64	-10.69	1.03

Table 4.14 Difference between the mean of each parameter of each group and that of all groups in Section 5

Parameter / Comparative Item	Group Label	pLF	pHF	nLF	nHF	LF/HF Ratio
Difference between the mean of each parameter of each group and that of all groups in Section 5	E_full_male	632	-143	8.56	-8.99	1.66
	E_full_female	-370	-183	-3.33	4.53	-0.16
	E_half_male	-23	339	-12.05	3.47	-1.21
	E_half_female	-72	330	-12.56	15.75	-1.52
	C_male	81	-186	12.45	-9.78	0.90
	C_female	-248	-155	6.94	-4.99	2.90

Table 4.15 The mean value of the differences in 5 sections (‘difference’ means the difference between the mean of each parameter of each group and that of all groups in one of the 5 sections)

Parameter / Comparative Item	Group Label	pLF	pHF	nLF	nHF	LF/HF Ratio
The mean value of the differences in 5 sections (‘difference’ means the difference between the mean of each parameter of each group and that of all groups in one of the 5 sections)	E_full_male	237	-262	13.50	-12.97	1.31
	E_full_female	-280	-42	-6.21	6.23	-0.42
	E_half_male	206	499	-9.51	4.70	-0.78
	E_half_female	-565	105	-20.24	21.57	-1.43
	C_male	251	-194	14.08	-12.41	0.92
	C_female	151	-105	8.39	-7.12	0.91

The items listed in Table 4.10-14 are the difference between the mean of each parameter of each group and that of all groups in Section 1-5, and the items listed in Table 4.15 are the mean values of the differences in 5 sections (‘difference’ means the difference between the mean of each parameter of each group and that of all groups in one of the 5 sections). From Table 4.16, it can be found that at the three parameters, nLF, nHF, and LF/HF Ratio, the three groups, E_full_female, E_half_male, and E_half_female, have the same phenomenon, and for the other three groups, E_full_male, C_male, and C_female, the phenomenon is on the opposite side. About the pLF, E_full_male, E_half_male, C_male, and C_female have mean differential value of five sections which is bigger than zero; the mean differential value of five sections of E_full_female and E_half_female is smaller than zero. About the pHF, E_full_male, E_full_female, C_male, and C_female have mean differential value of five sections which is smaller than zero, and the mean differential value of five sections of E_half_male and E_half_female is bigger than zero. Therefore it infers that the activation of the parasympathetic of E_full_female, E_half_male, and E_half_female is more active than that of E_full_male, C_male, and C_female.

4.2.2 Analysis with Fuzzy *C*-Means Clustering

Like the time domain analysis, feature clustering help establishing a systematic data structure for medical research and clinical application. We thus apply the Fuzzy *C*-means algorithm to the quantitative features to study their clustering behaviors. From Tables 4.10-15, in parameter pLF, the evident deviation only exists between the experimental female subjects and the control subjects. Parameter pHF of the experimental subjects in half-lotus posture deviates from that of the control subjects. Then the parameters, nLF, nHF, and ratio of LF/HFof the experimental female subjects and the experimental subjects in half lotus position deviate from those of the control subjects. The physiological meaning of nLF is similar to that of pLF. The physiological meaning of nHF is similar to that of pHF. Ratio of LF/HF can be obtained from nLF and nHF. Therefore, in the analysis of FCM, only the parameters, nLF and nHF, are chosen as the feature vectors.

From Tables 4.10-4.15, the comparison of the parameters in frequency domain among six groups is performed in each section. Thus nLF and nHF are selected as feature vectors only in a section once in the analysis of FCM. Firstly, we discuss the classified results in Section 1. As shown in Fig. 4.12, the patterns are divided into 3 clusters based on the 2-dimensional feature vectors reconstructed by nLF(Section1), and nHF(Section1). The classified condition of each group is tabulated in Table 4.16. Cluster 1 mainly consists of the female experimental subjects and the subjects in half lotus position. Control subjects mainly distribute in Cluster 2, and the male experimental subjects in full lotus position are mainly grouped into Cluster 3. Note that members of Cluster 1 have higher nHF value and lower nLF value than those of Cluster 2 and Cluster 3. On the other hand, nHF value of the members in Cluster 3 is lower than that in Cluster 1 and Cluster 2. Thus, the female experimental subjects

and the subjects in half lotus position have the highest nHF value and the lowest nLF value. The control subjects have the mid-range nHF and nLF value, and the male experimental subjects in full lotus position have the lowest nHF value, and the highest nLF value in Section 1 (pre-test section).

Table 4.16 The classified results of nLF vs. nHF in Section 1; the number of subjects (of a group) being classified to a particular cluster

Cluster / Group	Cluster 1	Cluster 2	Cluster 3	unclassified
E_full_male	0	1	9	1
E_full_female	3	1	2	0
E_half_male	2	2	1	1
E_half_female	2	0	0	0
C_male	0	6	2	1
C_female	1	6	1	1

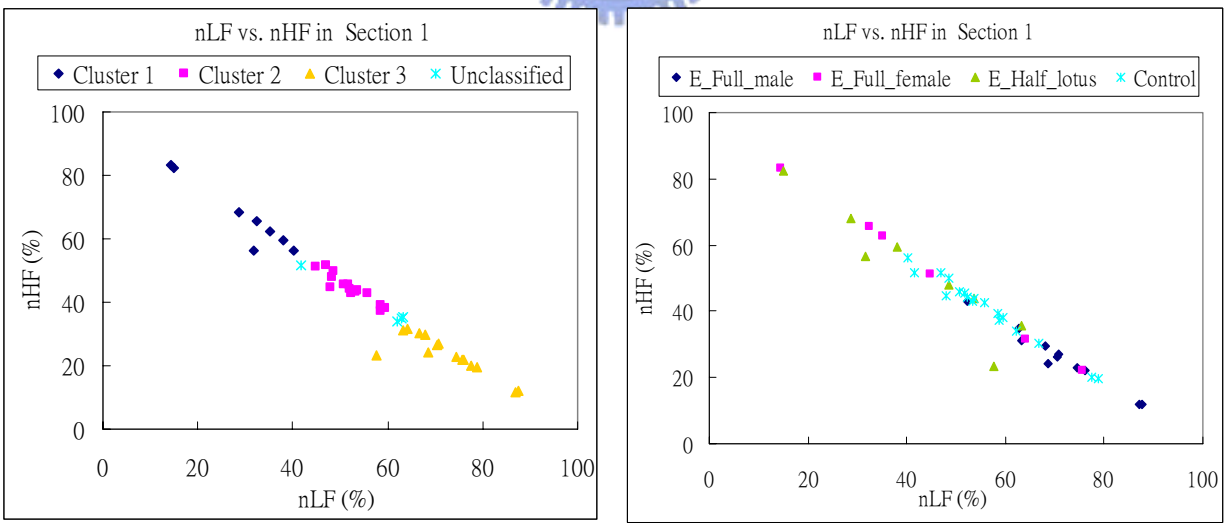

(a) (b)

Figure 4.12 The classified result of nLF vs. nHF in Section 1 using Fuzzy *C*-means algorithm

Then we discuss the classified results in Section 2. As shown in Fig. 4.13, the patterns are divided into 2 clusters based on the 2-dimensional feature vectors reconstructed by nLF(Section2) and nHF(Section2). The classified condition of each group is tabulated in Table 4.17. The female experimental subjects and the subjects in half lotus position probably distribute in Cluster 1, and Cluster 2 mainly consists of the control subjects and the male experimental subjects in full lotus position. The members of Cluster 1 have higher nHF value and lower nLF value than those of Cluster 2. According to the literature, the female have higher nHF and lower nLF values than the male. From Table 4.17, all female subjects are almost classified to Cluster 1 except the control female subjects, and all male subjects are almost classified to Cluster 1 except the experimental male subjects in half lotus position.

Table 4.17 The classified results of nLF vs. nHF in Section 2; the number of subjects (of a group) being classified to a particular cluster

Group \ Cluster	Cluster 1	Cluster 2	unclassified
E_full_male	2	8	1
E_full_female	5	1	0
E_half_male	5	1	0
E_half_female	2	0	0
C_male	0	8	1
C_female	4	5	0

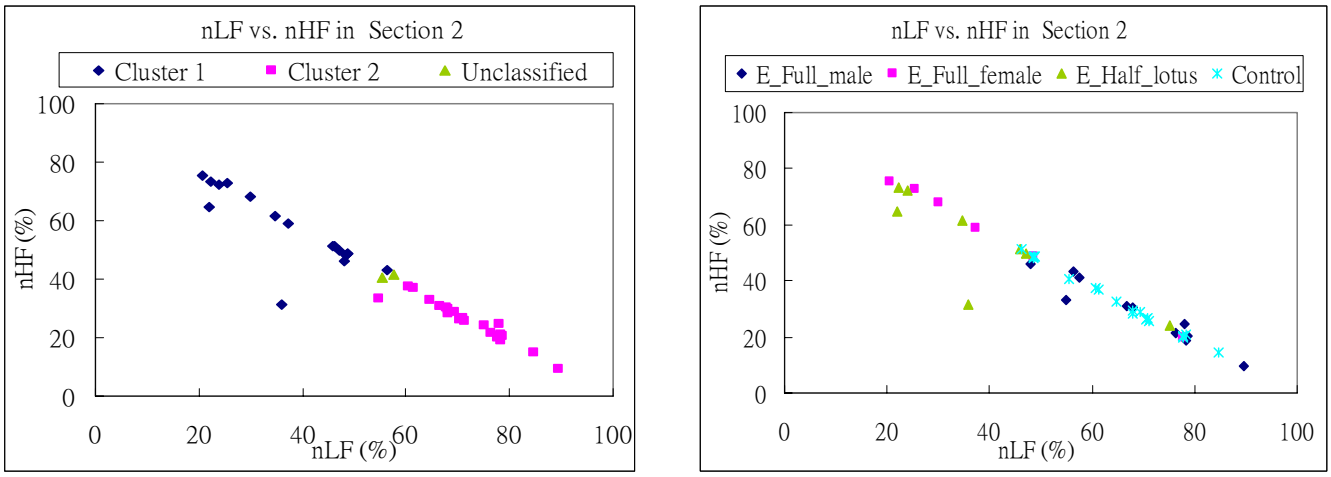

(a) (b)

Figure 4.13 The classified results of nLF vs. nHF in Section 2using Fuzzy *C*-means algorithm

Then we discuss the classified results in Section 3. As shown in Fig. 4.14, the patterns are divided into 2 clusters based on the 2-dimensional feature vectors reconstructed by nLF(Section3) and nHF(Section3). The classified condition of each group is tabulated in Table 4.18. The female experimental subjects and the subjects in half lotus position probably distribute in Cluster 2, and Cluster 1 mainly consists of the control subjects and the male experimental subjects in full lotus position. The members of Cluster 2 have higher nHF value, and lower nLF value than those of Cluster 1. Like the classified result in Section 2, from Table 4.18, all female subjects are almost classified to Cluster 2 except the control female subjects, and all male subjects are almost classified to Cluster 1 except the experimental male subjects in half lotus position in Section 3. Therefore it infers that meditation in half lotus position does better to cheer up the parasympathetic activation than normal resting.

Table 4.18 The classified results of nLF vs. nHF in Section 3; the number of subjects (of a group) being classified to a particular cluster

Cluster / Group	Cluster 1	Cluster 2	unclassified
E_full_male	8	1	2
E_full_female	1	5	0
E_half_male	1	5	0
E_half_female	0	2	0
C_male	9	0	0
C_female	5	3	1

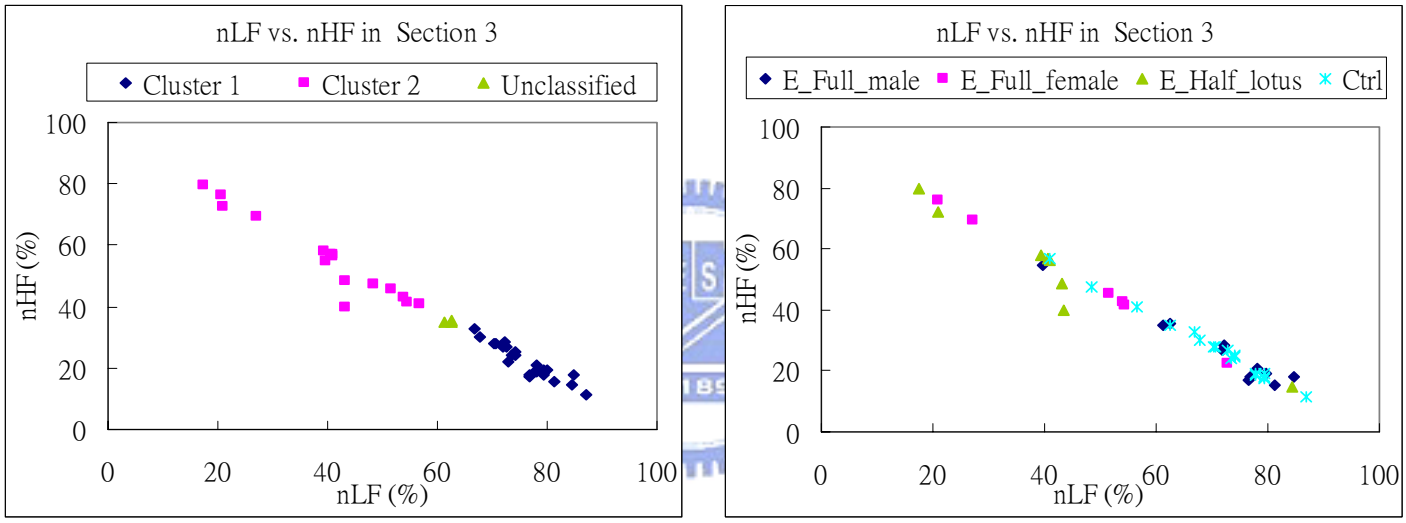

(a) (b)

Figure 4.14 The classified results of nLF vs. nHF in Section 3 using Fuzzy *C*-means algorithm

Then we discuss the classified results in Section 4. As shown in Fig. 4.15, the patterns are divided into 2 clusters based on the 2-dimensional feature vectors reconstructed by nLF(Section4) and nHF(Section4). The classified condition of each group is tabulated in Table 4.19. The male experimental subjects and the control subjects probably distribute in Cluster 2, and Cluster 1 mainly consists of the experimental subjects. The members of Cluster 1 have higher nHF value, and lower

nLF value than those of Cluster 2. Most control subjects and experimental male subjects in full lotus position keep lower nHF and higher nLF value in Section 4 as in the Section 2 and Section 3. However, some parts of the experimental female subjects in full lotus position and male subjects in half lotus position do not remain so high nHF and low nLF value in the Section 4 as in the Section 2 and Section 3.

Table 4.19 The classified results of nLF vs. nHF in Section 4; the number of subjects (of a group) being classified to a particular cluster

Cluster / **Group**	Cluster 1	Cluster 2	unclassified
E_full_male	3	7	1
E_full_female	2	3	1
E_half_male	4	2	0
E_half_female	2	0	0
C_male	1	8	0
C_female	1	8	0

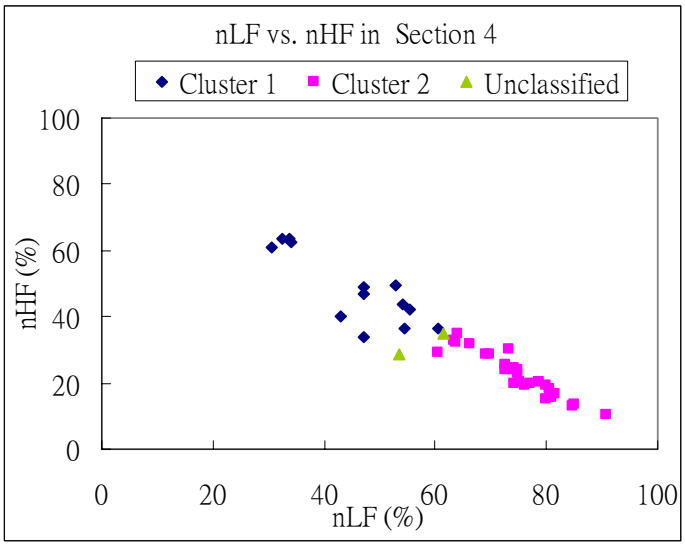

(a)

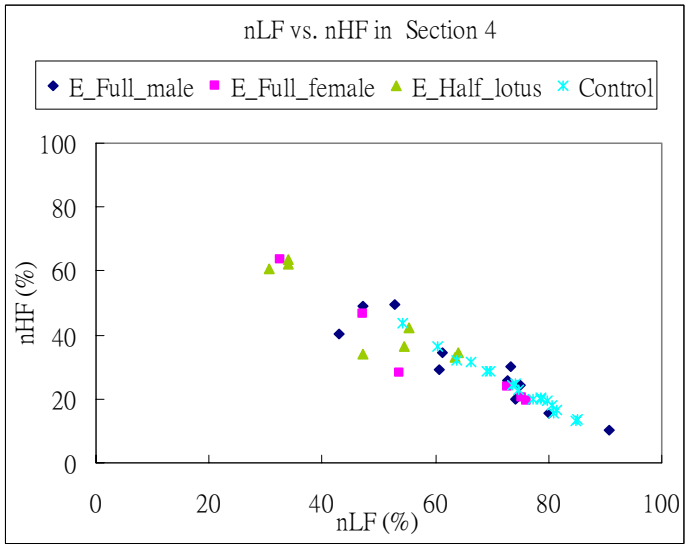

(b)

Figure 4.15 The classified results of nLF vs. nHF in Section 4 using Fuzzy *C*-means algorithm

Then we discuss the classified results in Section 5. As shown in Fig. 4.16, the patterns are divided into 2 clusters based on the 2-dimensional feature vectors reconstructed by nLF(Section5) and nHF(Section5). The classified condition of each group is tabulated in Table 4.20. Like the Section 4, the male experimental subjects and the control subjects probably distribute in Cluster 2, and Cluster 1 mainly consists of the experimental subjects. The members of Cluster 1 have higher nHF value, and lower nLF value than those of Cluster 2. Most control subjects and experimental male subjects in full lotus position keep lower nHF and higher nLF value in Section 5 as in the Section 4. Some of experimental female subjects in full lotus position and male subjects in half lotus position have high nHF and low nLF value, and some of them have low nHF and high nLF value in the Section 5. The female experimental subjects in half lotus position keep the high nHF and low nLF value from Section 1 to Section 5.

Table 4.20 The classified results of nLF vs. nHF in Section 5; the number of subjects (of a group) being classified to a particular cluster

Cluster / **Group**	Cluster 1	Cluster 2	unclassified
E_full_male	2	9	0
E_full_female	3	3	0
E_half_male	3	2	1
E_half_female	2	0	0
C_male	1	8	0
C_female	1	8	0

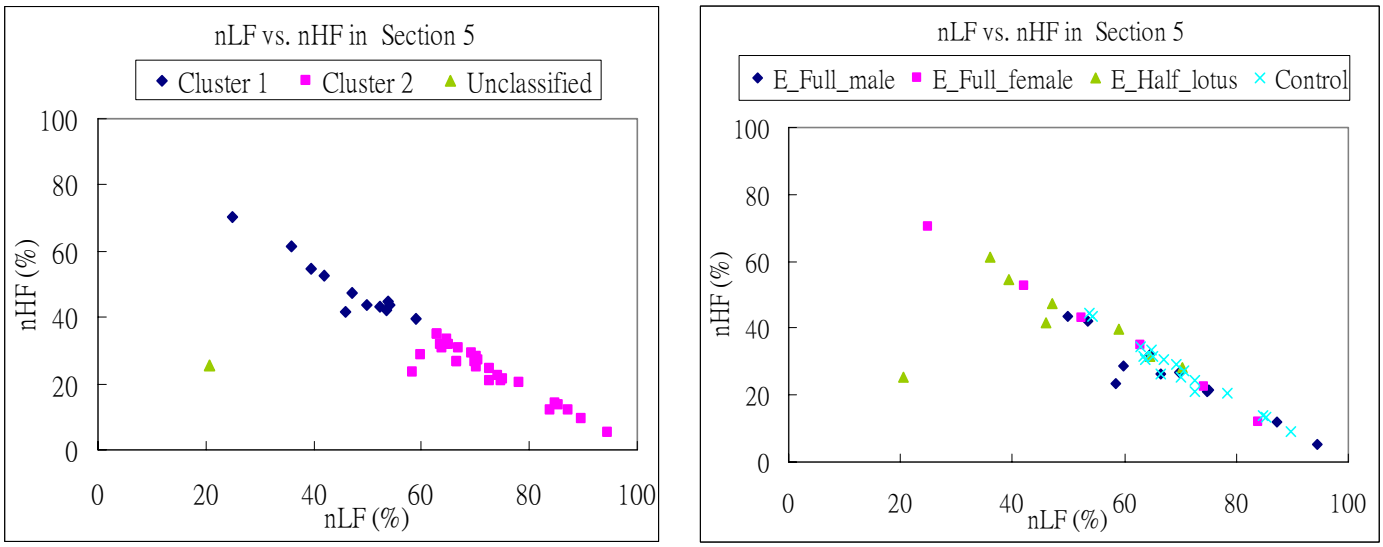

(a) (b)

Figure 4.16 The classified results of nLF vs. nHF in Section 5 using Fuzzy *C*-means algorithm

Chapter 5

Conclusion and Discussion

5.1 Summary of the current Work

The aim of this research is to investigate the difference of the extent of HRV and the modulation of ANS between the experimental subjects (Zen-Buddhist practitioners) and the control subjects (normal healthy people without meditation experiences) in those sections before, during, and after the meditation /resting. The items listed in Table 5.1 are the P-values of some parameters selected from Table 4.3 and Table 4.9, and they present obvious distinction between the experimental and control group. For these four parameters, the difference between the two groups is getting more obvious from Section 2 to Section 4, that is, the meditation (resting) time. Therefore it can be inferred that meditation does a different effect on heart rate, HRV, and the modulation of the autonomic nervous system from normal resting does.

Table 5.1 P-value

Comparative Item \ Parameter		MRR	SDRR	nLF	nHF
P-value between Experimental and Control group from Section 1 to Section 5	Section 1	0.124	0.569	0.931	0.959
	Section 2	0.314	0.474	0.015	0.028
	Section 3	0.045	0.016	0.009	0.015
	Section 4	0.011	0.008	0.0004	0.002
	Section 5	0.248	0.699	0.019	0.095

The items listed in Table 5.2 are the comparison of the magnitude of each parameter between male and female in the same position during the five sections. For the parameters, nLF, nHF, and LF/HF Ratio, the comparisons between male and female in the same position are in accordance among the three groups. Then for the parameters, pLF, and MRR, the comparisons between male and female in control group are different from those in the other two experimental groups. And then for the parameters, SDRR, and RMSSD, the comparisons between male and female in E_Full_Lotus group are different from those in E_Half_Lotus and control group. Finally, for the parameter, pHF, the comparisons between male and female in E_Half_Lotus group are different from those in E_Full_Lotus and control group.

Table 5.2 Parameter (male) $_{\text{Section I}}$ – parameter (female) $_{\text{Section I}}$ based on the same posture in 5 sections (M: male; F: female)

Parameter / Group Label	E_Full_Lotus	E_Half_Lotus	Ctrl
MRR(sec)	M＜F(-0.043, -0.053, -0.002, -0.006, -0.067)	M＜F(-0.025, -0.036, -0.024, -0.035, -0.042)	M＞F(0.064, 0.072, 0.073, 0.067, 0.077)
SDRR(msec)	M≈F (-2.7, -4.6, 1.4, 0.6, 3.7)	M＞F (22.4, 11.0, 18.4, 18.8, 5.4)	M＞F (11.0, 8.9, 22.4, 19.5, 5.8)
RMSSD(msec)	M＜F (-10.2, -13.3, -2.0, -2.6, -4.6)	M＞F (13.1, 11.3, 12.9, 18.3, 18.9)	M＞F (4.6, 4.5, 7.6, 10.3, 5.9)
pLF (bpm^2)	M＞F (445, 280, 608, 250, 1003)	M＞F (1052, 638, 1188, 925, 49)	M≈F (-50, -185, 424, -19, 328)
pHF (bpm^2)	M＜F (-404, -430, -304, 1, 40)	M＞F (414, 491, 403, 653, 9)	M＜F(-100, -113, -137, -62, -31)

nLF (%)	M＞F (26.66, 28.48, 24.62, 6.9, 11.89)	M＞F (27.03, 4.62, 17.1, 4.37, 0.51)	M＞F (5.44, 7.04, 10.18, 0.27, 5.5)
nHF (%)	M＜F(-26.84, -28.16, -23.48, -4, -13.52)	M＜F(-30.81, -11.04, -20.89, -9.35, -12.28)	M＜F(-5.19, -7.21, -9.17, -0.08, -4.79)
LF/HF Ratio	M＞F (2.09, 1.99, 2.02, 0.68, 1.83)	M＞F (0.98, 0.46, 1.14, 0.37, 0.32)	M＞F (0.54, 0.3, 1.07, 0.17, 0.56)

The descriptions listed in the Table 5.3 are the tendencies during the meditation(resting) period, and those during the period from the the end of meditation(resting) to the post test of six groups. In the E_full_male and E_full_female groups, the tendencies of the time domain parameters, MRR, SDRR, and RMSSD from Section 2 to Section 4 all present falling trends, and on the contrary, those from Section 4 to Section 5 all present rising trends. On the other hand, in the C_male and C_female groups, the tendencies of the two time domain parameters, SDRR, and RMSSD from Section 2 to Section 4 both present rising trends, and on the contrary, those from Section 4 to Section 5 both present falling trends. For the E_half_male and E_half_female group, there exist rising trends of the two parameters, MRR, and RMSSD from Section 4 to Section 5, but they do not exhibit an identical trend from Section 2 to Section 4.

Table 5.3 Tendency from Section 2 to Section 5 (from the beginning of the meditation to the post test)

Parameter / Group Label	MRR		SDRR		RMSSD	
	Tendency	Sect3 - Sect2	Tendency	Sect3- Sect2	Tendency	Sect3- Sect2
		Sect4 - Sect3		Sect4- Sect3		Sect4- Sect3
		Sect5 - Sect4		Sect5 - Sect4		Sect5 - Sect4
E_full_male	falling	-0.013 sec	falling	-0.2 msec	falling	-0.2 msec
		-0.033 sec		-2.0 msec		-3.1 msec
	rising	0.008 sec	rising	5.8 msec	rising	3.0 msec

E_full_female	falling	-0.064 sec	falling	-6.2 msec	falling	-11.5 msec
		-0.029 sec		-1.3 msec		-2.5 msec
	rising	0.069sec	rising	2.8msec	rising	5.0msec
E_half_male	not obvious	0.004 sec	rising	8.1 msec	rising	1.1 msec
		-0.010 sec		1.3 msec		4.2 msec
	rising	0.003sec	falling	-0.9msec	rising	4.5msec
E_half_female	not obvious	-0.008 sec	rising	0.8 msec	falling	-0.5 msec
		0.001 sec		0.8 msec		-1.2 msec
	rising	0.011sec	rising	12.5msec	rising	3.9msec
C_male	not obvious	0.010 sec	rising	16.8 msec	rising	4.2 msec
		-0.007 sec		3.4 msec		3.4 msec
	falling	-0.022sec	falling	-20.2msec	falling	-11.4msec
C_female	not obvious	0.009 sec	rising	3.4 msec	rising	1.1 msec
		-0.001 sec		6.2 msec		0.7 msec
	falling	-0.031sec	falling	-6.5msec	falling	-7.1msec

From the Fig. 5.1(a)(b), the tendencies of MRR and RMSSD of the experimental subjects in full lotus posture are mostly descending from Section 2 to Section 4, and the tendencies of SDRR of the control subjects are mostly ascending from Section 2 to Section 4. These results are in accordance with those in the statistical analysis. From the Fig. 5.1(c)(d), in the experimental group, the number of the subjects whose MRR ,SDRR, and RMSSD present ascending tendencies from Section 4 to Section 5 is more than that of the subjects whose MRR ,SDRR, and RMSSD present descending tendencies during the same period. On the contrary, in the control group, the number of the subjects whose MRR, SDRR, and RMSSD present descending tendencies from Section 4 to Section 5 is more than that of the subjects whose MRR, SDRR, and RMSSD present ascending tendencies during the same period. These results are also in accordance with those in the statistical analysis. From the above, it can be inferred that meditation in full lotus position can

make heart rate speed up and instantaneous HRV lower down, and normal resting lead HRV to rise up. And it also exhibits that the heart rate slows down and HRV increases for most subjects in the experimental group from the end of meditation to post test, and the condition is just opposite for control group during the same period.

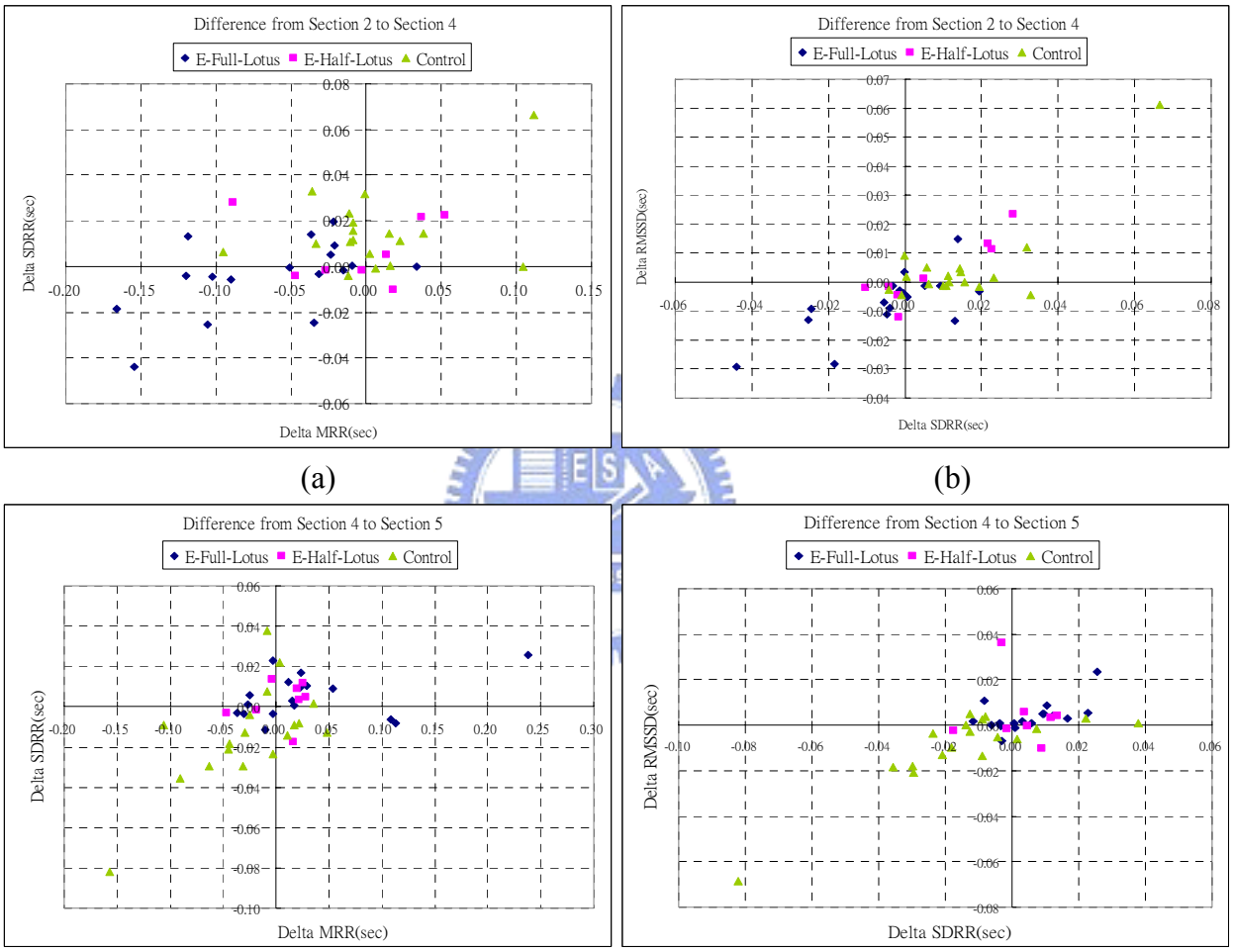

Fig. 5.1 (a)(b) Difference of MRR, SDRR, and RMSSD from Section 2 to Section 4; (c)(d) Difference of MRR, SDRR, and RMSSD from Section 4 to Section 5

The items listed in Table 5.4 are the mean values of the differences in 5 sections (‘difference’ means the difference between the mean of each parameter of each group and that of all groups in one of the 5 sections). From Table 5.4, it can be found that at the three parameters, nLF, nHF, and LF/HF Ratio, the three groups, E_full_female, E_half_male, and E_half_female, have the same phenomenon, and for the other three groups, E_full_male, C_male, and C_female, the phenomenon is on the opposite side. About the pLF, the mean differential value of five sections of E_full_male, E_half_male, C_male, and C_female is bigger than zero, and the mean differential value of five sections of E_full_female and E_half_female is smaller than zero. About the pHF, the mean differential value of five sections of E_full_male, E_full_female, C_male, and C_female is smaller than zero, and the mean differential value of five sections of E_half_male and E_half_female is bigger than zero.

Table 5.4 The mean value of the differences in 5 sections (‘difference’ means the difference between the mean of each parameter of each group and that of all groups in one of the 5 sections)

Parameter / Comparative Item	Group Label	pLF	pHF	nLF	nHF	LF/HF Ratio
The mean value of the differences in 5 sections (‘difference’ means the difference between the mean of each parameter of each group and that of all groups in one of the 5 sections)	E_full_male	237	-262	13.50	-12.97	1.31
	E_full_female	-280	-42	-6.21	6.23	-0.42
	E_half_male	206	499	-9.51	4.70	-0.78
	E_half_female	-565	105	-20.24	21.57	-1.43
	C_male	251	-194	14.08	-12.41	0.92
	C_female	151	-105	8.39	-7.12	0.91

From the Fig. 5.2(a), the female experimental subjects and the subjects in half lotus position have the highest nHF value, and the lowest nLF value, the control subjects have the intermediate nHF and nLF value, and the male experimental subjects in full lotus position have the lowest nHF value, and the highest nLF value in Section 1 (pre-test section). According to the literature, the female have higher nHF and lower nLF values than the male. From the Fig. 5.2(b)(c), all female subjects are almost classified to a cluster except the control female subjects, and all male subjects are almost classified to the other cluster except the experimental male subjects in half lotus position during Section 2 and Section 3. Therefore it can be inferred that meditation in half lotus position does better to cheer up the parasympathetic activation than normal resting. From Fig. 5.2(d)(e), most control subjects and experimental male subjects in full lotus position keep the lower nHF and higher nLF value in Section 4 and Section 5 as in the Section 2 and Section 3. Some of experimental female subjects in full lotus position and male subjects in half lotus position have high nHF and low nLF value, but hoever, some of them have low nHF and high nLF value in the Section 4 and Section 5. The female experimental subjects in half lotus position keep the high nHF and low nLF value from Section 1 to Section 5. Therefore it can be inferred that the activation of the parasympathetic of E_Full_female, and E_Half_lotus group is more active than that of E_full_male, and Control groups.

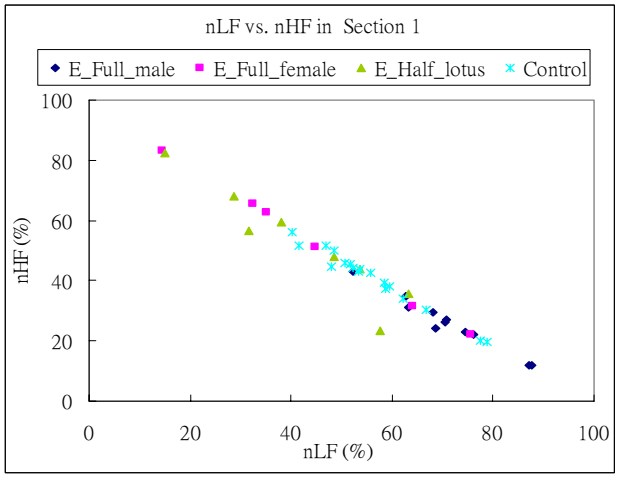

(a)

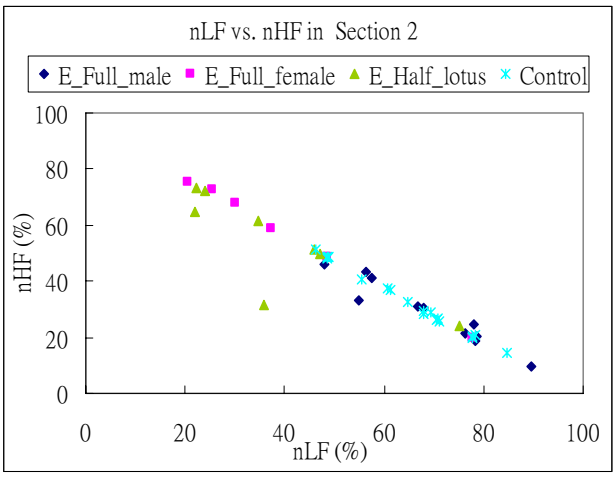

(b)

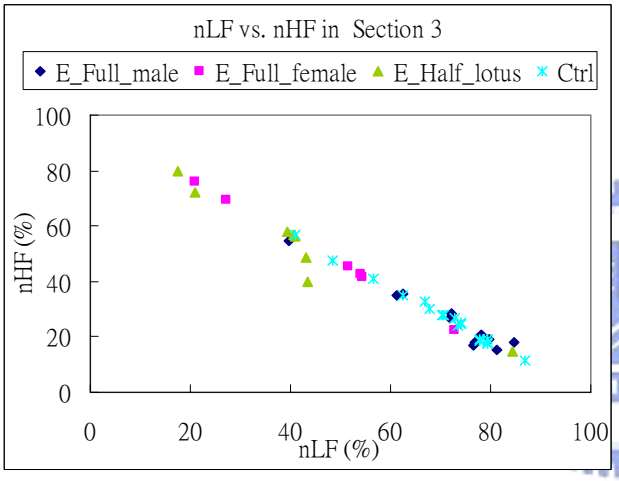

(c)

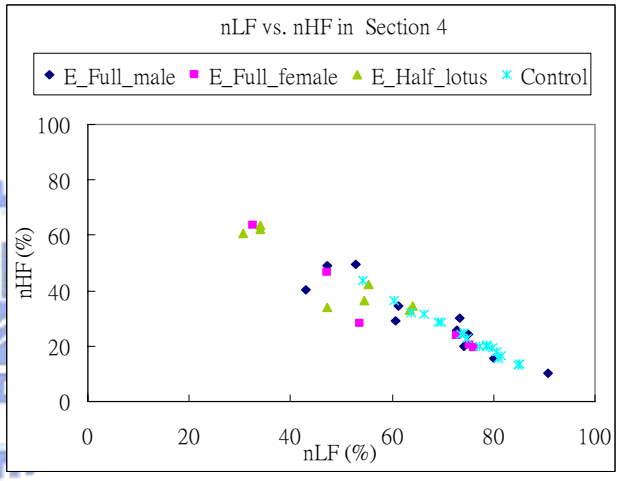

(d)

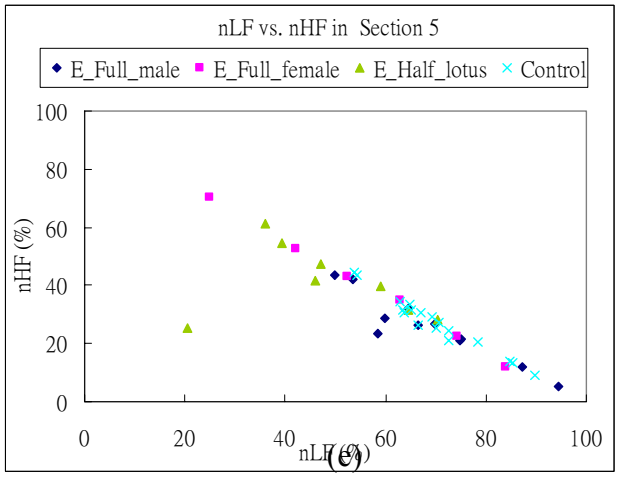

(e)

Fig. 5.2 (a) nLF vs. nHF in Section 1;
(b) nLF vs. nHF in Section 2;
(c) nLF vs. nHF in Section 3;
(d) nLF vs. nHF in Section 4;
(e) nLF vs. nHF in Section 5;

5.2 Future Work

In this research, for the subjects in experimental group, the number of male and that of female are not equal. Then the number of the subjects adopting full-lotus posture and that of the subjects adopting half-lotus posture are not equivalent, either. Therefore this condition can be modified so that the result will be more significant in statistics. The experiment can be designed like that the respiratory signal can be measured with ECG synchronously in the future, because it is mentioned in the literature [12] that the frequency of the respiration is related to the high frequency component of the power spectrum of RR intervals. ECG and EEG can also be examined together because it is mentioned in the literature [25] that during meditation, in terms of mean values in all subjects, an increase in slow alpha interhemispheric EEG coherence in the frontal region, an increase in high-frequency power, and a decrease in the ratio of low-frequency to high-frequency power were observed.

Bibliogrphy

[1] Biswas AK, Scott WA, Sommerauer JF, Luckett PM. “Heart rate variability after acute head injury in children,” Critical Care Medicine, vol.28(12), pp:3907-3912 Dec. 2000

[2] Baillard C, Vivien B, Mansier P, Mangin L, Jasson S, Riou B, Swynghedauw B. “Brain death assessment using instant spectral analysis of heart rate variability,” Critical Care Medicine, vol.30(2), pp:306-310, Feb. 2002

[3] Berger R.D., Akselrod S, Gordon D, Cohen R.J. “An Efficient Algorithm for Spectral Analysis of Heart Rate Variability,” IEEE transaction on biomedical engineering, vol.33(9), pp:900-904, Sep. 1986

[4] Brennan M., Palaniswami M., Kamen P.W., “A new cardiac nervous system model for heart rate variability analysis,” Engineering in Medicine and Biology Society, 1998 Proceedings of the 20th Annual International Conference of the IEEE, vol. 1, pp:349-352, 1998

[5] Brennan M, Palaniswami M, Kamen P., “Do Existing Measures of Poincare Plot Geometry Reflect Nonlinear features of Heart Rate Variability?” IEEE Transaction Biomedical Engineering, vol.48(11), pp:1342-1347, Nov 2001

[6] Crasset V, Mezzetti S, Antoine M, Linkowski P, Degaute JP, van de Borne P “Effects of Aging and Cardiac Denervation on Heart Rate Variability During Sleep,” Circulation, vol.103(1), pp:84-88, Jan 1 2001

[7] Elizabeth Monk-Turner, “The benefit of meditation: experimental findings,” The Social Science Journal, vol.40, pp.465-470, 2003

[8] Gregory A. Tooley, Stuart M. Armstrong, Trevor R. Norman, Avni Sali, “Acute increases in night-time plasma melatonin levels following a period of meditation,” Biological Psychology, vol.53, pp.69-78, 2000

[9] Gu HG, Ren W, Liu G, Shen XY, Meng JR. “Approximate entropy and its application in heart rate variability analysis,” Space Medicine & Medical Engineering, vol.13(6), pp:417-421, Dec 2000

[10] G D'Addio, GD Pinna, R Maestri, D Acanfora, C Picone, G Furgi, F Rengo, "Correlation between Power-Law Behavior and Poincare Plots of Heart Rate Variability in Congestive Heart Failure Patients," IEEE Computers in Cardiology, vol.26, pp:611-614, 1999

[11] Huikuri HV, Seppanen T, Koistinen MJ, Airaksinen J, Ikaheimo MJ, Castellanos A, Myerburg RJ. "Abnormalities in Beat-to-Beat Dynamics of Heart Rate Before the Spontaneous Onset of Life-Threatening Ventricular Tachyarrhythmias in Patients With Prior Myocardial Infarction," Circulation, vol.93(10), pp:1836-1844, May 15 1996

[12] Hayano J, Mukai S, Sakakibara M, Okada A, Takata K, Fujinami T., "Effects of respiratory interval on vagal modulation of heart rate," American Journal of Physiology, vol. 267(1 Pt 2), pp: H33-40, Jul 1994

[13] John Ding-E Young and Eugene Taylor, "Meditation as a voluntary hypometabolic state of biological estivation," News in Physiological Sciences, vol.13, June 1998

[14] John J. Miller, M.D., Ken Fletcher, Ph.D., and Jon Kabat-Zinn, Ph.D., "Three-Year Follow-up and Clinical Implications of a Mindfullness Meditation-Based Stress Reduction Intervention in the treatment of Anxiety Disorders," General Hospital Psychiatry, vol.17(3), pp:192-200, May 1995

[15] Kamen P.W., Krum H., Tonkin A.M. "Poincare plot of heart rate variability allows quantitative display of parasympathetic nervous activity in humans," Clinical Science, vol.91(2), pp:201-208, Aug 1996

[16] Linda E. Carlson, Michael Speca, Kamala D. Patel, Eileen Goodey, "Mindfulness-based stress reduction in relation to quality of life, mood, symptoms of stress and levels of cortisol, dehydroepiandrosterone sulfate (DHEAS) and melatonin in breast and prostate cancer outpatients," Psychoneuroendocrinology, vol.29, pp.448-474, 2004

[17] Laurie Keefer, Edward B. Blanchard, "The effects of relaxation response meditation on the symptoms of irritable bowel syndrome: results of a controlled treatment study," Behaviour Research and Therapy, vol.39, pp.801-811, 2001

[18] L. Keefer, E.B. Blanchard, “A one year follow-up of relaxation response meditation as a treatment for irritable bowel syndrome,” Behaviour Research and Therapy, vol.40, pp.541-546, 2002

[19] Lombardi F, Mortara A., “Heart rate variability and cardiac failure,” Heart, vol.80(3), pp:213-214, 1998

[20] Liao Duanping, Barnes RW, Chambless LE, Simpson RJ, Sorlie P, Heiss G. “Age, Race, and Sex Differences in Autonomic Cardiac Function Measured by Spectral Analysis of Heart Rate Variability—The ARIC Study,” American Journal of Cardiology, vol.76(12), pp:906-912, 1995

[21] Lau Ying-Tung, “Practical Physiology,” Fayfar Publishing Co.,Ltd., 1996

[22] Lessard A, Salevsky FC, Bachelard H, Cupples WA. “Incommensurate frequencies of major vascular regulatory mechanisms,” Canadian Journal of Physiology and Pharmacology, vol.77(4), pp:293-299, Apr 1999

[23] Mastrocola C, Vanacore N, Giovani A, Locuratolo N, Vella C, Alessandri A, Baratta L, Tubani L, Meco G. “Twenty-four-hour heart rate variability to assess autonomic function in Parkinson’s disease,” Acta Neurologica Scandinavica., vol.99(4), pp:245-247, April 1999

[24] Massin MM, Maeyns K, Withofs N, Ravet F, Gerard P. “Circadian rhythm of heart rate and heart rate variability,” Archives of Disease in childhood, vol.83(2), pp:179-182, 2000

[25] Murata T, Takahashi T, Hamada T, Omori M, Kosaka H, Yoshida H, Wada Y., “Individual trait anxiety levels characterizing the properties of zen meditation,” Neuropsychobiology, vol.50(2), pp:189-94, 2004

[26] Nakagawa M, Iwao T, Ishida S, Yonemochi H, Fujino T, Saikawa T, Ito M. “Circadian rhythm of the signal averaged electrocardiogram and its relation to heart rate variability in healthy subjects,” Heart, vol.79(5), pp:493-496, May 1998

[27] Ponikowski P, Anker SD, Chua TP, Szelemej R, Piepoli M, Adamopoulos S, Webb-Peploe K, Harrington D, Banasiak W, Wrabec K, Coats AJ. “Depressed heart rate variability as an independent predictor of death in chronic congestive heart failure secondary to ischemic or idiopathic dilated cardiomyopathy,” American Journal of Cardiology, vol.79(12), pp:1645-1650, Jun. 15 1997

[28] Pieper S J, Hammill, SC., “Heart Rate Variability Standards of Measurement, Physiological Interpretation, and Clinical Use,” Circulation, vol.93(5), pp:1043-1065, Mar 1 1996

[29] Parati G, Frattola A, Di Rienzo M, Castiglioni P, Mancia G. “Broadband spectral analysis of blood pressure and heart rate variability in very elderly subjects,” Hypertension, vol.30(4), pp:803-808, Oct. 1997

[30] Pierro C, Pierro V, Iacono A. “New experimental evidence of complex dynamics of heart beat. II. Correlation dimension, Lyapunov's exponents,” Cardiologia, vol.43(8), pp:819-824, Aug 1998

[31] Pomeranz B, Macaulay RJ, Caudill MA, Kutz I, Adam D, Gordon D, Kilborn KM, Barger AC, Shannon DC, Cohen RJ, et al. “Assessment of autonomic function in humans by heart rate spectral analysis,” American Journal of Physiology Vol.248, pp:H151-153, Jan 1985

[32] Pan J, Tompkins W.J. “A real-time QRS detection algorithm,” IEEE transaction on biomedical engineering, vol.32(3), pp:230-236, Mar. 1985

[33] Ramita Bonadonna, PhD, “Meditation’s impact on chronic illness,” Holistic Nursing Practice, vol.17(6), pp.309-319, Nov-Dec 2003

[34] Solange Akselrod, David Gordon, F. Andrew Ubel, Daniel C. Shannon, A. Clifford Barger, and Richard J. Cohen, “Power Spectrum analysis of Heart Rate Fluctuation: A Quantitative Probe of Beat-To-Beat Cardiovascular Control,” Science, Vol.213, No.4504, pp: 220-222, Jul.10 1981

[35] Singh JP, Larson MG, Tsuji H, Evans JC, O'Donnell CJ, Levy D. “Reduced Heart Rate Variability and New-Onset Hypertension: Insights Into Pathogenesis of Hypertension: The Framingham Heart Study.,” Hypertension, vol.32, pp:293-297, 1998

[36] Sato N, Miyake S, Akatsu J, Kumashiro M. “Power Spectral Analysis of Heart Rate Variability in Healthy Young Women during the Normal Menstrual Cycle,” Psychosomatic Medicine, vol.57(4), pp:331-335, Jul-Aug 1995

[37] Stein PK, Kleiger RE, Rottman JN. “Differing Effects of Age on Heart Rate Variability in Men and Women,” American Journal of Cardiology, vol.80(3), pp:302-305, 1997

[38] Vernon A. Barnes, Frank A. Treiber, Harry Davis, “Impact of Transcendental Meditation on cardiovascular function at rest and during acute stress in adolescents with high normal blood pressure,” Journal of Psychosomatic Research, vol.51, pp.597-605, 2001

[39] Vanoli E, Adamson PB, Ba-Lin, Pinna GD, Lazzara R, Orr WC. “Heart rate variability during specific sleep stages, A comparison of healthy subjects with patients after myocardial infarction,” Circulation, vol.91(7), pp:1918-1922, April 1995

[40] Watanabe T, Sugiyama Y, Sumi Y, Watanabe M, Takeuchi K, Kobayashi F, Kono -K. “Effects of vital exhaustion on cardiac autonomic nervous functions assessed by heart rate variability at rest in middle-aged male workers,” International Journal of Behavioral Medicine, vol.9(1), pp:68-75, 2002

[41] Woo MA, Stevenson WG, Moser DK, Trelease RB, Harper RM. “Patterns of beat-to-beat heart rate variability in advanced heart failure,” The American Heart Journal, vol.123(3), pp:704-710, Mar 1992

[42] Young L H, Chyun D A, Inzucchi S E, Sun V, Davey J A, Wackers F J. “Heart Rate Variability (HRV) in Patients with Type 2 Diabetes (T2DM) without Symptomatic Coronary Artery Disease (CAD),” Diabetes, (51S):A525, 2002

[43] Yataco AR, Fleisher Lee A, Katzel Leslie I. “Heart Rate Variability and Cardiovascular Fitness in Senior Athletes,” American Journal of Cardiology, vol.80(10), pp:1389-1391, 1997

[44] 陳德輝 主編 心電圖學原理與實用 合記圖書出版社 民 61

[45] 原著 Nora Goldshlager / Mervin J. Goldman 編譯 廖述朗. 譯自 Principles of Clinical Electrocardiography(臨床心電圖學), 藝軒圖書出版社 1995

[46] 蔡仁隆,"禪定心電圖研究,"交通大學電機與控制工程研究所碩士論文, 2003.